


Summer 2024

Investigation of Mechanically Fatigue Low-Frequency Energy Harvesting Effects on Isotropic Materials

Daniel J. Meade

Follow this and additional works at: <https://digitalcommons.georgiasouthern.edu/etd>

 Part of the [Ceramic Materials Commons](#), [Electro-Mechanical Systems Commons](#), and the [Other Materials Science and Engineering Commons](#)

Recommended Citation

Meade, Daniel J., "Investigation of Mechanically Fatigue Low-Frequency Energy Harvesting Effects on Isotropic Materials" (2024). *Electronic Theses and Dissertations*. 2809.
<https://digitalcommons.georgiasouthern.edu/etd/2809>

This thesis (open access) is brought to you for free and open access by the Jack N. Averitt College of Graduate Studies at Georgia Southern Commons. It has been accepted for inclusion in Electronic Theses and Dissertations by an authorized administrator of Georgia Southern Commons. For more information, please contact digitalcommons@georgiasouthern.edu.

Investigation of Mechanically Fatigue Low-Frequency Energy Harvesting Effects on Isotropic Materials

by

DANIEL MEADE

Under the Direction of Hossain Ahmed

ABSTRACT

This research project reports an exploratory investigation of energy harvesting effect on isotropic material that goes through low frequency mechanical fatigue. Energy harvesting is a growing field of study that can recycle ambient energy back into a system that would otherwise be lost. This is a significantly useful method for the ongoing energy crisis and provides an alternate route to design and upgrade systems to be more efficient and last longer than current system designs. However, it is time to investigate if there is any effect vibration-based energy harvesting has on the structure from which energy is being harvested. To answer this novel research question, both numerical and experimental studies are designed to determine the ultimate tensile strength and fatigue life of Aluminum structures with and without employing energy harvesting technique. Numerical studies are performed by commercial finite element solver and the experimental studies are performed by well controlled material testing systems. Two sets of specimens are prepared following ASTM standards. While the first set is reserved for baseline tests to determine ultimate tensile strengths and fatigue life without energy harvesting, the second set is used for inducing fatigue test with varying fatigue loads (3 Hz and 5 Hz). Energy is harvested from the second set of specimens. To quantify the material property degradations, linear ultrasonic wave velocity and non-linear normalized second harmonic frequencies are determined. Finally, the remaining strengths of the fatigued specimens are determined, and a correlation is drawn if energy harvesting has any effects on these mechanically fatigued specimens. A good match is found between the experimental and simulation results. The results show an average decrease in ultimate strength of 8% at 5Hz frequency and 13% at 3Hz frequency.

INDEX WORDS: Energy Harvesting, Material Properties, Material Structure, Piezoelectric Energy Harvesting, PZT, Fast Fourier Transformation

Investigation of Mechanically Fatigue Low-Frequency Energy Harvesting Effects on
Isotropic Materials by

DANIEL MEADE

B.S., Georgia Southern University, 2023

M.S., Georgia Southern University, 2024

A Thesis Submitted to the Graduate Faculty of Georgia Southern University

in Partial Fulfillment of the Requirements for the Degree

MASTER OF SCIENCE

STATESBORO, GEORGIA

© 2024

DANIEL MEADE

All Rights Reserved

Investigation of Mechanically Fatigue Low-Frequency Energy Harvesting Effects on
Isotropic Materials by

DANIEL MEADE

Major Professor:

Hossain Ahmed

Committee:

Mohammad Ahad

Mosfequr Rahman

Riaz Ahmed

Electronic Version Approved:

July 2024

ACKNOWLEDGMENTS

This thesis would not have been possible without the constant support of my mother, father, and sister, the grammar checks from Rebecca, the encouragement and knowledge from Dr. Ahmed, and the help, support, and laughs from Patrick, Sadaf, and Arif.

TABLE OF CONTENTS

	Page
ACKNOWLEDGMENTS	2
TABLE OF CONTENTS.....	3
LIST OF TABLES.....	6
LIST OF FIGURES.....	7
CHAPTER	
1 INTRODUCTION	12
1.1 Background and Motivation	12
1.2 Purpose of Research.....	12
1.3 Hypothesis	13
1.4 Objectives	13
2 LITERARY REVIEW.....	15
2.1 Background of Energy Harvesting.....	15
2.2 Piezoelectric Effect	17
2.2.1 Piezoelectric Energy Harvesting	19
2.3 Material Properties.....	19
2.4 Stress and Strain.....	20
2.5 Testing and Harvesting Methods.....	20
2.6 Circuit Design.....	21
2.7 Internal Stress Relaxation.....	24
3.1 Overview of Methodology.....	25
3 METHODOLOGY	25
3.2 Simulation Work	25
3.2.1 COMSOL Simulation	26
3.2.2 Simulated Force Calculations.....	26

3.2.3	Simulations with COMSOL	26
3.2.4	Simulation Setup in COMSOL.....	27
3.2.5	Changing Parameters of the Simulation.....	29
3.2.6	Simulations with Different Materials.....	29
3.3	Previous Testing Method Types	30
3.4	Material Relaxation Periods with Composite Materials Setup	32
3.5	Materials Relaxation Periods with Composite Materials Analysis	32
3.6	Material Properties Table for Aluminum 6061	33
3.7	Experimental Tensile Testing.....	34
3.7.1	Test Specimen Dimensions	34
3.7.2	Energy Harvesting Plate Setup.....	35
3.7.3	PZT Sensor Dimensions.....	36
3.7.4	Round PZT Location	37
3.7.5	Equipment Used During Testing	38
3.7.6	Reason for Baseline Fatigue Test	40
3.8	Preliminary Tensile Testing	41
3.8.1	Fatigue Force Calculations.....	41
3.9	Energy Harvesting Testing List.....	42
3.9.1	Fatiguing Material with Three Dispersed Relaxation Periods without PZT	42
3.9.2	Fatiguing Material with Three Dispersed Relaxation Periods with PZT	43
3.10	Material Relaxation Pitch and Catch Setup	43
3.11	Analysis of Data.....	44
3.12	Criteria for Success	45
4	DATA, RESULT, AND ANALYSIS	46
4.1	Simulation Data	46
4.2	Experimental Data Baseline Testing Results	48
4.2.1	Baseline Fatigue Results	51

4.3	Experimental Data.....	52
4.3.1	Specimen Break Locations.....	52
4.4	Energy Harvesting Results	55
4.4.1	Energy Harvesting Results for 3Hz and 5Hz	56
4.5	Material Relaxation Results.....	58
4.5.1	FFT Results – 5Hz.....	59
4.5.2	FFT Results – 3Hz.....	71
4.5.3	Velocity Results – 5Hz.....	84
4.5.4	Velocity Results – 3Hz.....	87
4.5.5	Total Max Stress of 5Hz and 3Hz Samples.....	90
4.6	Analysis of Data and Results	92
5	FINDINGS, CONCLUSION, AND RECOMMENDATION.....	93
5.1	Discussion of Findings and Results	93
5.2	Conclusion of Research.....	95
5.3	Recommendations of Improvements.....	96
5.4	Recommendations for Future Work	96
	REFERENCES.....	97

LIST OF TABLES

	Page
Table 1: Material Properties of Aluminum 6061	33
Table 2: ASTM Dog bone Dimensions for Testing.....	35

LIST OF FIGURES

	Page
Figure 1: Energy Harvesting Sources	15
Figure 2: Frequency Chart for a range of Applications.....	16
Figure 3: Sample experiencing necking in a tensile test (Roylance, 01).....	20
Figure 4: Modes of Energy Harvesting	21
Figure 5: Option 1 for Circuit Design (Covaci, 20).....	22
Figure 6: Option 1 Circuit Design with Cantilever Beam Model (Covaci, 20)	22
Figure 7: Option 3 for Circuit Design with Rectification (Covaci, 20).....	23
Figure 8: Option 3 with further Rectification to Increase Efficiency (Covaci, 20).....	23
Figure 9: S-S curve for Aluminum.....	26
Figure 10: Force Vs. Time from Force Calculations.....	26
Figure 11: Simulation Model with Fixed End, Force Direction, and PZT	27
Figure 12: Test Specimen Used in Simulation.....	28
Figure 13: Dimensions of PZT used for Simulation and Experimentation	28
Figure 14: Simulation Flow Chart	30
Figure 15: Material Degradation Properties (Patra, 17).....	31
Figure 16: Fatigue Loading with Relaxation Periods	31
Figure 17: Tensile Alignment Tool	34
Figure 18: Dimensions of the Test Specimen	35
Figure 19: Square PZT Location	36
Figure 20: Round PZT for Pitch and Catch and Dimensions	37
Figure 21: Round PZT Location Compared to Square PZT Location	37
Figure 22: Full Circuit Setup.....	38
Figure 23: Function Generator Used During Data Collection.....	39

Figure 24: Oscilloscope Used for Data Collection	39
Figure 25: 810 MTS for Fatigue and Tensile Loading	40
Figure 26: Stress Strain Curve Example for Aluminum.....	42
Figure 27: Specimen Holder for Relaxation Periods	43
Figure 28: Function Generator and Oscilloscope Setup for Data Collection	44
Figure 29: Simulation Data for 1mm Displacement (Meade, 23).....	46
Figure 30: Simulation Data for 1.5mm Displacement (Meade, 23).....	47
Figure 31: Comparison of Specimens used in Base Test and Actual Experimentation.....	48
Figure 32: Combine Base Tensile Test Results.....	49
Figure 33: Base Tensile Test 1 Break Location	49
Figure 34: Base Tensile Test 2 Break Location	49
Figure 35: Base Tensile Test 3 Break Location	50
Figure 36: Baseline Fatigue Test Results	51
Figure 37: Break Locations of Baseline Fatigue Samples.....	52
Figure 38: 5Hz Sample 1 Break Location	53
Figure 39: 5Hz Sample 2 Break Location.....	53
Figure 40: 5Hz Sample 3 Break Location	54
Figure 41: 3Hz Sample 1 Break Location	54
Figure 42: 3Hz Sample 2 Break Location	54
Figure 43: 3Hz Sample 3 Break Location	54
Figure 44: 5Hz Specimen Ultimate Strength vs Baseline Strength	55
Figure 45: 5Hz Specimen Ultimate Strength vs Baseline Strength	55
Figure 46: 3Hz Average Voltage Output Trend.....	56
Figure 47: 5Hz Average Voltage Output Trend.....	57
Figure 48: 5Hz Sp1 Time Series	59
Figure 49: 5Hz Sp1 FFT Full View.....	59

Figure 50: FFT Analysis of 5Hz Specimen 1	60
Figure 51: Second Harmonic Beta Value vs All Relaxation Cycles – SP1.....	60
Figure 52: 5Hz Specimen 1 – Average Beta Values before and after Relaxation Period	61
Figure 53: 5Hz Specimen 1 - Unrelaxed vs Relaxed - 35k	62
Figure 54: 5Hz Specimen 1 - Unrelaxed vs Relaxed - 70k	62
Figure 55: 5Hz Specimen 1 - Unrelaxed vs Relaxed - 105k	62
Figure 56: 5Hz Sp2 Time Series	63
Figure 57: 5Hz Sp2 FFT Full View.....	63
Figure 58: FFT Analysis of 5Hz Specimen 2	64
Figure 59: Second Harmonic Beta Value vs All Relaxation Cycles – SP2.....	64
Figure 60: 5Hz Specimen 2 - Average Beta Values before and after Relaxation Period.....	65
Figure 61: 5Hz Specimen 2 - Unrelaxed vs Relaxed - 35k	66
Figure 62: 5Hz Specimen 2 - Unrelaxed vs Relaxed - 70k	66
Figure 63: 5Hz Specimen 2 - Unrelaxed vs Relaxed - 105k	66
Figure 64: 5Hz Sp3 Time Series	67
Figure 65: 5Hz Sp3 FFT Full View.....	67
Figure 66: FFT Analysis of 5Hz Specimen 3	68
Figure 67: Second Harmonic Beta Value vs All Relaxation Cycles – SP3.....	68
Figure 68: 5Hz Specimen 3 - Average Beta Values before and after Relaxation Period.....	69
Figure 69: 5Hz Specimen 3 - Unrelaxed vs Relaxed - 35k	69
Figure 70: 5Hz Specimen 3 - Unrelaxed vs Relaxed - 70k	70
Figure 71: 5Hz Specimen 3 - Unrelaxed vs Relaxed - 105k	70
Figure 72: Average Beta Value for all 5Hz Specimen.....	71
Figure 73: 3Hz Sp1 Time Series	71
Figure 74: 3Hz Sp1 FFT Full View.....	72
Figure 75: FFT Analysis of 3Hz Specimen 1	72

Figure 76: Second Harmonic Beta Value vs All Relaxation Cycles – SP1.....	73
Figure 77: 3Hz Specimen 1 - Average Beta Values before and after Relaxation Period.....	73
Figure 78: 3Hz Specimen 1 - Unrelaxed vs Relaxed - 30k	74
Figure 79: 3Hz Specimen 1 - Unrelaxed vs Relaxed - 60k	74
Figure 80: 3Hz Specimen 1 - Unrelaxed vs Relaxed - 90k	75
Figure 81: 3Hz Sp2 Time Series	75
Figure 82: 3Hz Sp2 FFT Full View.....	76
Figure 83: FFT Analysis of 3Hz Specimen 2	76
Figure 84: Second Harmonic Beta Value vs All Relaxation Cycles – SP2.....	77
Figure 85: 3Hz Specimen 2 - Average Beta Values before and after Relaxation Period.....	77
Figure 86: 3Hz Specimen 2 - Unrelaxed vs Relaxed - 30k	78
Figure 87: 3Hz Specimen 2 - Unrelaxed vs Relaxed - 60k	78
Figure 88: 3Hz Specimen 2 - Unrelaxed vs Relaxed - 90k	79
Figure 89: 3Hz Sp3 Time Series	79
Figure 90: 3Hz Sp3 FFT Full View.....	80
Figure 91: FFT Analysis of 3Hz Specimen 3	80
Figure 92: Second Harmonic Beta Value vs All Relaxation Cycles – SP3.....	81
Figure 93: 3Hz Specimen 3 - Average Beta Values before and after Relaxation Period.....	81
Figure 94: 3Hz Specimen 3 - Unrelaxed vs Relaxed - 30k	82
Figure 95: 3Hz Specimen 3 - Unrelaxed vs Relaxed - 60k	82
Figure 96: 3Hz Specimen 3 - Unrelaxed vs Relaxed - 90k	83
Figure 97: Average Beta Value for all 3Hz Specimen.....	83
Figure 98: Amplitude vs Time Graph for 5Hz Specimen.....	84
Figure 99: Specimen 1 – Relaxation Velocity	85
Figure 100: Specimen 2 Relaxation Velocity	86
Figure 101: Specimen 3 – Relaxation Velocity	86

Figure 102: 5Hz Average Velocity for all Three Specimen	87
Figure 103: Amplitude vs Time Graph for 3Hz Specimen.....	87
Figure 104: 3Hz - Specimen 1 - Relaxation Velocity.....	88
Figure 105: 3Hz - Specimen 2 - Relaxation Velocity.....	89
Figure 106: 3Hz - Specimen 3 - Relaxation Velocity.....	89
Figure 107: 3Hz Average Velocity for all Three Specimens.....	90
Figure 108: Max Stress for 5Hz Samples.....	91
Figure 109: Max Stress for 3Hz Samples.....	91

CHAPTER 1

INTRODUCTION

1.1 Background and Motivation

The world is constantly looking for a source of energy that is efficient, clean, and sustainable for future generations. This is because as mankind and the world as a whole grow and evolve, the demand for energy increases. Energy production, transportation, and use is currently as efficient as it has ever been, however, the United States Government estimates that 5%-10% of energy is lost in distribution due to inefficiency (EIA, 22). This is just one example of scenarios like this that happen constantly in many other areas and industries. Energy harvesting is a fast-developing science that can be implemented in many of the mechanical, civil, and electro-mechanical areas to minimize the loss of ambient energy and increase the efficiency of energy conversion and transportation systems.

Ambient energy is the energy that is composed of natural sources of energy, and combination of two or more combination of energy systems. Ambient energy is not intended to be used for a designated purpose. This energy can be a byproduct of an inefficient system or natural phenomena that are possible sources of energy. Some examples of this natural phenomena are sunlight, ocean waves, gravity, and wind. All these sources naturally converts energy that can be harvested if the energy harvesting components such as smart materials and tools are combined in a specific configurations. There are also smaller sources of ambient energy that can be harvested from stresses in materials, heat byproducts of systems, etc. (Rashad, 21).

1.2 Purpose of Research

The purpose of this research is to investigate the effects of energy harvesting. As discussed previously, energy harvesting can be very useful when technology is implemented properly (Fan, 15; Covaci, 20; Yang, 22). Looking into possible advantages and disadvantages of energy harvesting can open new areas of research, open doors for new technology, and push mankind towards a future that is cleaner, efficient, and sustainable. No research exist that details the effects that energy harvesting has on material strength while

energy is actively being harvested. Some of the disadvantages with energy harvesting include the limited energy output, variability sources, initial cost and complexity, durability, storage and management, size and form factor for existing systems, energy conversion and conditioning, and application specific challenges. These are known disadvantages but currently no research exist that definitively defines a relationship between energy harvesting and material strength and the effect the two have on each other. The degradation in the material introduced in mechanically fatigued structures are associated with previous studies. The previous studies look at the effect that relaxation has on composite material. There is no research to look at the effects of relaxation on isotropic materials and how relaxation can influence the strength of the material in this study. The plan for fatiguing the specimen to extract energy allows for the introduction of relaxation periods that can be used to compare with the composite material research. Current investigation is an attempt to address the research gap for these two major points of interest for isotropic materials.

1.3 Hypothesis

In this study a numerical and an experimental approach are used to investigate the effects of mechanically fatigued energy harvesting effect on isotropic material such as Aluminum. The internal stresses of material play a pivotal role in the fatigue life and terminal strengths of all materials (Domanski, 07). This is why various methods like heat treatment, cold work etc. have been developed to relieve some of those stresses. It has been well established that heat treatment improves mechanical properties such as yield strength and tensile strength (Chandra, 21). Considering this phenomenon, the hypothesis for this research is that when harmonic vibration energy is harvested from an isotropic material (say, Aluminum), using smart materials, changes occur to the material properties and hence remaining strength of the isotropic materials gets affected as the internal stresses are relieved.

1.4 Objectives

The philosophy of the objectives is to find the effects of energy harvesting on material structure and to observe the effects that relaxation has on isotropic materials and compare these results to simulations and previous research.

The objectives of this research are to fill several gaps in the current research regarding piezoelectric energy harvesting, material science, and effects that relaxation can have on isotropic materials. The goals are to collect data while harvesting energy from the material and to analyze the effects the harvesting has on the material. Another objective is to collect data while the material is in a relaxed state. The state of relaxation has shown to introduce improvements to material in similar studies conducted with other materials. This study aims to close the gap and establish a relationship between harvesting energy from isotropic materials and the material science properties of isotropic materials.

CHAPTER 2

LITERARY REVIEW

2.1 Background of Energy Harvesting

Energy harvesting is a topic that is broad and has many complex parts and pieces. The reason for the complexity of energy harvesting is due to the vast array of types of energy. Many types of energy exist in many different forms. The two major categories of energy are kinetic and potential. Kinetic is the energy of motion and potential is stored energy. Three major forms of energy include mechanical energy, thermal energy, and radiant energy (U.S. EIA, 23). These three forms of energy are the forms of energy that are most often harvested. Thermal energy can be harvested from body heat and external heat. Mechanical energy can be harvested from body motion, vibrations, and air flow. Radiant energy can be harvested from solar rays, RF fields, and RF waves. These types of energy harvesting sources are shown in *figure 1*. Due to a lack of 100% efficiency in any system, all systems have wasted energy if the energy is not collected (Covaci, 20).

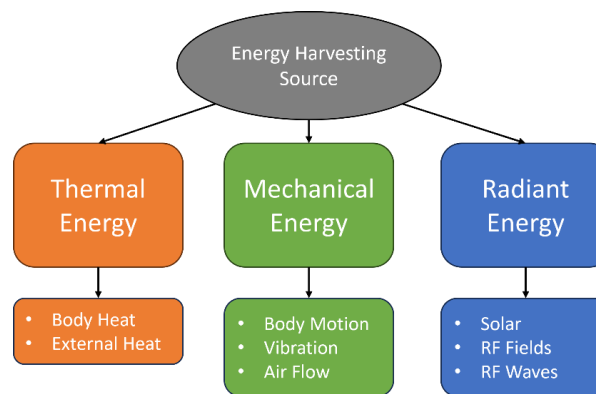


Figure 1: Energy Harvesting Sources

This study looks specifically at systems that generate ambient mechanical energy. Abundant research has been conducted around mechanical energy harvesting. Some projects have focused on the human motion aspect of ambient energy and uses typical human movements like walking, running, lifting weights, etc. to harvest and store ambient energy that can later be used to charge electronics like phones, computers,

or speakers. An example of this is using a piezoelectric heel strike generator in shoes that collects and stores ambient energy from a common human motion, walking (Howells ,09,2; Kim, 11; Mitcheson, 08). The results of this study yielded results that were lower than average due to several factors, such as unbalanced bimorph forces on the cam which cancelled some of the downward force of the heel on the generator. Other issues included stiffness variations and location of the PZT (Howells, 09, 4).

Vibration based energy harvesting is the major focus of this study. This type of energy harvesting can occur at a wide variety of frequencies. Different examples are shown in figure 2, along with the average frequency of the applications.

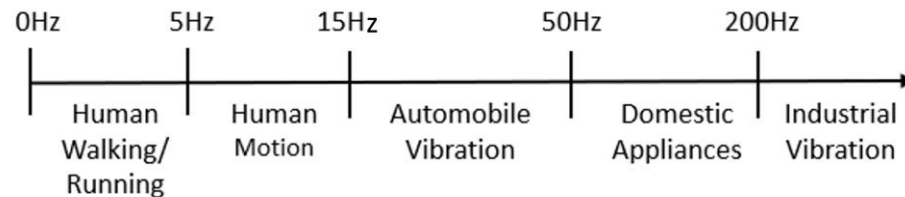


Figure 2: Frequency Chart for a range of Applications

Low energy harvesting is used in this study for multiple reasons. The main reason being the greater number of applications of use with lower frequency. Many everyday items do not have the large frequency output of a major industrial environment. The other reason for picking the lower frequency is due to the material selection, specimen size, and limits of the testing machine. This testing fills a major gap in the energy harvesting research and how it connects to another major area of engineering, which is material science.

Other studies take a deeper approach to energy harvesting and look at microsystem applications of energy harvesting. The three major systems of energy harvesting explored are piezoelectric, electromagnetic, and electrostatic. Piezoelectric energy harvesting consists of harvesting energy with piezoelectric crystal and ceramic materials and using a beam and mass to apply force and harvest energy. Electromagnetic energy harvesting uses a system of magnets to apply to force and harvest the energy. The

third microsystem application looked at was electrostatic generators that use capacitors to apply the force and then collect and store the energy (Beeby, 06).

Research has also been done to review energy harvesting techniques with microelectronic applications. Batteries are most used in portable devices. As portable devices shrink down the batteries are also expected to shrink down while still maintaining similar levels of efficiency. Batteries also require proper maintenance to function at full capacity. Both aspects of batteries pose issues now but also future issues that may occur. Compared to electric technology evolution over the past 50 years, battery technology has been slow. One of the solutions to this problem is a secondary battery or a system that can recharge using environmental factors like solar power and motion from the human body. (Mateu, 05, 360). In Mateu and Moll's review paper the definition of energy harvesting devices is provided and is used in this research. The first application is classified as a device that uses energy from the user of the electronic device to provide power. Some of these examples include shoes that charge a battery or automatic watches that use arm motion to rewind the spring instead of quartz watch that uses a battery. The second type of harvest energy comes from three main types of energy. These types include kinetic energy, electromagnetic radiation, and thermal energy. These energy sources are classified as environmental energy sources (Mateu, 05, 362)

2.2 Piezoelectric Effect

The piezoelectric effect is described the capabilities of certain materials to generate separated opposite electrical charges in response to mechanical deformation by an external force (Surmenev, 19). A typical quartz crystal is made of two elements, oxygen and silicon. When these elements bond atomically the results shape is a hexagon made of three oxygen and three silicon. There is a covalent bond between the two which results in the shared electron being closer to the smaller atom, which in this case is the oxygen atom. Since the electron is closer to the oxygen atom it makes the oxygen atoms slightly electro-negative which results in a more electro-positive silicon. This is typically called a dipole, and the dipoles of the hexagon result in a point at the center of the hexagon that is referred to as the center of charge. When a tensile or compressive load is applied on the individual hexagons this separates the center of charge and creates two points that are

oppositely charged. The charge separation creates an electromagnetic field that produces voltage. The hexagonal structure of the PZT is in series and lacks symmetry (Lesics, 21).

$$S = s \cdot T \quad 1$$

The equation above is a common equation among engineers, Hooke's law. The equation, in words, states that Strain is equal to Compliance multiplied by Stress.

$$D = \varepsilon \cdot E \quad 2$$

Piezoelectric Materials also have electrical properties as well so equations for common dielectrics must be used as well. The equation, shown above, simply states that Charge Density is equal to permittivity multiplied by the electric field.

$$D_i = e_{ij}^{\sigma} E_j + d_{im}^d \sigma_m \quad 3$$

$$\varepsilon_k = d_{jk}^c E_j + S_{km}^E \sigma_m \quad 4$$

Equations 1 and 2 can be combined to generate the constitutive equations of piezoelectric materials. The first is the direct piezoelectric effect equation. The second equation is the converse piezoelectric effect equation (Kim, 11). These equations help to provide a connection between Hooke's law and stress and strain and with the electrical side of the piezoelectric material.

Another major component of piezoelectric material is the polarization effect. This effect occurs in the material when a force is applied. The force creates polarization inside of the material due to the center of charge between the atomic bonds separating into a positive and negative side. This polarization creates an electromagnetic field within the bonds of the molecules.

2.2.1 Piezoelectric Energy Harvesting

Part of this research is because environments are subjected to ambient vibrations energy that typically go unused. Some of these sources are electromagnetic (Glynne-Jones, 04), Electrostatic generation (Mitcheson, 04), dielectric elastomers (Kornbluh, 02), and piezoelectric (Sodano and Anton, 07). Piezoelectric devices can transform mechanical stress into energy, but they can also transfer electrical energy to mechanical stress, by converting applied electric potential into mechanical strain.

The sources for this energy harvesting can be biological (Shenck and Paradiso, 01; Gonzalez, 02), water currents (Taylor et al., 01), and structural systems (Sodano, 05). Piezoelectric energy harvesting has led to tons of applications such as blenders (Lesieutre, 04; Sodano, 05; Sodano, 06), Thunder actuators (Shenck and Paradiso, 01) and Microelectromechanical systems (MEMS) (Duggirala, 04; Mitcheson, 04). These applications are useful in showing the expansive areas that PZT can be used in. From everyday household products like blenders, to structural systems of bridges and buildings, to water currents in streams and rivers, and rainbow and thunder actuators in weather. The expansive uses of the PZT are very useful in my different areas that are very different from each other.

2.3 Material Properties

The goal of this research is to look at the structural effects that energy harvesting can have on a material. The material properties are some of the most important things to look at when designing, implementing, or troubleshooting issues that a system may have (Liao, 09). If a system was designed or upgraded to include piezoelectric (PZT) plates it is likely that some side effect may result from the implementation. This study looks to answer the question of how piezoelectric energy harvesting affects material structure and strength (Bergmann, 10). There are three possible outcomes to this question. The first is that the piezoelectric energy harvesting plate reduces the material strength and breaks down the structure at an accelerated rate. The second scenario is that the effects of the piezoelectric material on the material strength and structure is minimal and only has a small increase that could be chalked up to the increase support from the PZT plate and the glue that holds it on. The final scenario is that the piezoelectric material

increases the strength of the material and the life of the material. This scenario would be ideal due to the advantage of harvesting ambient energy and increasing the life of the material.

2.4 Stress and Strain

The stress and strain curve is a very useful tool in this research to compare the results in the experiment. The stress strain curve can be generated from a tensile test and can be used to show the point that a specimen changes from the elastic deformation region to the plastic deformation region which is also close to the point that the specimen would begin necking as seen in *figure 3 (Roylance, 01)*. The stress strain curve is used to compare the results of testing specimen that energy have not been harvested from and test specimens that have undergone energy harvesting. The harvesting is conducted in the elastic region of the stress strain curve and then the specimen is broken to determine the effects that the harvesting has on the material.

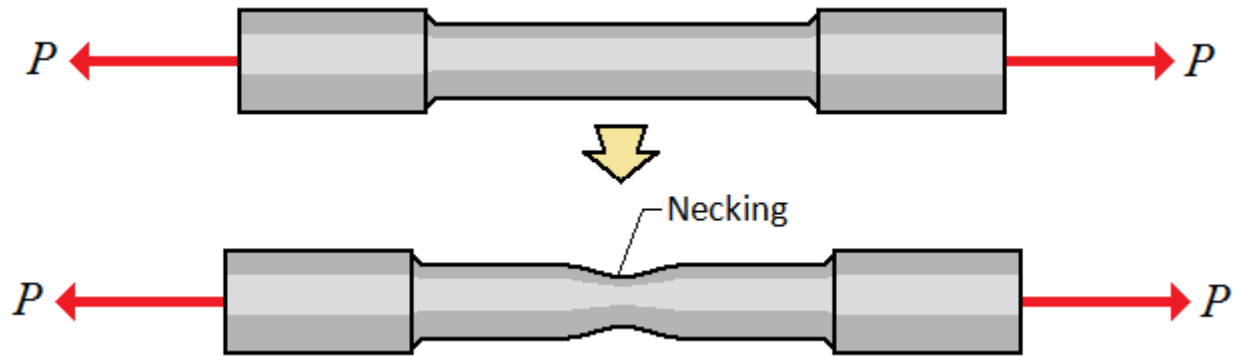


Figure 3: Sample experiencing necking in a tensile test (Roylance, 01)

2.5 Testing and Harvesting Methods

There are several modes of testing that can be used when working with piezoelectric materials. These modes depend on two things, the direction of the force, and the direction of the flow of voltage. These modes give you a standard XYZ plane to show these directions however, instead of XYZ the modes use 123 respectively. The two most common mode types are 31 and 33. 31 is when the force of the mechanical input is in the 1 direction and the circuit path is in the 3 direction which would be common in tensile testing.

33 mode is used with cantilever beam designs (Erturk, 09) because the direction of the force is parallel to the direction of the circuit. For this research the 31 method is used along with a standard tensile test. While the circuit is connected in the 3 direction the force is applied in the 1 direction. Which is shown in *figure 4*. The d33 applications are more suited for cantilever beam testing. The research utilizes the d31 method of harvest and the d31 method for wave data acquisition. To achieve the desired frequency the 810 MTS tensile machine is used. Using a tensile load with the frequency provides more output and accurate results. The d31 method is also used to send a receive signal through the material to evaluate material properties.

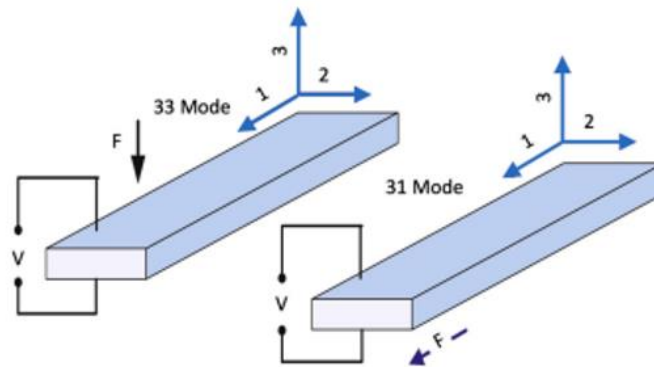


Figure 4: Modes of Energy Harvesting

2.6 Circuit Design

Circuit design is very important in this research due to the low amounts voltage that is produced. An efficient circuit is a key part of seeing results. A big area of energy harvesting right now is circuit design and how to design circuits that are more efficient. In the case of this research a circuit that is inefficient may yield voltage that is too low to be measured or too low to so significant results. Circuits that have been examined as more efficient are different and diverse, but most share some common components such as a whetstone bridge and a capacitor as seen in *figure 5 and 6* (Covaci, 20; Kim, 11). Typical systems that produce small amounts of voltage, due to size or area of PZT zone.

The use of a whetstone bridge to rectify the signal of the electrical output to detect the power levels more accurately. These systems also use a capacitor to store charge and then release the charge on a time interval to decrease the frequency of the results but increase the size of the results (Yang, 20). *Figure 8* shows a model of the cantilever beam setup. The electrical circuit set up is the same for both concepts.

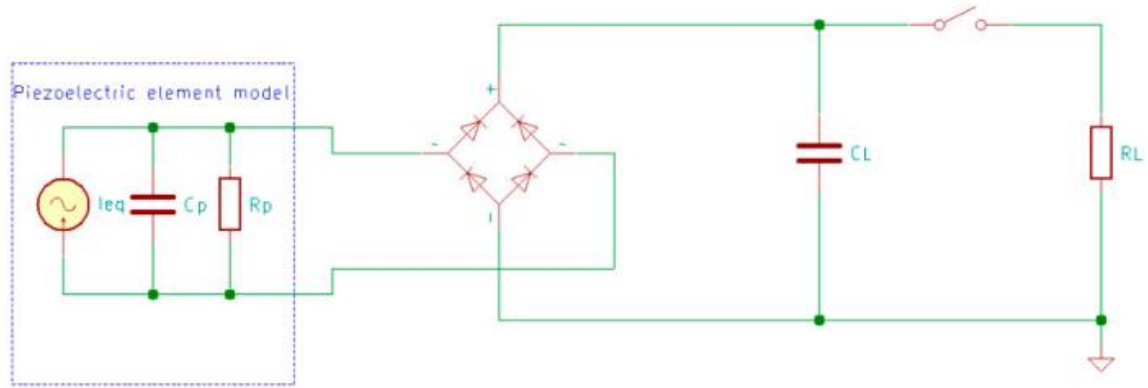


Figure 5: Option 1 for Circuit Design (Covaci, 20)

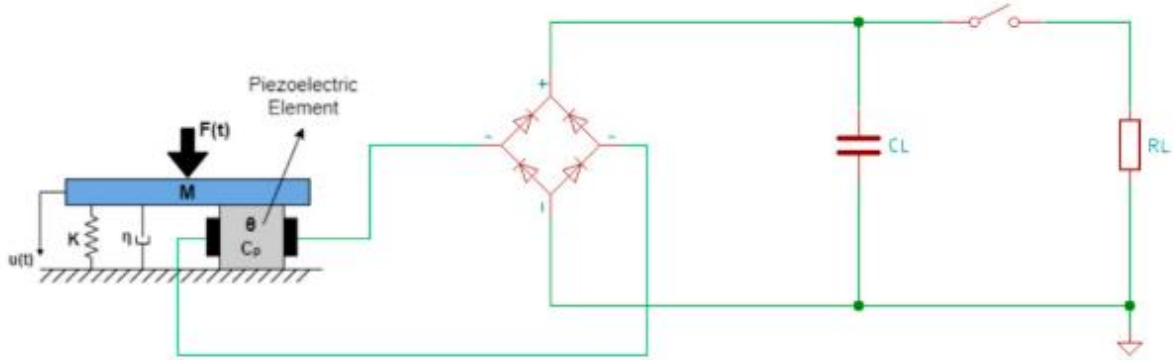


Figure 6: Option 1 Circuit Design with Cantilever Beam Model (Covaci, 20)

Typical PZT output AC current. Some studies have looked at the rectification of AC to DC. These studies found that power extraction depends on the input vibration characteristics, generator mass, electrical load, frequency, and damping ratio (Shu, 06). The effects of this study are useful in designing a circuit for this research that is useful and efficiently harvest the energy for the data analysis. The circuits in *figure 7 and 8* show circuits that have been improved to increase the efficiency of the electrical output. A larger and

more efficient electrical output is useful in measuring the electrical output in experimentation and eliminates the need for more precise tools and equipment.

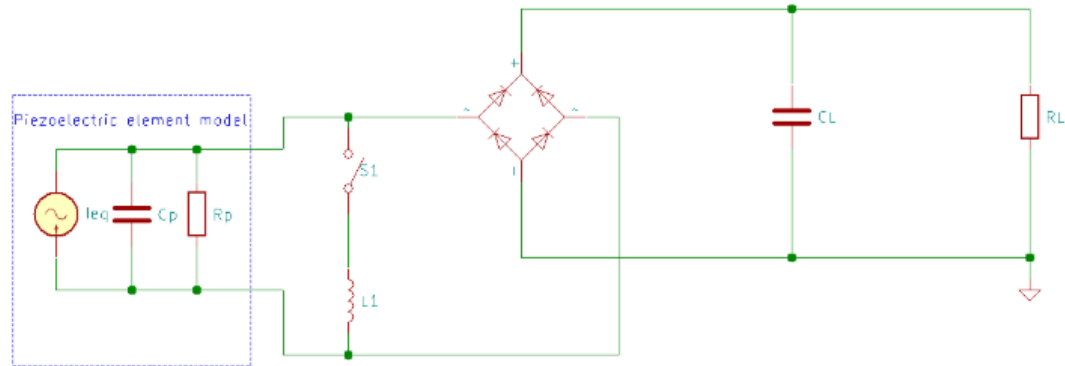


Figure 7: Option 3 for Circuit Design with Rectification (Covaci, 20)

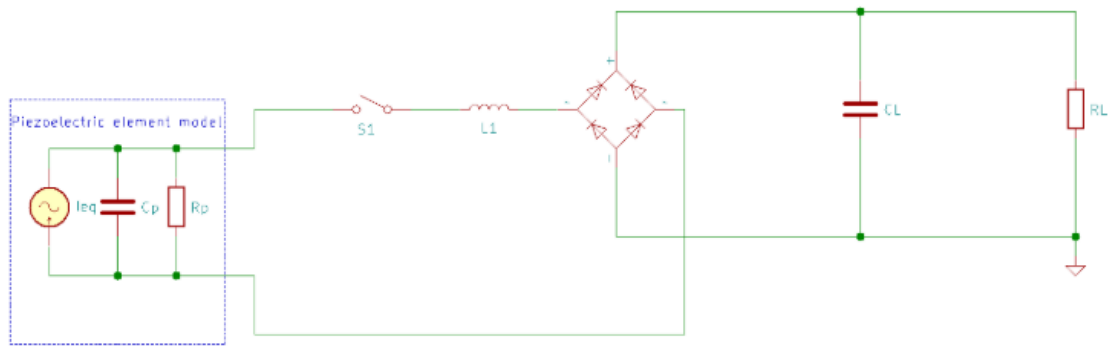


Figure 8: Option 3 with further Rectification to Increase Efficiency (Covaci, 20)

There are methods that are used to increase the performance of piezoelectric energy harvesting circuits. These methods are more recently developed compared to some older circuit designs that have been reviewed. The biggest areas of improvement have been amplification techniques, resonance tuning methods and nonlinear oscillations (Yildirim, 17,1). Some of these methods were very effective in increasing the energy output of the piezoelectric materials.

Mechanical amplifiers were one technique that increases the mass displacement, power output, operating frequency, and works well in low frequency environments. The main disadvantage of this method

is the increased amount of space needed to implement this technique (Yildirim, 17, 38). Given that the amount of space in this research is not a major issue mechanical amplifiers are beneficial in amplifying the output even more to make the measurement of the voltage easier.

Frequency up conversion was also beneficial in this study and works well with MEMS devices and low frequency environments. Hybrid systems were also studied to look at the advantages and disadvantages. Some of the main advantages were increased power output, and broader operating frequency. The disadvantage of this method is the increased complexity of the circuit design (Yildirim, 17, 38).

These methods are useful in amplifying smaller frequency systems. This is due to the fact that larger systems have increased the output of electricity and are trying to increase. These improvements are very useful in this research due to the small voltages that are extracted due to the small size of the piezoelectric material. Issues like space and circuit design are unimportant if those methods are chosen for use due to limited restrictions on space.

These circuits were analyzed to compare with the built in components of the function generator and oscilloscope used in the study. These effect circuits have similar components to the tools used in this study and the collection efficiency of these tools can be verified.

2.7 Internal Stress Relaxation

The internal stresses of the material are one aspect that is studied due to controversy in the field of material science and energy harvesting. Research has been conducted that shows techniques for relieving the internal stresses in composite material using ultra-sonic techniques to monitor the stresses during fatigue cycles. The techniques used in the study use lamb waves and scanning acoustic microscope to monitor the stress relaxation in the composite materials (Saadatzi, 19). This relates to the research through the hypothesis and can be utilized this tool for any other materials with similar results to the composite materials.

CHAPTER 3

METHODOLOGY

3.1 Overview of Methodology

The overview of the research includes several distinct parts. The methodology involves numerical and experimental are adopted to analysis previous work, simulate the problem with FEA, and conduct experimentation to generate meaningful data. The data generated is used to look at multiple properties of the material. The methodology analyzes previous work and established methods that are applicable in the field of composites and apply the same testing to verify if the results are transferable to isotropic materials. The testing conducted actively harvests energy from a specimen of aluminum 6061 while the specimen is undergoing a fatigue load. While not underload the specimen is placed in a relaxed state and a signal is sent a receive by piezoelectric materials to look at changes in properties such as time, frequency, and velocity.

3.2 Simulation Work

A key part of this research is background testing using simulations. An abundant amount of work has been conducted, both with simulations and experimentation, using cantilever beams in a 33-mode testing setup, where the force is in the same direction as the circuit flow (Elvin, 08; Lerch, 08; Staworko, 08). Some research has been conducted using the tensile test and the 31-mode method, where the force and circuit flow are perpendicular to each other. This form of testing is not as common and does not have as much background information. As a result, the current method of piezoelectric simulation is remodeled to fit the necessary standards for tensile testing (Popovici, 08; Farshchi, 19). The simulation side of this research is used to find several things. The first is to look at the correlation of electrical output while manually changing the yield strength of the material. The second is to look at the effect of frequency on electrical output, and the third is to look at the displacements effect on the electrical output. The experimental side of this research is to look at these three things in the reverse direction to determine how harvesting electrical energy affects the material structure.

3.2.1 COMSOL Simulation

Simulations was first conducted in COMSOL to apply forces and validate the areas of the test specimen that undergo the highest points of stress. The model is designed in SolidWorks and then imported into COMSOL Multiphysics (version 6.1). A fixed boundary condition is applied at one end of the specimen and a force boundary condition is applied at the other end. The simulation runs as a static structural simulation and a dynamic simulation with the same set up for both (Meade, 23).

3.2.2 Simulated Force Calculations

The force is calculated using the stress-strain curve of aluminum. The average yield point is used from the stress-strain curve to find the 50% point of the curve and the force that is needed. This 50% point is used in calculating the force by multiplying 50% of the yield point by the cross-sectional area of the testing region of the specimen (Brown, 41). The force point is shown in *figure 9* and the force applied over time is shown in *figure 10*.

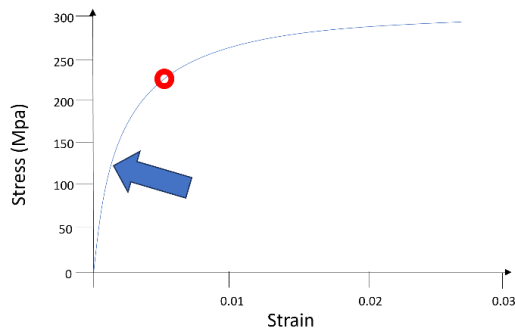


Figure 9: S-S curve for Aluminum

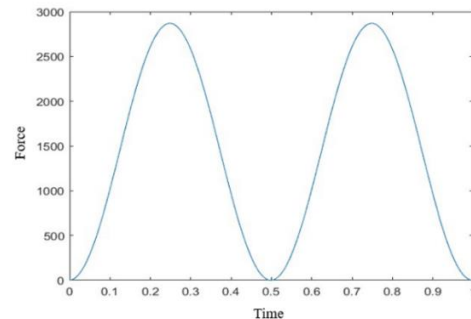


Figure 10: Force Vs. Time from Force Calculations

3.2.3 Simulations with COMSOL

COMSOL was used for the simulations due to the piezoelectric tools available through the base software. COMSOL also had previous examples of an energy harvesting setup using a cantilever beam with

a mass fixed at the end. This simulation is helpful in determining where the PZT plates should be attached and in which orientation closed the circuit to yield results. The simulation setup is shown in *figure 11*.

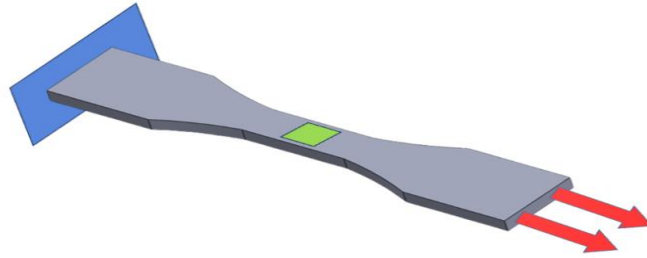


Figure 11: Simulation Model with Fixed End, Force Direction, and PZT

The cantilever beam set up is be modified to fit the design parameters and adjusted to use a 31-mode compared to the basic 33-mode. COMSOL has many features and more customizable settings that fit the parameters needed for the design experiment (Meade, 23).

3.2.4 Simulation Setup in COMSOL

The testing parameter uses ASTM standard dog bone testing shape, see *figure 12*, to attach the PZT to and used in a tensile testing apparatus. The testing is based on the standard in the American Society for Testing and Materials journal (Dreyfuss, 03). This journal gives dimension and ratios that were used to develop and design a specific test specimen for the tensile testing in this research.

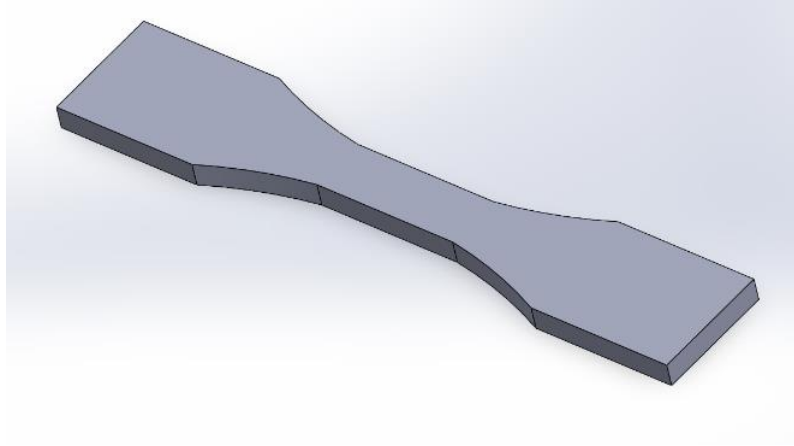


Figure 12: Test Specimen Used in Simulation

The simulation used a tensile test as the base for the set up. The specimen is uploaded to COMSOL from SolidWorks and the corner of the test specimen was centered at the origin of the 3-D plane. The PZT is modeled using COMSOL and aligned in the center region of the testing area of the specimen.

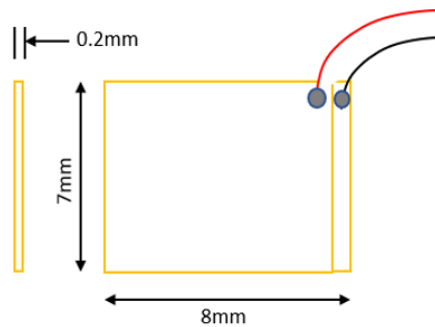


Figure 13: Dimensions of PZT used for Simulation and Experimentation

After the dimensions and geometry of the specimen and piezoelectric material were verified and spatially correct the forces are applied at both ends of the specimen. A displacement of 1mm is applied at one end and a fixed end at the other to simulate the tensile test. The final part of the simulation setup in COMSOL is applying the piezoelectric faces and circuit parameter to create a closed circuit to measure the electrical output. To make the piezoelectric element work the plate must be identified as piezoelectric material. After the piezoelectric material is identified a positive side and a ground side must also be

identified. The ground is assigned to the side of the PZT that encounters the testing specimen, while the positive is assigned to the side facing away from the specimen. This is assigned on both PZT plates in the simulation. The result output is the last part of the simulation setup. After the setup is complete the output should be assigned to generate a graph of electrical output verses frequency on a range for 2Hz to 200Hz. This frequency range is only for the simulation aspect of this research (Meade, 23).

3.2.5 Changing Parameters of the Simulation

To determine the most effective way to harvest the energy and see the results, the same experiment is conducted with a 1.5mm displacement. The 50% increase in displacement is used to show if the electrical output in the simulations is linear with the displacement or if the displacement is exponential (Meade, 23).

The second parameter that is changed is the yield strength of the material. The yield strength is manually lowered in the material properties section of COMSOL. The material starts off at 100% strength, then lowered to 80% and 50%. Nothing is tested below 50% due to the fluctuations that take place in material properties after the 50% point has been reached.

3.2.6 Simulations with Different Materials

After the initial simulation of aluminum 6061 the same test is conducted on two other materials that have properties that differ from aluminum. The first material is copper, and the second material is structural steel. The exact same test is conducted to determine if the result of the aluminum matches the results of the copper and structural steel. If the results of these two new materials are the same as the aluminum, then it can be inferred that the experimental result from the aluminum follows the same pattern with copper and structural steel (Meade, 23).

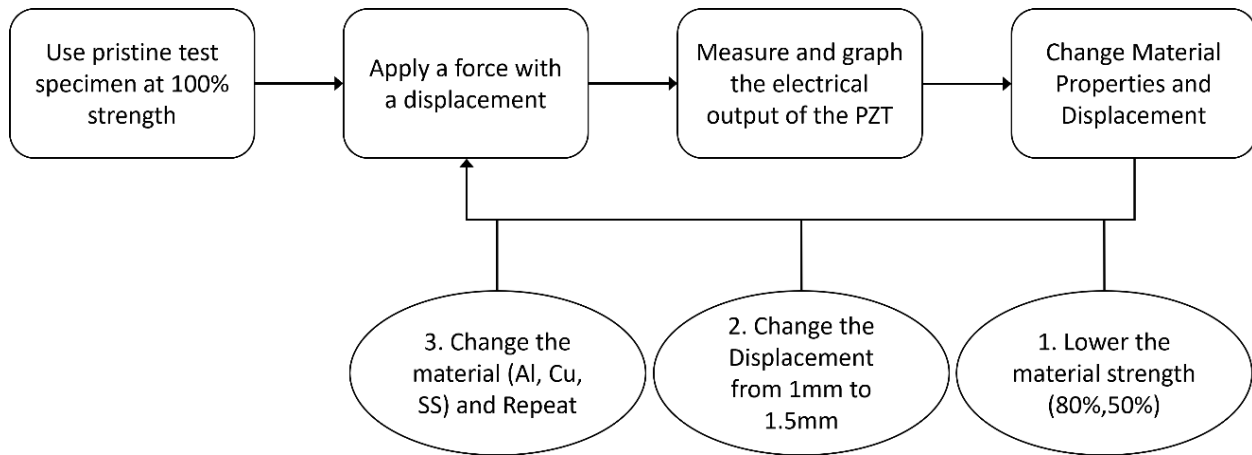


Figure 14: Simulation Flow Chart

3.3 Previous Testing Method Types

The testing parameters for this research were chosen based on data from several previous research projects. The first related to material strength and which values were chosen. Material properties are a very important part of this research project. Looking into material properties a correlation has been made that shows that material properties vary more significantly when a material has reached 50% of its remaining life (Patra, 17) as shown in *figure 15* . This is very important for this study due to the amount of material properties that may change and could affect the data that is yielded. The figure below shows the importance of identifying damage early in the structural materials life cycle.

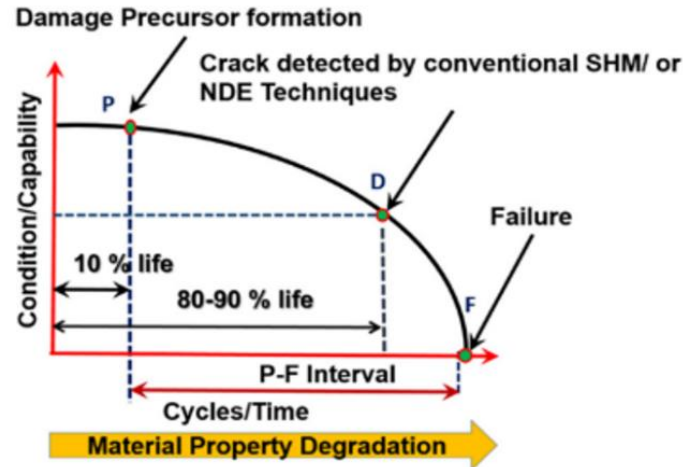


Figure 15: Material Degradation Properties (Patra, 17)

Research has been conducted to show the effects that a relaxation period can have on the number of fatigue cycles. The first test that is used is conducted in this manner. The test applies a predetermined number of cycles at a set frequency based on the total number of fatigue cycles. The cycles are run at the lower volume and then the material is returned to a relaxation state for a set number of hours. The same fatigue cycle is run again and then rested for 2 more full rounds. After these cycles of three fatigue loads and three relaxation periods the sample is broken to observe changes in material properties. An example of the output of this fatigue testing method is shown below.

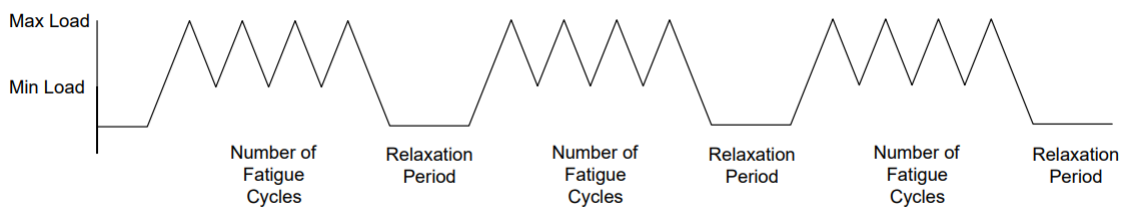


Figure 16: Fatigue Loading with Relaxation Periods

3.4 Material Relaxation Periods with Composite Materials Setup

A similar study was conducted with composite material research that followed the same pattern. Prepared composites were fatigued to introduce damage for a given number of cycles. After the fatigue was applied, the materials were left to rest for at least 8 hours while a pitch and catch was performed every 15 minutes. The results were analyzed and presented to show that the material regained strength as it stayed in recovery. The full strength was obviously not regained but the strength slowly recovered linearly for the first few hours and then plateaued towards the end indicating the max amount of restoration possible from the damage that was induced.

3.5 Materials Relaxation Periods with Composite Materials Analysis

Fast Fourier Transformation, or FFT is a measurement method that converts different signals to frequencies and is useful in providing information about the signal. The use cases for FFT analysis range from a variety of areas. The FFT analysis in this research is used to take the time data from the relaxation periods and convert the data into frequency graphs. The frequency graphs are then be normalized, smoothed, and analyzed for analysis of the harmonic peaks (Mitchell, 1982). Previous studies have shown that after the normalization and FFT analysis the time graph should appear as a frequency graph that has three distinct peaks that can be classified as first, second, and third harmonics. The second and third non-linear harmonics can be expressed as β and γ . The equations for these two values are found below. These formulas and methods were conducted and pulled from a similar study with composites (Patra, 20)

$$\tilde{\beta} = \frac{A_2}{A_1^2} \propto \beta x$$

5

$$\tilde{\gamma} = \frac{A_3}{A_1^3} \propto \gamma x^2$$

6

These values can be used to determine several properties of the specimen. The location and shift of the values indicate a change in the strength of the material during the relaxation phases. Previous studies noted that FFT graphs that contained a shift to the left during relaxation phases indicate a restoration of material strength during the relaxation period (Patra, 20)

3.6 Material Properties Table for Aluminum 6061

Table 1: Material Properties of Aluminum 6061

Hardness, Brinell	95	95
Hardness, Knoop	120	120
Hardness, Rockwell A	40	40
Hardness, Rockwell B	60	60
Hardness, Vickers	107	107
Tensile Strength, Ultimate	310 MPa	45000 psi
Tensile Strength, Yield	276 MPa	40000 psi
Modulus of Elasticity	68.9 GPa	10000 ksi
Notched Tensile Strength	324 MPa	47000 psi
Ultimate Bearing Strength	607 MPa	88000 psi
Bearing Yield Strength	386 MPa	56000 psi
Poissons Ratio	0.33	0.33
Fatigue Strength	96.5 MPa	14000 psi
Fracture Toughness	29.0 MPa-m ^{1/2}	26.4 ksi-in ^{1/2}
Machinability	50%	50%

Shear Modulus	26.0 GPa	3770 ksi
Shear Strength	207 MPa	30000 psi
Electrical Resistivity	0.00000399 ohm-cm	0.00000399 ohm-cm

3.7 Experimental Tensile Testing

The experimental side of this research is completed in a reverse method to the simulation. The first step is to determine a base line for the aluminum specimens that is used. For this baseline two tests are performed, the tensile and the fatigue test (LaVan, 99; Lee, 05; Weibull, 13). To ensure perfectly accurate tensile test a major assumption is that the specimen is loaded perfectly straight to prevent damage from bending. The guide in figure 17 was used to ensure the specimen was loaded perfectly parallel to the machine and loaded the same way for all specimens.

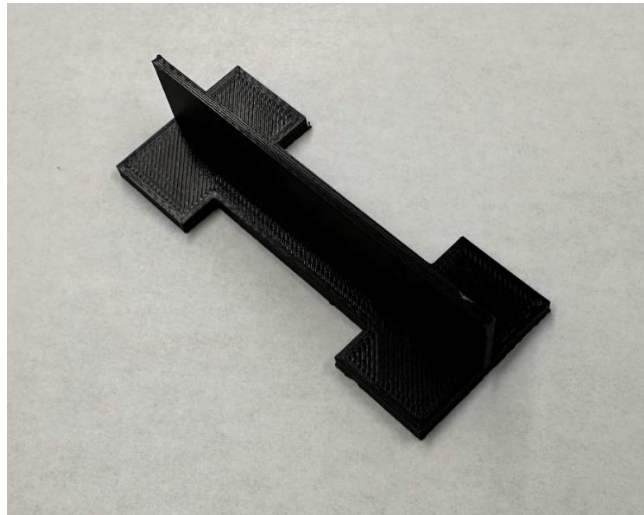


Figure 17: Tensile Alignment Tool

3.7.1 Test Specimen Dimensions

The test specimen dimensions are listed in the figure and table below. The specimen was designed to follow ASTM standard E466-15-5.2.2.1. This standard outlines the dimension parameters in relation to the

thickness of the material. The design of the specimen is made specifically for fatigue testing and works to focus the force within the confines of the gauge length of the specimen.

Table 2: ASTM Dog bone Dimensions for Testing

Dimension	Value (mm)
Length	90
Width	16
Thickness	3.175
Gauge Length	20
Gauge Width	7.5
Radius	60

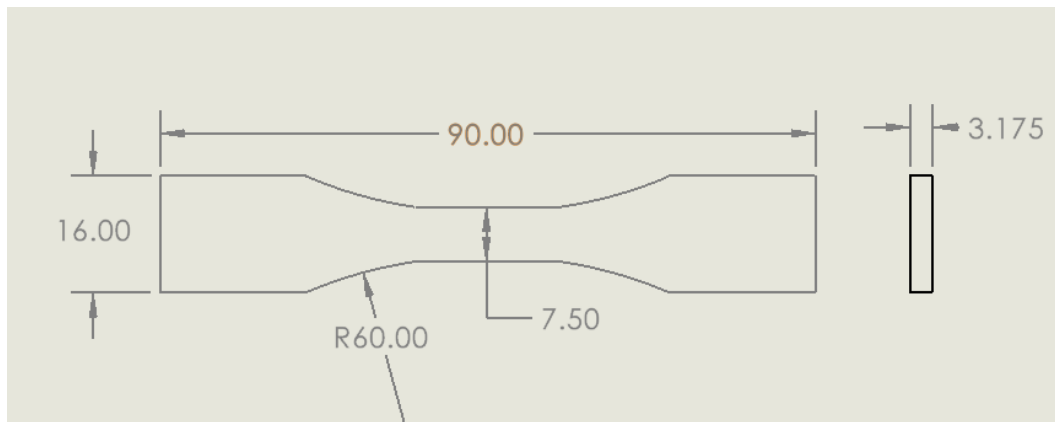


Figure 18: Dimensions of the Test Specimen

3.7.2 Energy Harvesting Plate Setup

The location of the plate is at the center of the gauge length. The plates are placed on both sides of the material to ensure symmetry in the testing and to ensure that the max amount of energy is taken from the material. The plates are applied with J-B Clear Weld Epoxy to ensure that the plate do not come loose during testing. The back location of the plate can be seen in the figure below. The plates were aligned to be

at the same location on either side of the specimen and to orient the wires in the proper direction. The square PZT dimensions are listed above in figure 13.

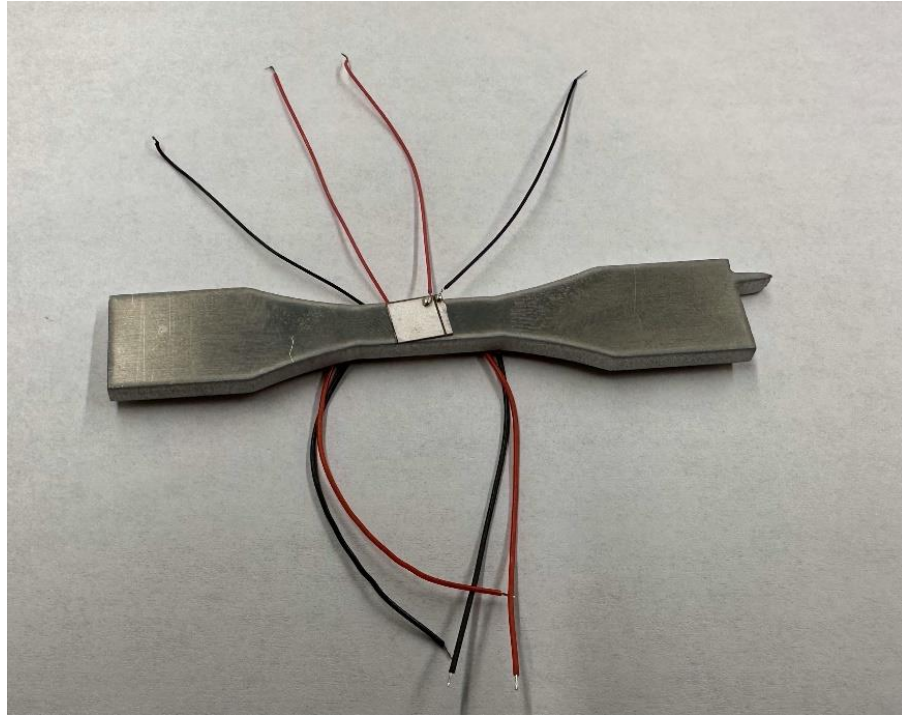


Figure 19: Square PZT Location

3.7.3 PZT Sensor Dimensions

The round PZTs serve a different purpose than the square PZTs. These PZTs are used to send a signal in one side of the material and another PZT is used to capture that signal due to the effects of the piezoelectric effect and coupling. The PZTs are also from STEMiNC and have a frequency of 450 KHz. The actual PZT can be seen below in figure 20. The dimensions of the PZT can also be seen below and include the thickness of the PZT and the diameter of the PZT in figure 20.

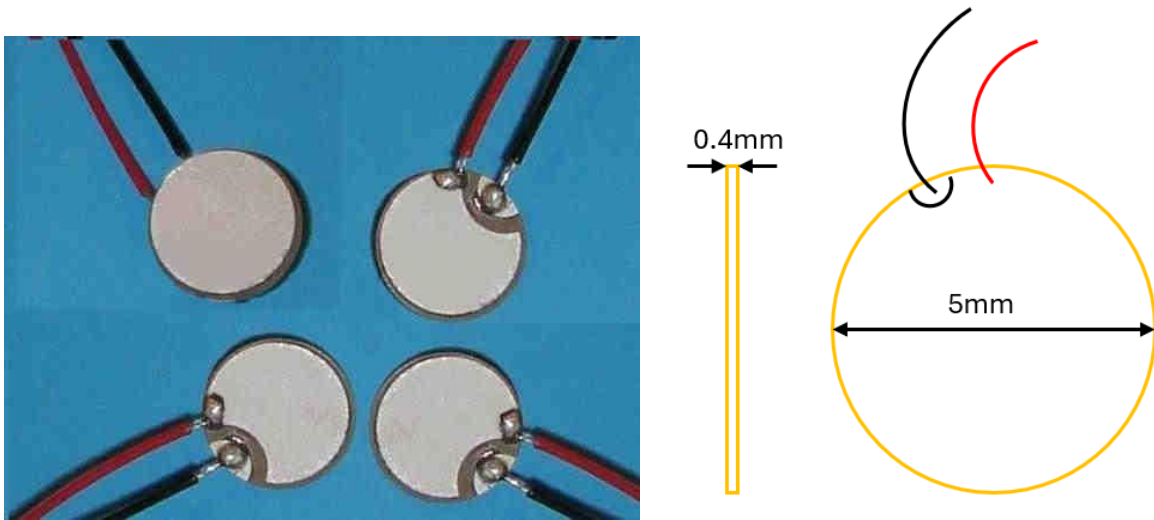


Figure 20: Round PZT for Pitch and Catch and Dimensions

3.7.4 Round PZT Location

The round PZT location was attached with the same epoxy used to secure the square PZTs. The location of all of the PZTs was on the edges of the gauge length. The distance between the center of the PZTs was measured and recorded for every sample and this distance was used to calculate the material velocity of the signal through the material.

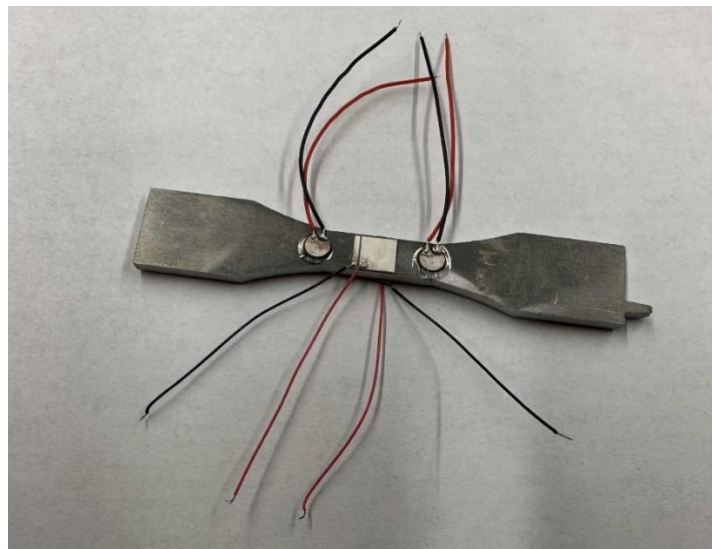


Figure 21: Round PZT Location Compared to Square PZT Location

3.7.5 Equipment Used During Testing

A full picture of the setup during an energy harvesting period can be found below. The computer running the MATLAB code is in the middle along with the relaxation period specimen holding apparatus. The function generator is on the right side and the oscilloscope is on the left side.



Figure 22: Full Circuit Setup

The function generator used can be seen below. It is the Tektronix AFG 31000. The only channel used was the first channel. This channel was used to generate an arbitrary burst wave with a peak-to-peak voltage of 10mV. The signal was split using a splitter to ensure that the signal was being sent out at the same time to ensure that the velocity value would not be compromised due to the small-time scale.



Figure 23: Function Generator Used During Data Collection

The oscilloscope used is picture below. This model is the Tektronix 3 series. This was one of the most crucial pieces for collecting the data. Three of the four channels were used. The first channel received the signal from that passed through the material. The second channel received the signal directly. The third channel was connected in parallel to the square PZT and used to measure the amount of energy harvested from the material. The first and second channels are compared to determine the time that both signals got there. The difference in the time the signals were received can be used in conjunction with the distance between the round PZTs to find the velocity of the signal through the material.



Figure 24: Oscilloscope Used for Data Collection

The final piece of equipment is the 810 MTS hydraulic 20-kip tensile machine. The hydraulic tensile machine is used to apply fatigue loads to the material. This machine was also used to conduct tensile test and fatigue test to achieve the baseline values for comparison. The 810 MTS can be seen below.



Figure 25: 810 MTS for Fatigue and Tensile Loading

3.7.6 Reason for Baseline Fatigue Test

Multiple fatigue tests are conducted to establish a temporary baseline that is used to determine the number of cycles used when damage has been introduced in the material. The number of cycles is significantly lowered from the lowest value to avoid prematurely breaking the specimen, unless the material has a flaw that is preexisting. An example conducted in a similar study used two hundred and twenty-five thousand total fatigue cycles for harvesting when the aluminum's full life ranged from 1 million to 2 million with the pitch-catch method. This method is one of the methods used in the experimentation (Patra, 20).

3.8 Preliminary Tensile Testing

These tests are repeated at least three times to generate an average stress strain curve of aluminum for the samples. The stress strain curve of aluminum is also used to calculate the forces that are applied while the material is being fatigued. The PZT is also tested to determine if the PZT plate can survive the full test, if the plate needs to be changed at certain intervals throughout, and if the breakdown of the plate could contribute to a decrease in the electrical output due to the atomic structure of the PZT.

3.8.1 Fatigue Force Calculations

The force applied while the material is fatigued is calculated from the Stress-Strain Curve of the baseline aluminum. Using the curve of aluminum shown in *figure 26* the force is calculated at 60% of the ultimate strength of the material. The fatigue reaches 60% at its peak strength and return to 10% to complete one full cycle. The selection of this force range was to keep the fatigue amounts inside of the elastic region of the stress strain curve. This would ensure that the forces could be applied to properly introduce damage into the material without causing major plastic deformation too early in the testing process. This force is applied in separate tests at multiple frequencies that range from 2Hz to 10Hz. Fatigue cycles are just part of the research, and the success of the research is not dependent on fatigue alone. This is just one of the observable outcomes that may or may not provide significant results.

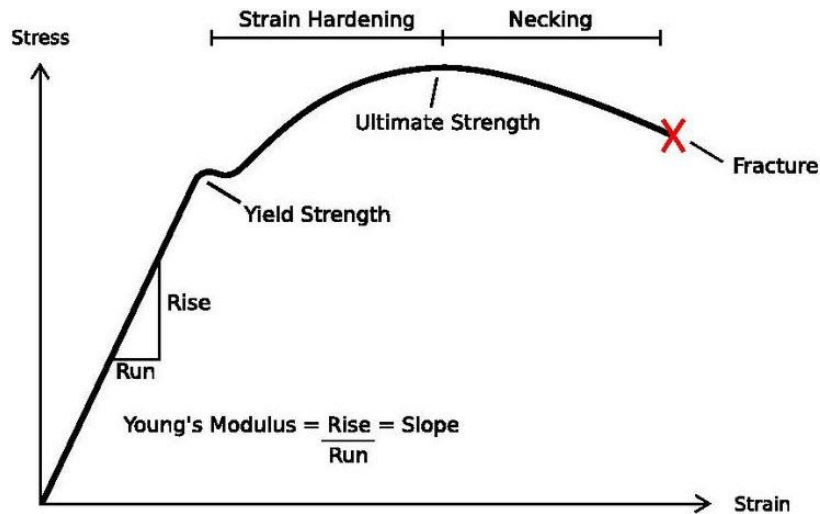


Figure 26: Stress Strain Curve Example for Aluminum

3.9 Energy Harvesting Testing List

The test conducted use the method above with the relaxation period and a test without the relaxation period. A fatigue test is used to excite the piezoelectric material to generate voltage. The fatigue test uses a small value that is significantly under the fatigue test limit. The fatigue is only used to excite the material. After the test is run, the material is broken using a tensile test and a stress strain curve is generated based on the break of the material.

3.9.1 Fatiguing Material with Three Dispersed Relaxation Periods without PZT

The first test is a cycle test that has a period of fatigue followed by a period of rest for at least eight consecutive hours. This process is repeated two more times for a total of three fatigue cycles and three relaxation periods. After this the sample is broken using a tensile test. The specimen is fatigued 35,000 cycles per fatigue section to ensure that damage is introduced in the material. After the three fatigue sections and three relaxation periods the specimen is then left alone for 24 hours and then broken with a standard tensile test.

3.9.2 Fatiguing Material with Three Dispersed Relaxation Periods with PZT

The second test is a repeated test of the first method, but energy is harvested with piezoelectric plates during the fatigue cycles. The specimen is fatigued for 35,000 cycles 5Hz. The number of fatigue cycles is decreased to 30,000 cycles for a set of samples run at 3Hz. This decrease in fatigue is due to issues that occurred with the machine. These issues were corrected but the cycles were lowered to preserve time and possible materials. This fatigue is followed by a period of rest that is at least eight hours long. This is repeated two more times for a total of three fatigue cycles and three relaxation periods. This is followed by a twenty-four-hour relaxation period and then the specimen is broken with a standard tensile test.

3.10 Material Relaxation Pitch and Catch Setup

During the relaxation period the specimen is placed in the holder shown below. The holder was designed to not introduce any external boundary conditions into the material while it was relaxing. The introduction of new forces could have skewed the results, so the holder was designed to combat this issue.

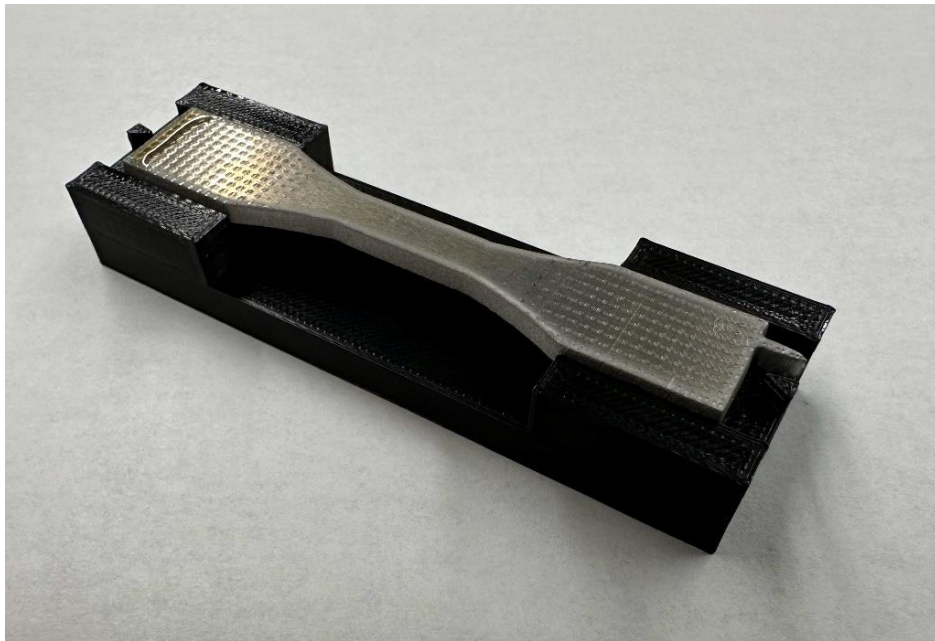


Figure 27: Specimen Holder for Relaxation Periods

The setup for the relaxation period utilized the function generator and the oscilloscope. The function generator utilized a splitter to send a single signal to two different places. The first signal was sent into the materials round PZT. That signal was picked up by the second PZT and sent to the oscilloscope. The second split signal from the function generator was sent to the second channel of the oscilloscope. These values can be used to calculate the velocity through the material and generate a time response graph through the material. The full setup is shown below.



Figure 28: Function Generator and Oscilloscope Setup for Data Collection

3.11 Analysis of Data

Several different properties and tests is used to conclude the final findings. Fatigue test is used to find a baseline of cycles that is significantly lower than the cycles needed to break. For example if five samples are tested and the results of cycles needed to break the samples are 1 million, 2 million, 5 million, 2.5 million, and 800 thousand, then a number that is significantly lower than 800 thousand is used for the total cycles in the test like 200 thousand cycles to make sure that the PZT can be excited without breaking the sample prematurely, unless of course the sample has internal defects that cause early breaking, which is

noted in the results due to the variability of fatigue life of aluminum. A tensile test is used to break the material after the PZT has been excited the specified number of cycles. The baseline tensile tests is compared with the tensile test obtained in the experiment to see if the strength of the material is increased stayed consistent or decreased after energy is harvested to confirm the reverse correlation that was established in simulations mentioned above. The relaxation data is analyzed in two different ways. The first is looking specifically at the velocity of the signal through the material by sending one signal through the material with PZTs and catching the signal with another PZT. This signal is compared with an identical signal sent directly to the oscilloscope. The same signal is sent from one channel of the function generator and uses a splitter to ensure symmetry of the signal due to the small magnitude of the time measurements. The second analysis of the relaxation data utilizes normalization and Fast Fourier Transformation or FFT. The FFT converts the time signal to a frequency signal that should have three distinct peaks. These peaks are the first, second, and third harmonics of the frequency. These are compared through the relaxation process and are expected to rise as the material relaxes. These tests are like other studies conducted in a similar manner with composite materials. The major analysis of the energy that is harvested during the fatigue is analyzed to determine if the energy extracted increases, decreases, or remains the same. The analysis of the energy harvested confirm or disprove the simulations conducted in COMSOL.

3.12 Criteria for Success

The criterion for success is not based on any one outcome of the research. Comparing the samples before and after energy harvesting with stress strain curves obtained through testing is used to determine if the sample increased, decreased, or remained the same before and after energy harvesting. This is the main point of the research. While looking at this correlation other criteria for success is studied to determine if there is any correlation with fatigue cycles and material structure. All together these are used to determine the correlation, if any, between material life and strength and harvesting energy. The outcomes are an increase in strength, a decrease in strength, or a neutral effect on the strength of the material that are confirmed with the tensile test and conducting the experiment multiple times and in multiple configurations.

CHAPTER 4

DATA, RESULT, AND ANALYSIS

4.1 Simulation Data

The simulation was conducted to look at several key factors of the PZT and the material properties. After the simulation was setup the material properties were adjusted while the energy output of the PZTs was recorded. The material strength was adjusted, and the force was then reapplied to measure the output of energy. The results are recorded below for three different isotropic materials, copper, structural steel and aluminum.

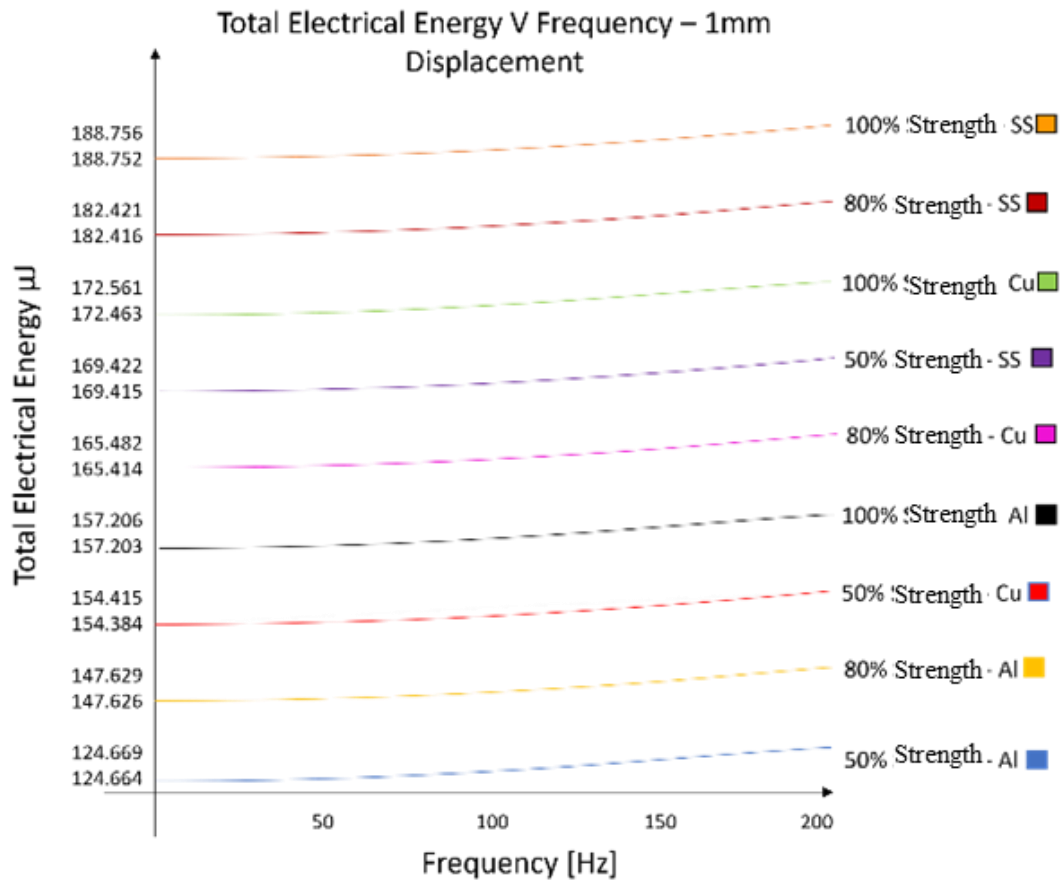


Figure 29: Simulation Data for 1mm Displacement (Meade, 23)

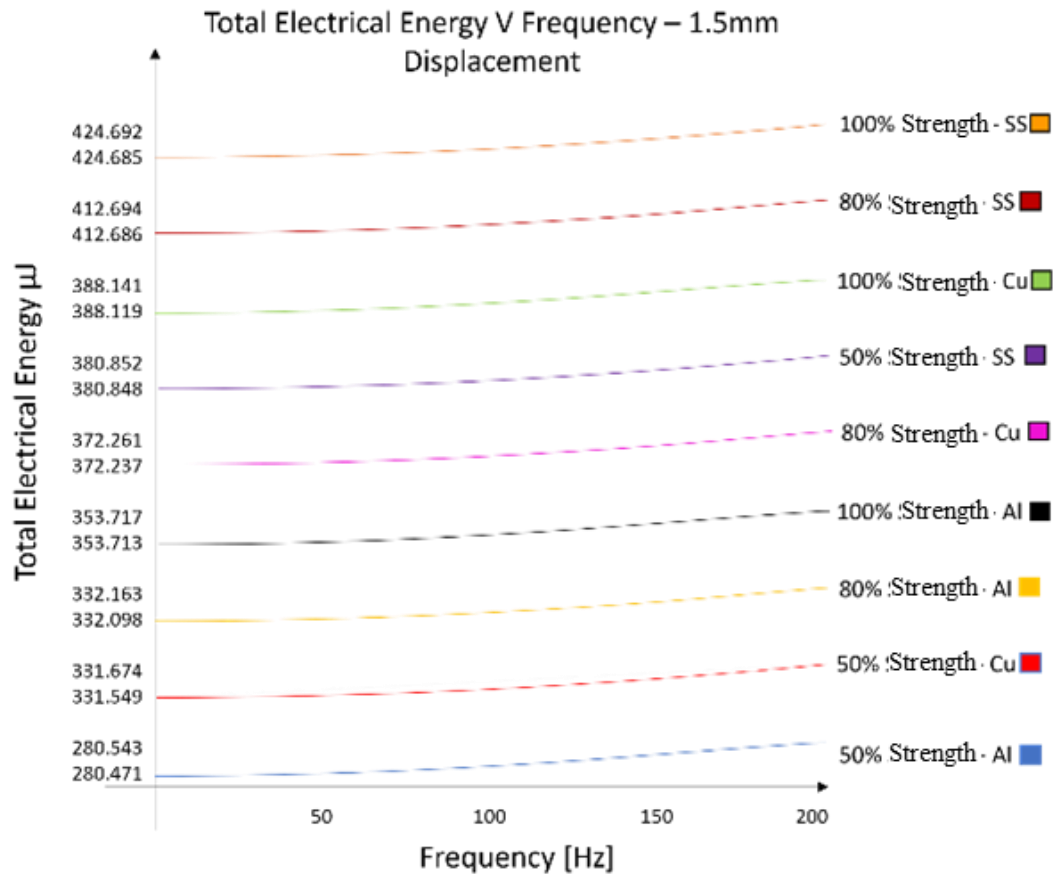


Figure 30: Simulation Data for 1.5mm Displacement (Meade, 23)

The results of the simulation show a solid connection between the amount of energy that can be harvested from a material and the materials remaining strength. This connection plays a crucial role in this research and presents the basis for a connection between these two properties that could go both ways. The amount of energy that can be extracted is affected by the material strength so does harvesting energy affect the material strength? The results show a clear correlation between the material strength and the amount of energy that can be extracted for all three materials. This simulation is significant because it creates the connection between the material properties and the amount of energy that can be harvested. This correlation is worked in the opposite way throughout this study to determine the effects that harvesting energy has on material properties.

4.2 Experimental Data Baseline Testing Results

The first test conducted on the specimens was a tensile test. This tensile data was used to set the baseline parameters for all further tests. A tensile test was conducted three times to determine the average ultimate tensile strength for the material. These tests were conducted on the same machine that the fatigue test was run to ensure that the results are consistent and to avoid possible issues with calibration errors due to machine maintenance.

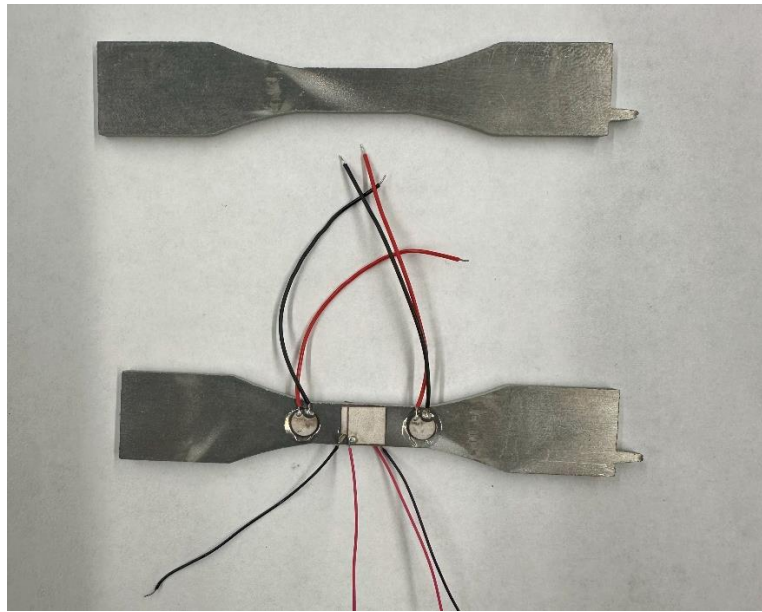


Figure 31: Comparison of Specimens used in Base Test and Actual Experimentation

Three different tensile tests were conducted as a basis for the entire project. The stress-strain curves of these three tests can be seen below in figure 32. The average ultimate tensile strength was used as a basis to determine the amount of force applied at the upper and lower bounds when the material is fatigued. For the upper and lower bounds values of 10% and 60% were used to apply to the material fatigue cycles for 5Hz. 10% and 50% were used to apply the force to the 3Hz set of specimens. The forces that were applied to the upper and lower bounds were 5000N as the upper limit and 1000N as the lower limit. The total cycles and limits were changed for the 3Hz specimen due to premature breaking in the 5Hz testing configuration.

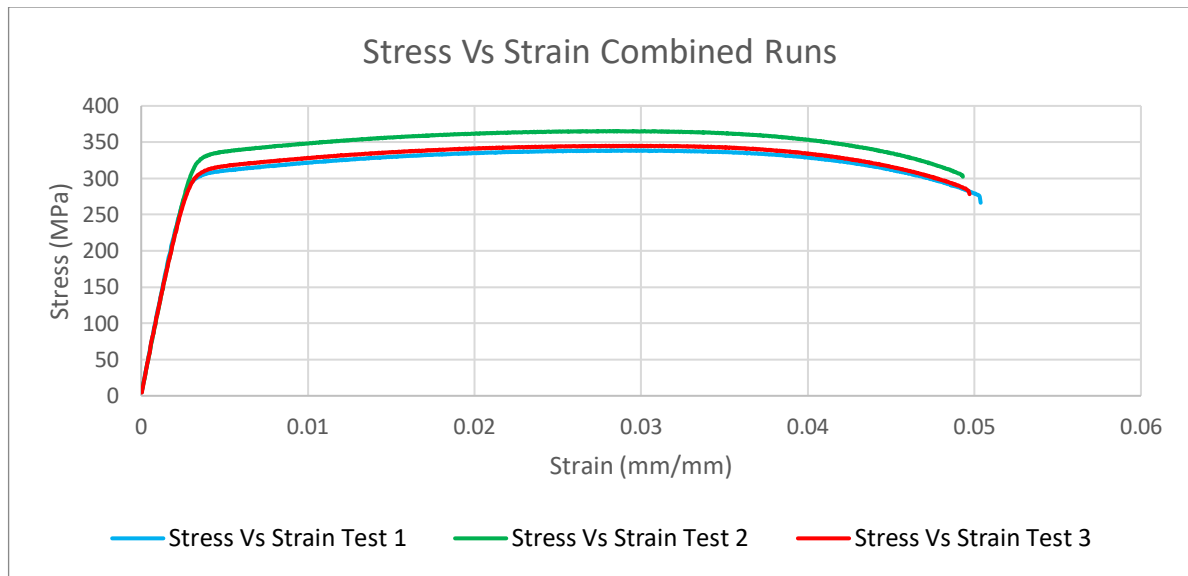


Figure 32: Combine Base Tensile Test Results



Figure 33: Base Tensile Test 1 Break Location



Figure 34: Base Tensile Test 2 Break Location



Figure 35: Base Tensile Test 3 Break Location

The second baseline testing that was done was a full fatigue test on the specimens. These tests are used to find a fatigue value that is enough to induce damage while energy is being harvested but not enough to break the material. Given the variability of the fatigue life of aluminum, 20% of the average fatigue life of three samples was used.

The fatigue life values varied a considerable amount, as expected. A total of 35,000 cycles was close to a value of 20% of the average fatigue life of the samples. Possible error in the fatigue test was considered and the total number lowered slightly under 20% of the average life. This value provides sufficient introduction of damage into the material without significantly increasing the chances that the material breaks in the middle or towards the end of a 30-hour test. The baseline tensile test was conducted on the MTS. The rate of force applied was 2mm/min. The average ultimate strength of the tensile test is used to set the parameters for the test. The fatigue test was conducted with 50% and 10% of the ultimate tensile strength.

4.2.1 Baseline Fatigue Results

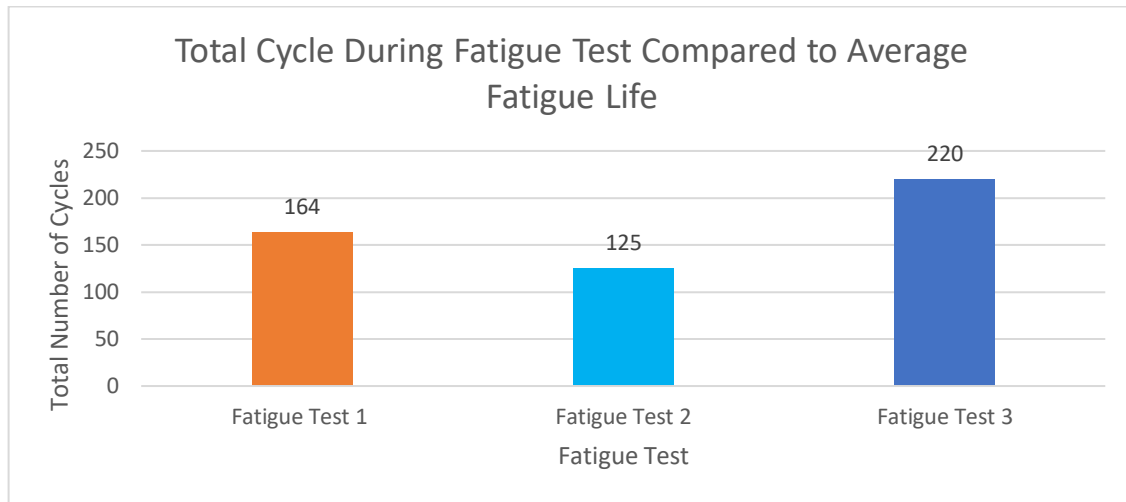


Figure 36: Baseline Fatigue Test Results

The fatigue test was conducted based off values from the tensile baseline test. The parameters were set with a range of 50% to 10% of the ultimate tensile strength. The specimen was loaded, and the test ramped to an initial value of 30% in the middle of the range. The fatigue began and alternated between 50% and 10% at the frequency of 5Hz. The specimen was fatigued until failure occurred.

The results of the test yield a minimum value that is used as a reference. The two total fatigue cycles values fall under this number for the factor of safety. The total number of cycles works out to be in between 30k and 35k cycles. These are the two values used through the testing stages of the research.

The broken fatigue specimens are shown below. The lifespan of aluminum 6061 varies significantly and some issues with slippage during the process required more tests to be conducted to verify the results of the fatigue testing.

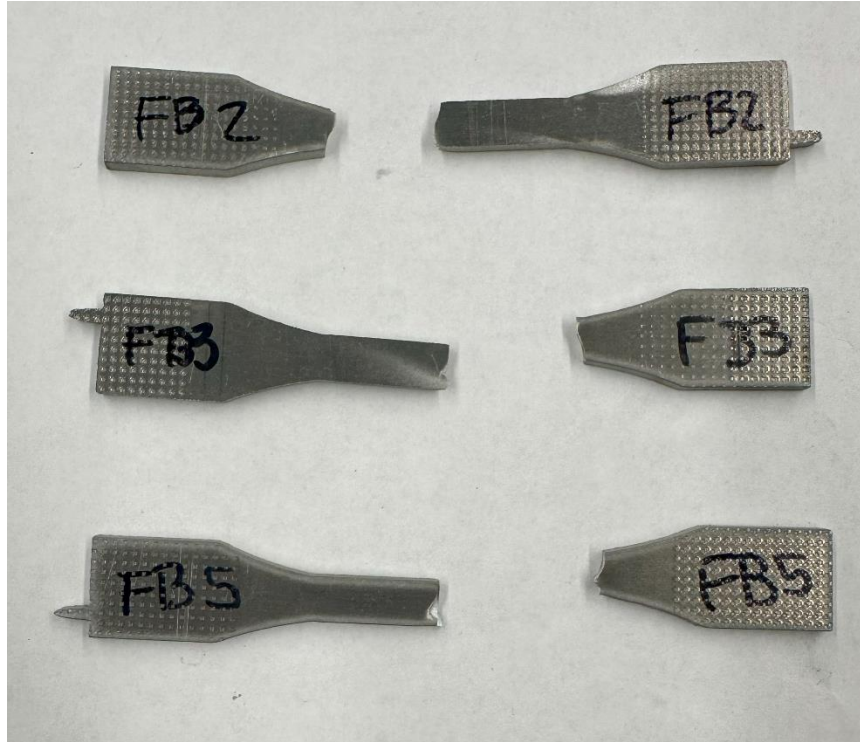


Figure 37: Break Locations of Baseline Fatigue Samples

4.3 Experimental Data

The experimental data section consists of data taken during the fatiguing of the material and the data taken while the data was in the relaxation phase for at least 8 hours. The results from the energy harvesting are displayed to show the amount of energy harvested as the material is fatigued and the strength of the material is decreased during fatiguing. The data during the relaxation period is used to analyze the velocity of a signal through the material and using the time data to convert to frequency and analyze the frequency data. This data is compared with results from a similar study conducted with composite materials (Patra, 20).

4.3.1 Specimen Break Locations

The location of the breaks reveals a lot about the specimen. An ideal break occurs in the center of the gauge length. This area has the highest concentration of stress when the material is under load. The design of these specimens is specifically for fatigue loading. The idea behind the design is for the specimen to

break at a location inside of the gauge length. A break inside the gauge length is considered a successful break even though the ideal break is in the middle under the PZT patch. The location of the PZT patch is in the area that should have the highest amount of stress. Several reasons exist that could cause the specimen to break at other locations in the gauge length. A major and uncontrollable factor are internal imperfections inside of the material. Outside effects on the location of the break can be reliant on the orientation of the specimen in the machine and vibrations through the machine while fatiguing. Specimens that are not loaded straight experience bending forces that begin at one side and propagate through causing a break. The vibrations of the lower clamp of the machine can also contribute to imperfections in the ends of the gauge length instead of the center. The 3Hz specimen were lowered to 30,000 cycles and fatigued between 4500 Newtons and 1000 Newtons. The change in testing parameters was due to premature breaking that occurred in the 3Hz specimen at 35,000. The failure occurred twice, and the test could not be completed in that configuration.

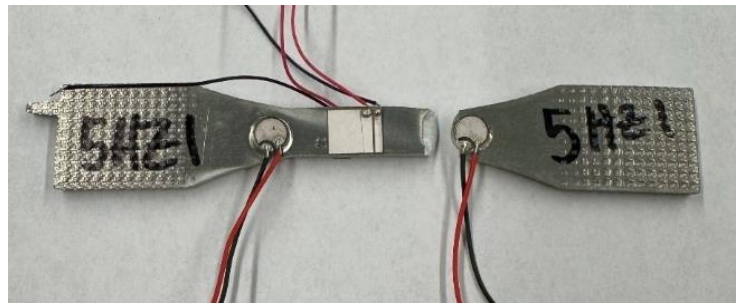


Figure 38: 5Hz Sample 1 Break Location



Figure 39: 5Hz Sample 2 Break Location

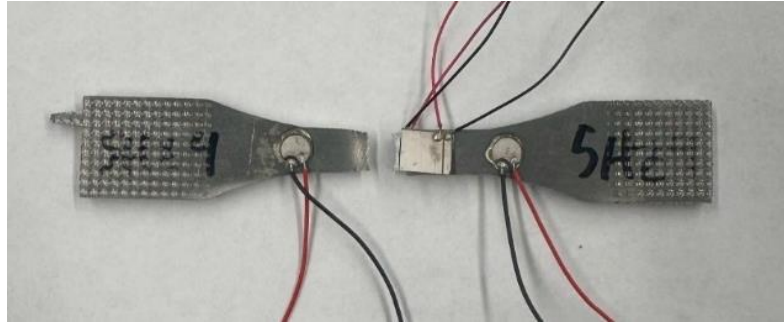


Figure 40: 5Hz Sample 3 Break Location

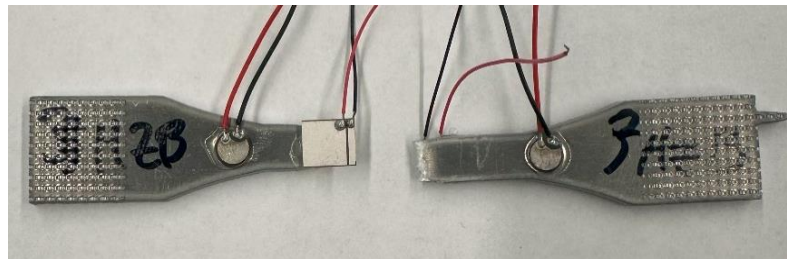


Figure 41: 3Hz Sample 1 Break Location

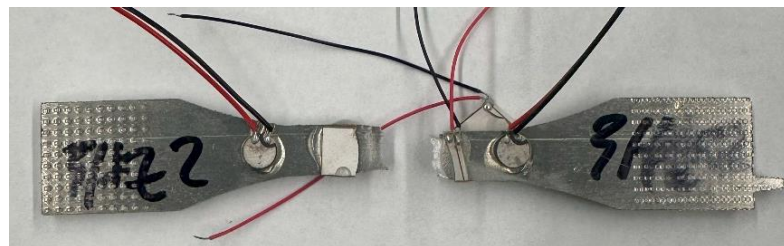


Figure 42: 3Hz Sample 2 Break Location



Figure 43: 3Hz Sample 3 Break Location

4.4 Energy Harvesting Results

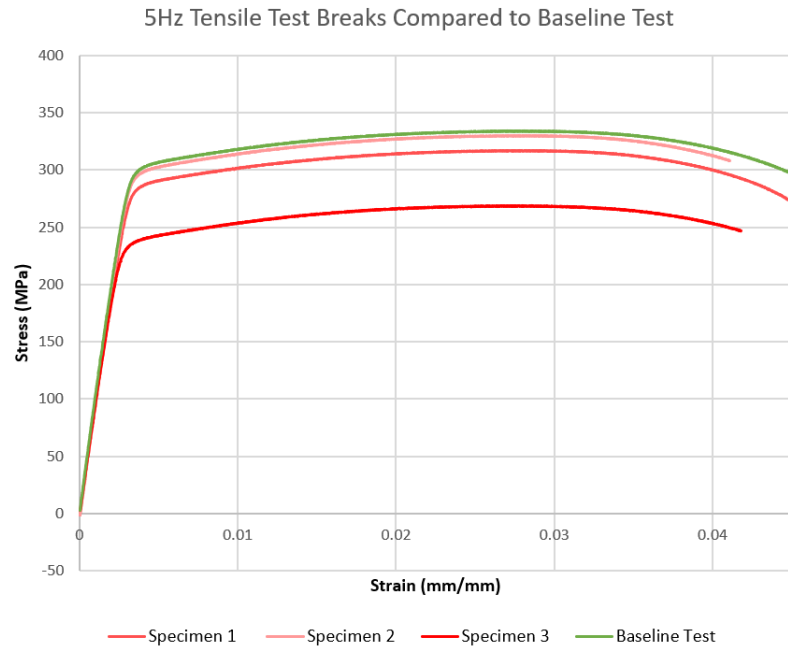


Figure 44: 5Hz Specimen Ultimate Strength vs Baseline Strength

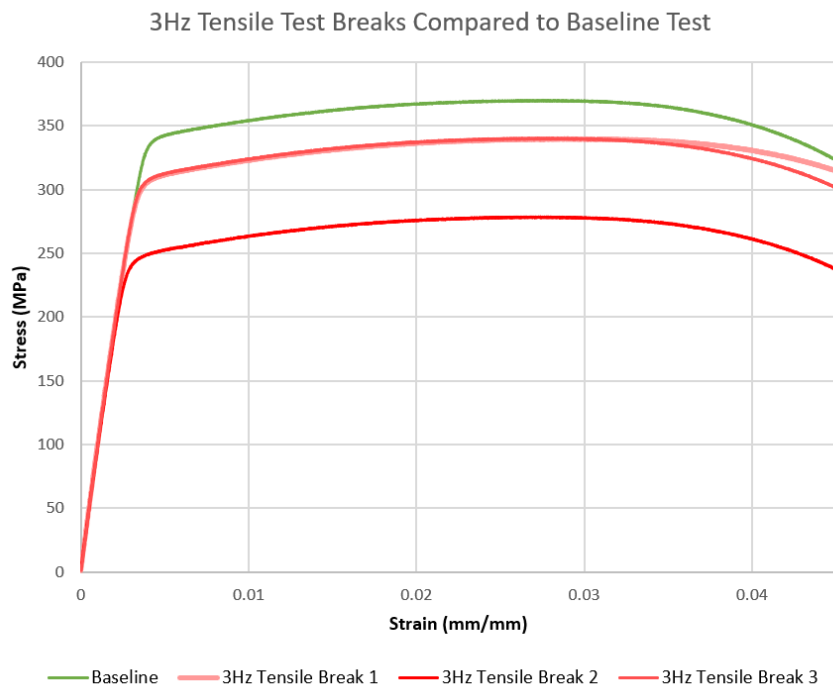


Figure 45: 5Hz Specimen Ultimate Strength vs Baseline Strength

The results of the tensile test break of all three specimen show a clear pattern that the strength of the material is lowered compared to the baseline. Some of the test show a slight change in the strength and other show a more significant change in the amount of strength lost while energy was harvested from the material. The total strength of the samples run at three hertz show an increased level of strength. The increase in strength is due to the test running for a lower number of cycles and at a lower strength range compared to the 5Hz specimens.

4.4.1 Energy Harvesting Results for 3Hz and 5Hz

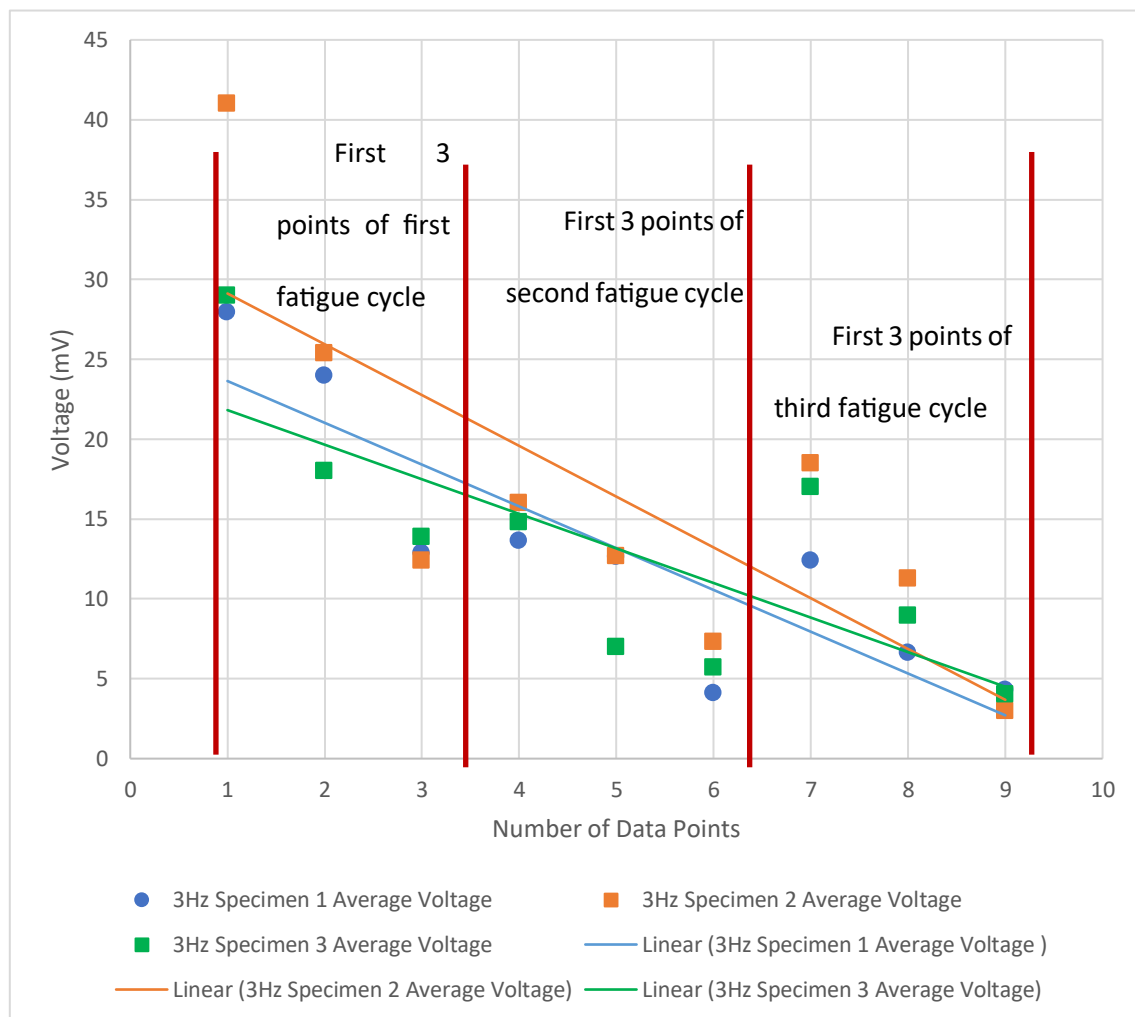


Figure 46: 3Hz Average Voltage Output Trend

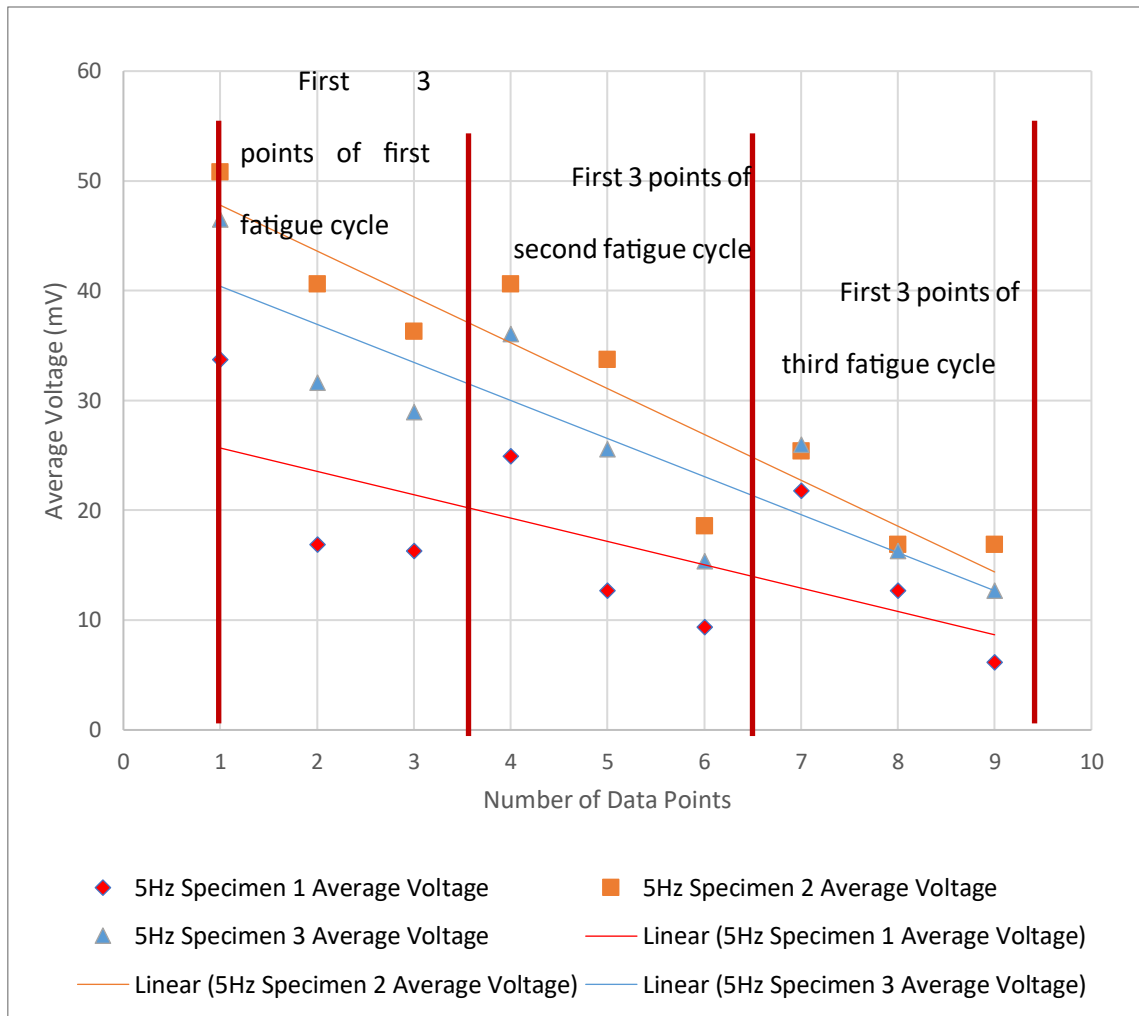


Figure 47: 5Hz Average Voltage Output Trend

Energy was extracted from the material constantly during the fatigue cycles on the material. Due to the size and number of PZTs attached to the material the energy extracted was in the millivolt range. The max average energy output for the 5Hz specimens ranged from 25mV to 50mV. A point was taken from the data at the beginning of the fatigue, the middle of the fatigue, and at the end of the fatigue. These three points, along with the three total fatigue cycles, make nine points. The nine points displayed show a clear downward trend in terms of the output of the energy from the PZT. The points are taken from an AC signal and an instantaneous point is taken to determine the max at each data point. The points are taken from three data points at the beginning, middle, and end of the fatigue cycles and three points are taken in these areas and averaged to generate the data points shown in figure 47 and 46. These results support the initial

simulation that was conducted. The points were taken through varies times in the fatiguing process. A total of 28 points were taken for all fatigue cycles. For 5Hz at 35,000 cycles the points were taken every 4 minutes. The points displayed were taken at the beginning, middle, and end of the range. The total ranged from 0-112 minutes. The time scale for 3Hz at 30,000 cycles was slightly different. Points were taken in 6-minute intervals to ensure collection through the entire fatigue cycle due to the slower introduction of force at 3Hz. The total range was from 0-168 minutes and points were taken from the beginning, middle, and end section of the range.

The results of the 3Hz specimens follow the same pattern as the 5Hz specimen and follow the same concept established in the experiment. The total max average energy output range was 20mV to 40mV which is slightly lower than the 5Hz. This decrease is due to the decrease in frequency, cycles, and total force. The data was analyzed in the same way and a trendline was used to show the correlation between all the points. Both 5Hz and 3Hz specimen show the same pattern and support the simulation. As the material strength decreases the amount of energy extracted decreases.

4.5 Material Relaxation Results

The material relaxation shows a lot of information in two major areas. The nonlinear FFT results and the velocity material properties. The relaxation was conducted, and the results were compared throughout all relaxation periods and comparisons were made at the start and end of the relaxation period for each one of the relaxation periods. The second harmonic or beta values were also compared to see the correlation between the beta values and the time during all three relaxation periods. The values were also compared at the start and end of each relaxation period.

4.5.1 FFT Results – 5Hz

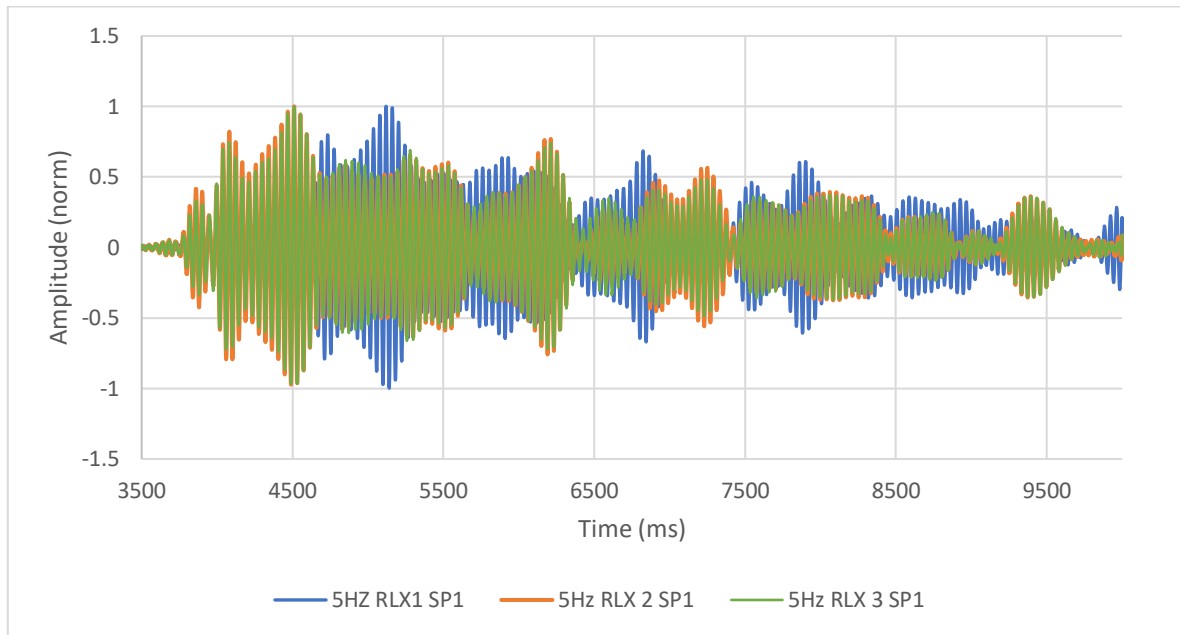


Figure 48: 5Hz Sp1 Time Series

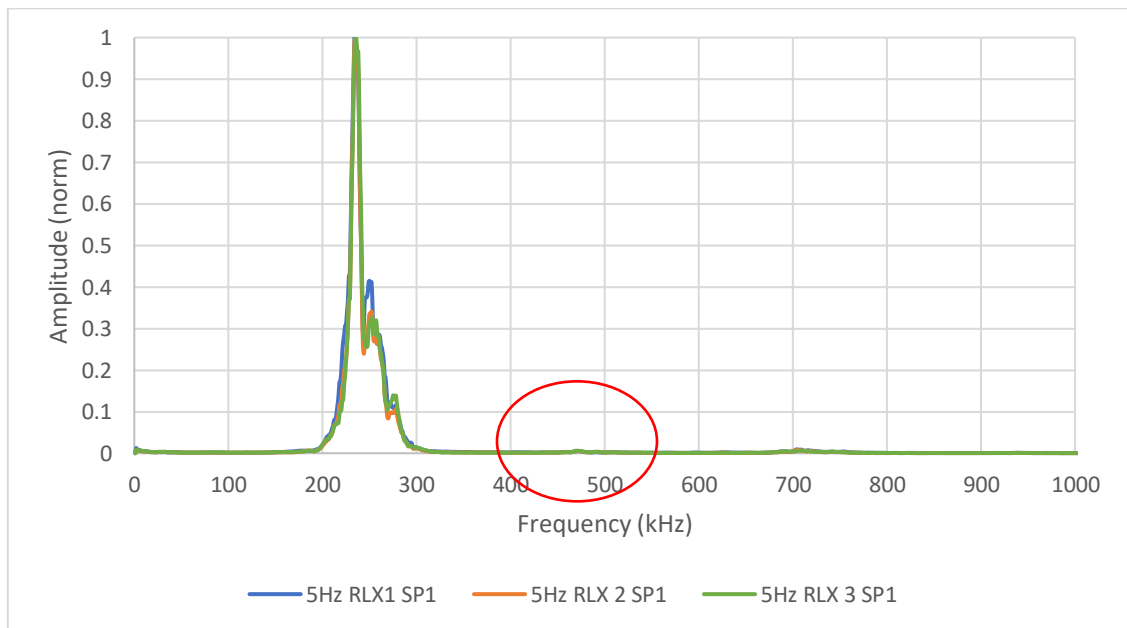


Figure 49: 5Hz Sp1 FFT Full View

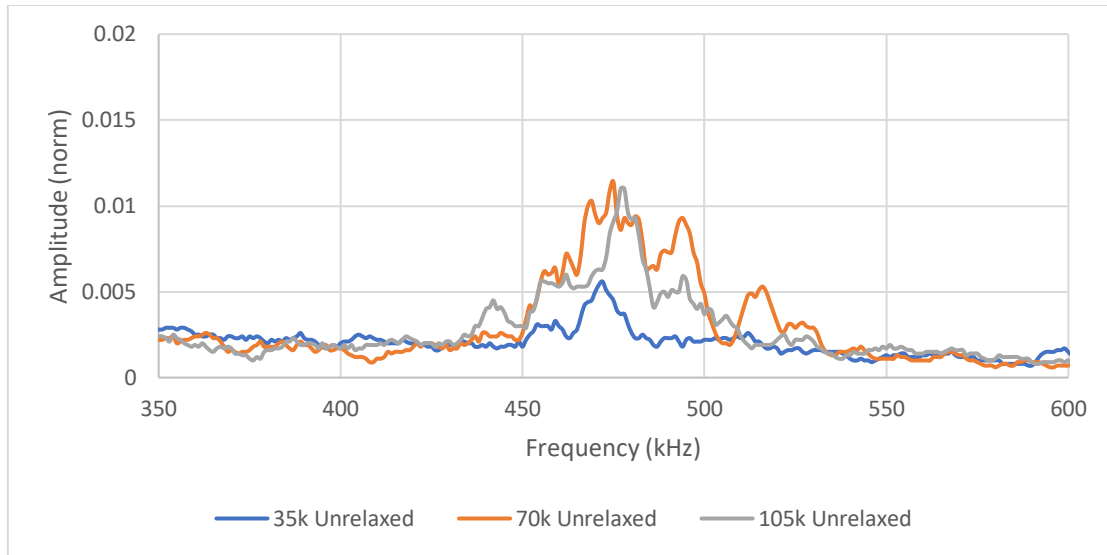


Figure 50: FFT Analysis of 5Hz Specimen 1

The FFT results show that in all relaxation periods of the specimen the first, second, and third harmonics at the beginning of the relaxation period were in a similar and expected position. The first harmonics peak reached a frequency in the range of 200Hz to 300Hz. Due to the placement of this point previous studies have shown the expected values of the second and third harmonic would double and triple respectively. The graphs for all three show similar points that follow similar patterns of previous research.

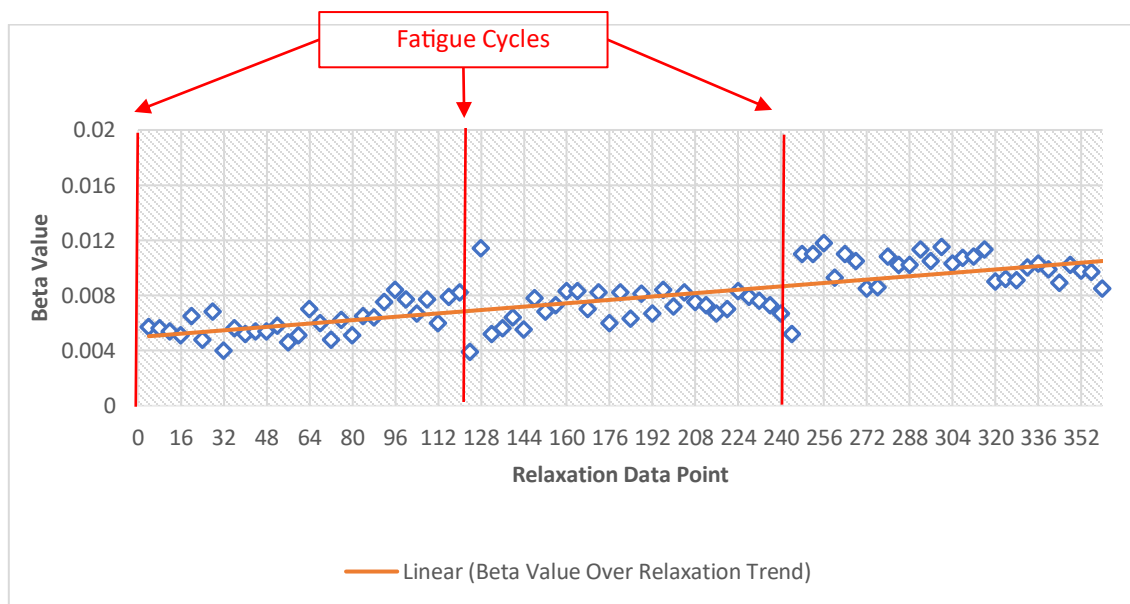


Figure 51: Second Harmonic Beta Value vs All Relaxation Cycles – SP1

The beta values show the peak of the second harmonic. Previous studies have indicated that in composite materials as the beta value increases the strength of the material increases. The results of this indicate that the material has regained part of its strength that was lost during fatigue. The beta values for all 5Hz specimen show an increasing trend throughout all ninety sets of data collected throughout relaxation for each specimen. Throughout all 90 points the beta values slightly increase for the first 5Hz specimen. The figure above used a range of 300 to 600 to find the peak second harmonics value. This beta value was found for all 30 relaxation points for all three relaxation periods of a total of 90 data points. Points 1-30 represent the first relaxation. Points 31-60 represent the second relaxation. Points 61-90 represent the third relaxation. A trendline was applied to show the average trend of the beta values throughout all three relaxation periods.

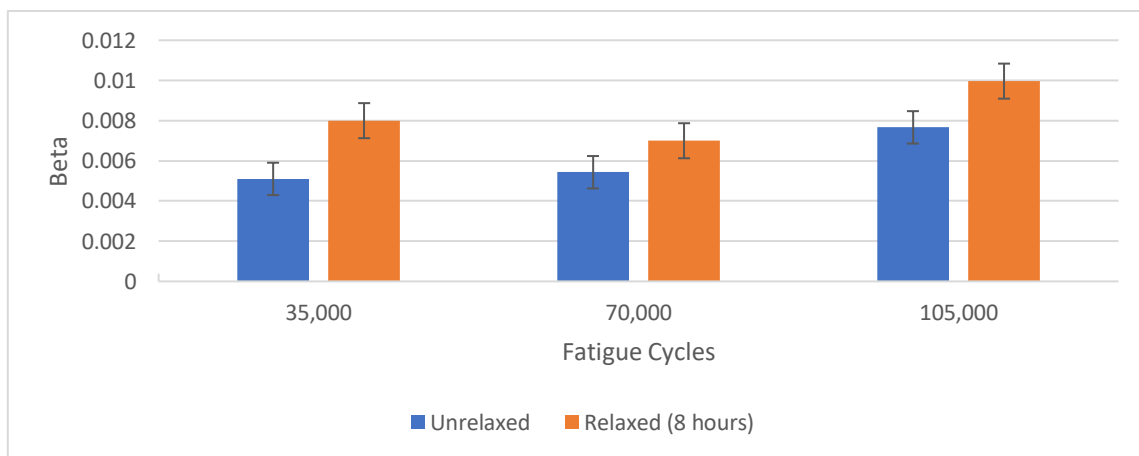


Figure 52: 5Hz Specimen 1 – Average Beta Values before and after Relaxation Period

The beta values throughout the relaxation periods should show an increase as the material settles into relaxation. Figure 52 shows a point taken at the beginning of the relaxation process and compares it with a point taken at the end of the relaxation process. The increase in the second point indicates that throughout each individual cycle the material is recovering some strength. This shows that the beta trend shown above in figure 52 occurs through all three cycles and is not concentrated on any one cycle. The beta values are taken as an average of 3 points in the unrelaxed state and three points in the relaxed state to generate the bar graph.

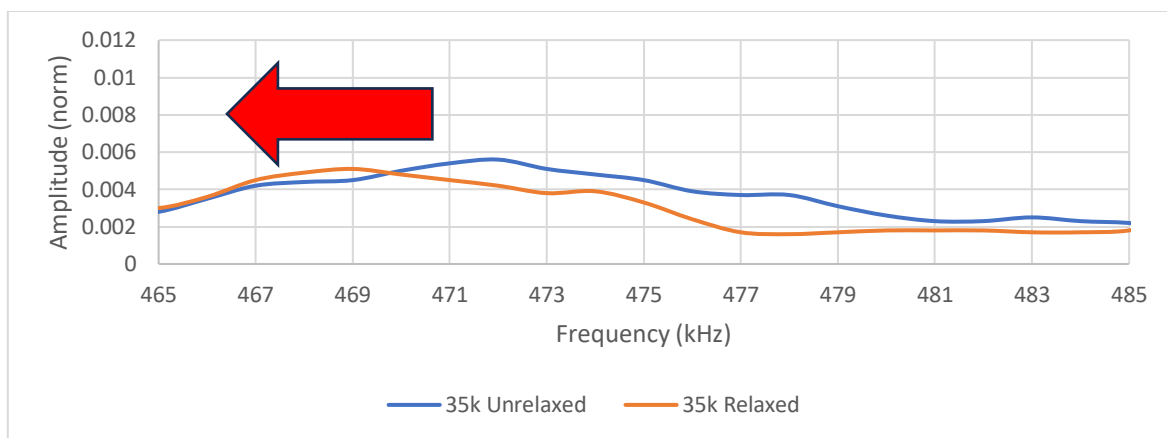


Figure 53: 5Hz Specimen 1 - Unrelaxed vs Relaxed - 35k

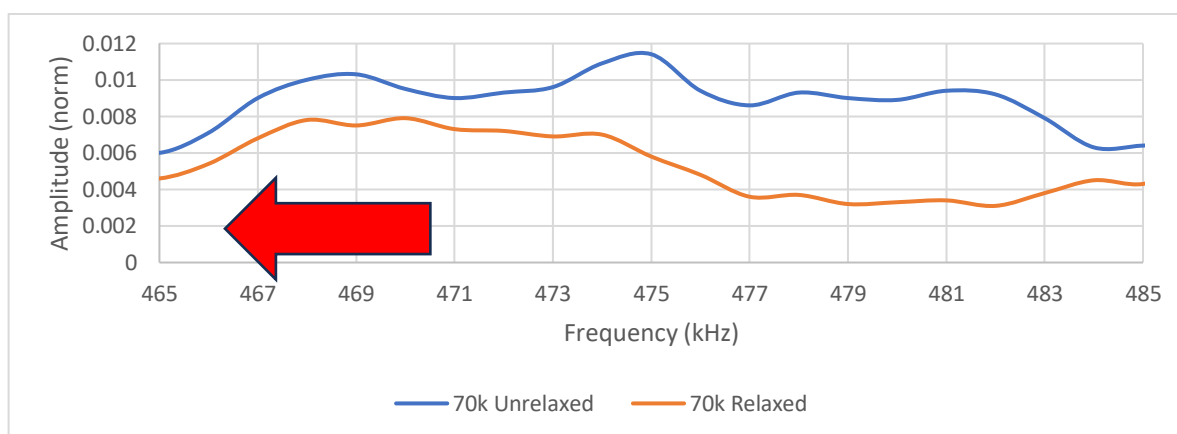


Figure 54: 5Hz Specimen 1 - Unrelaxed vs Relaxed - 70k

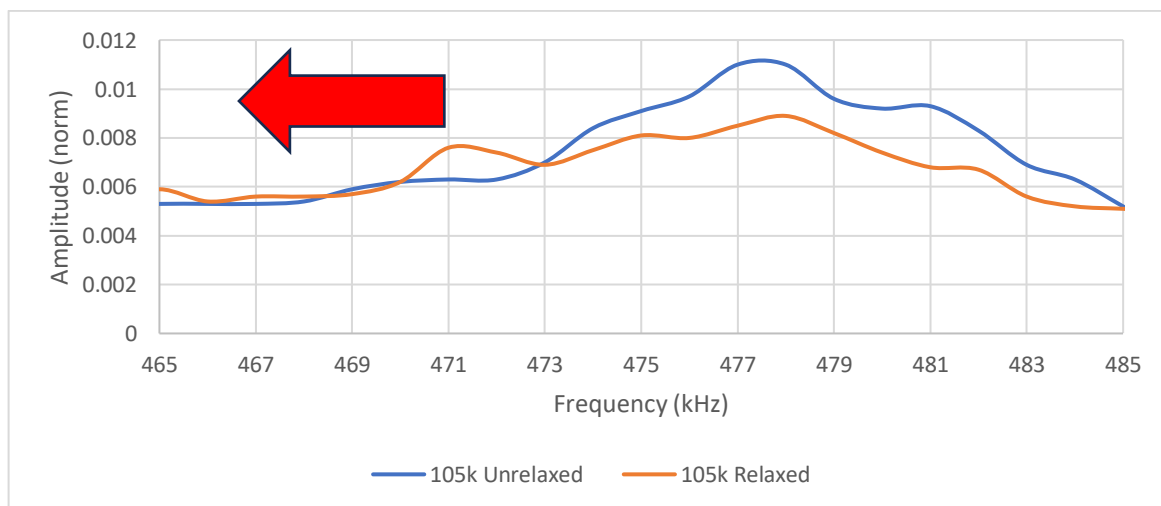


Figure 55: 5Hz Specimen 1 - Unrelaxed vs Relaxed - 105k

The final analysis of the FFT show a FFT graph that is focused on the second harmonic. The two FFT graphs were chosen and plotted from points take at the beginning and end of the data set while the material was unrelaxed after fatiguing and after the material was given at least 8 hours of relaxation. The shift to the left of most of the graphs indicates a regaining of strength to the material through the relaxation period. For specimen 1 the final graph in figure 55 shows minimal shift in the unrelaxed portion. This is likely due to an extensive amount of damage being introduced due to the approach of the end of the fatigue sets.

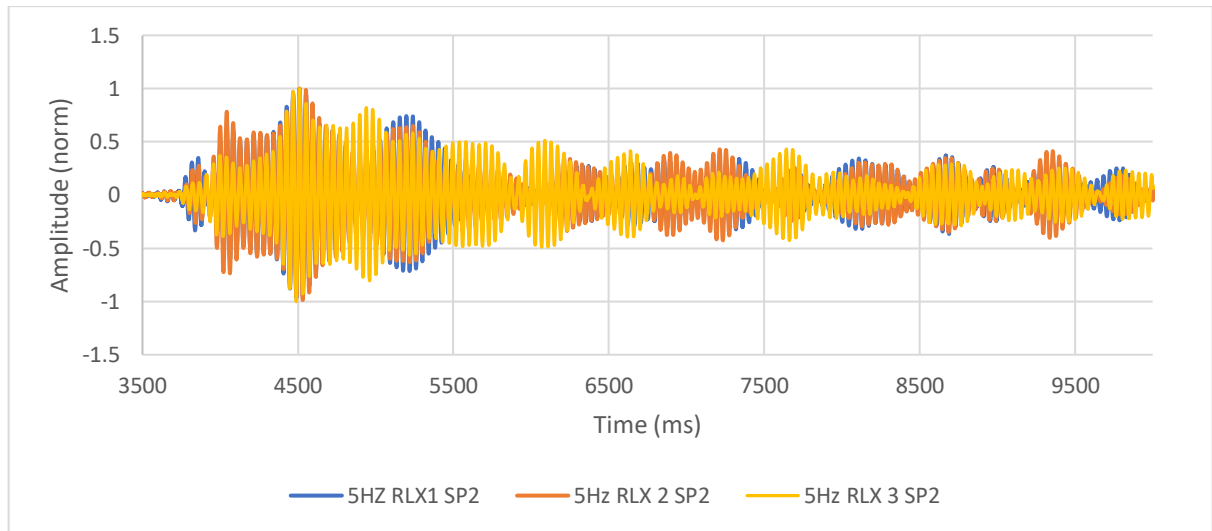


Figure 56: 5Hz Sp2 Time Series

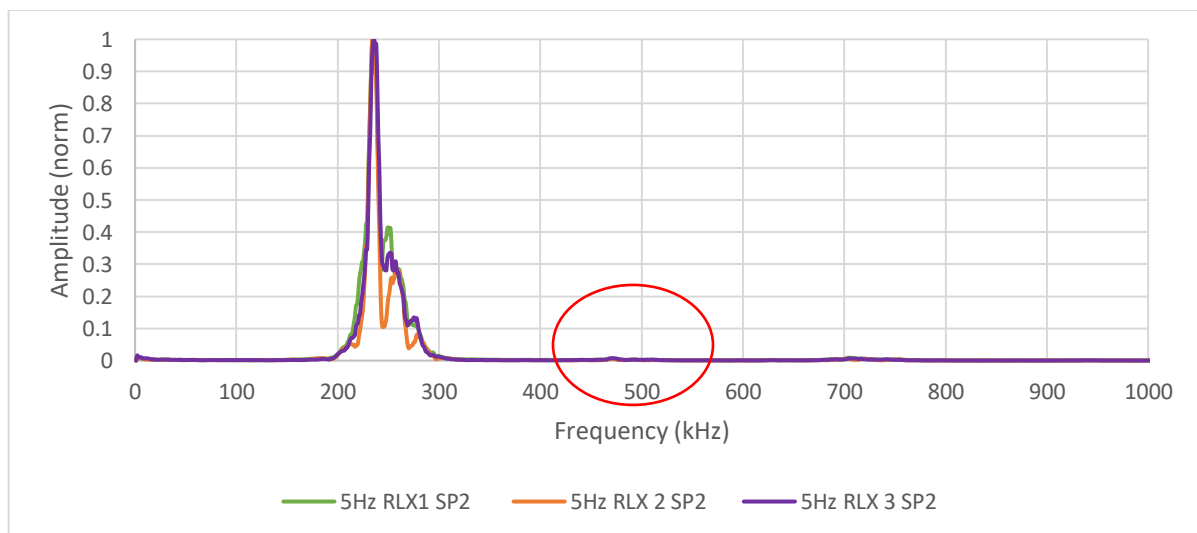


Figure 57: 5Hz Sp2 FFT Full View

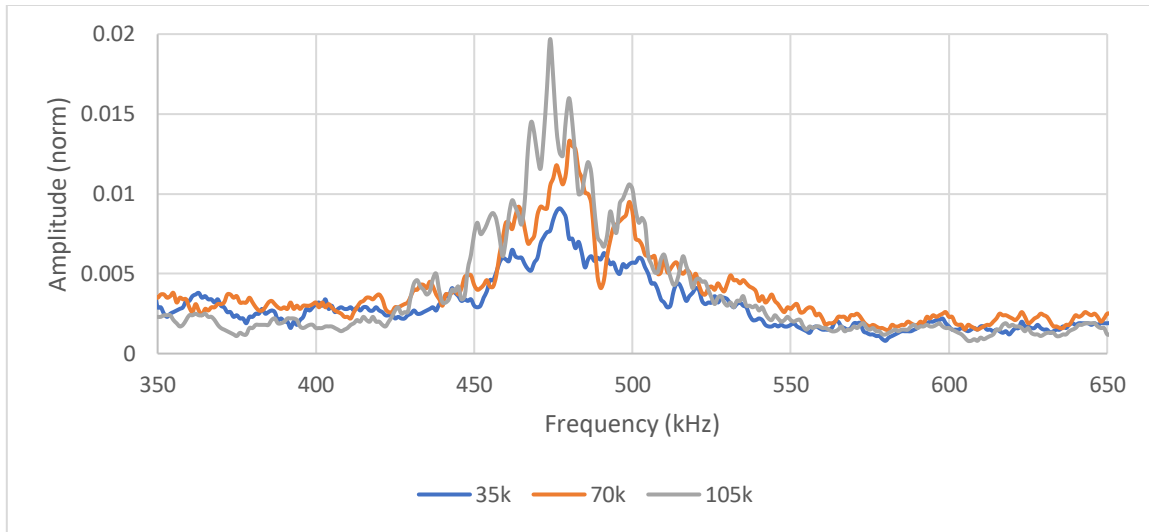


Figure 58: FFT Analysis of 5Hz Specimen 2

The second specimen at 5Hz frequency shows a similar pattern to the first. Visible harmonic points appear in the expected ranges. The results of all three 5Hz specimen show similar results to the similar study that was conducted with composite materials.

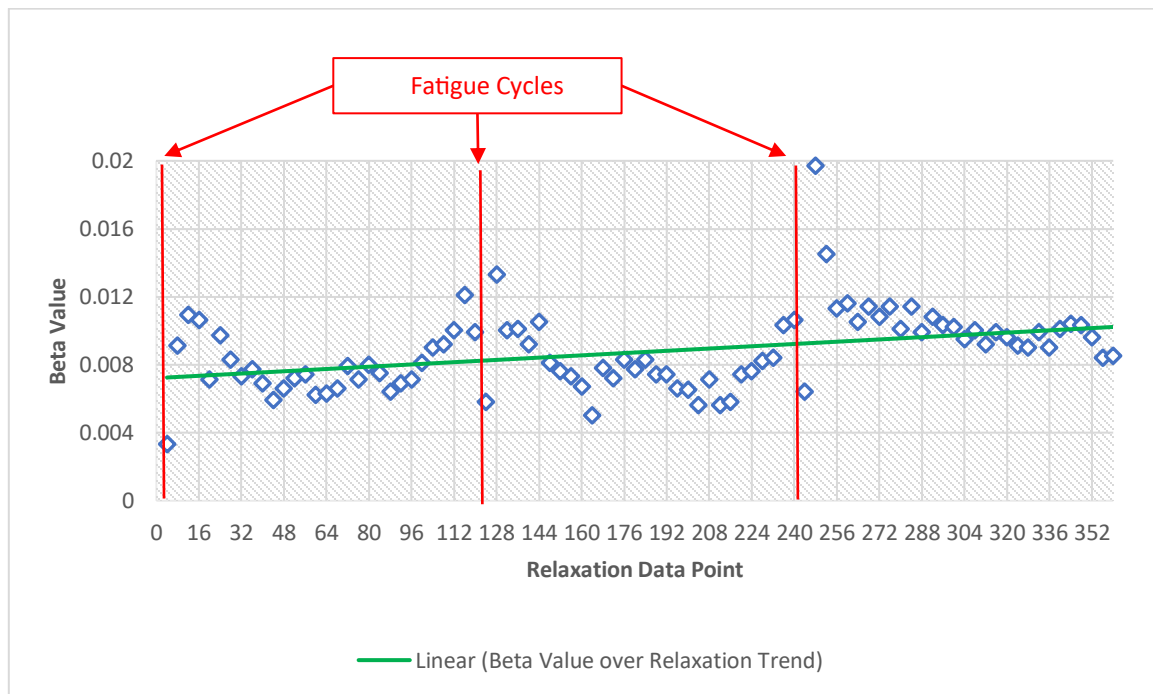


Figure 59: Second Harmonic Beta Value vs All Relaxation Cycles – SP2

The beta values taken at all 90 points taken during relaxation also show a similar pattern here compared to the first set. The range for this set is slightly lower overall compared to the first set but is not a significant amount. Throughout all 90 points the expected trend still appears with the second and third 5Hz sample. The time taken between each point was around 4 minutes throughout the collection.

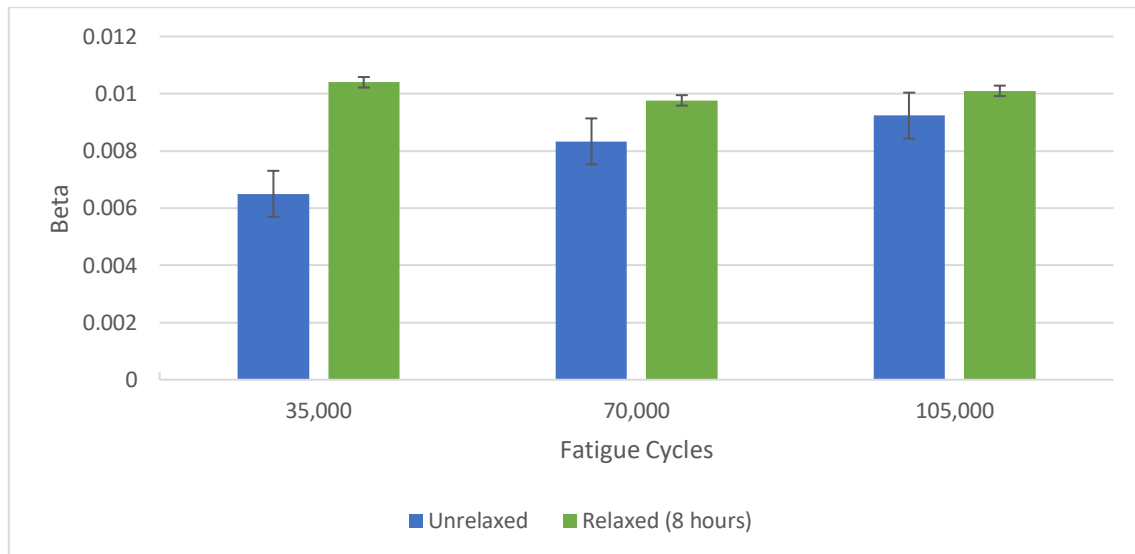


Figure 60: 5Hz Specimen 2 - Average Beta Values before and after Relaxation Period

The same method was used in the collection of these beta points and the same patterns appears compared to the first and third samples. The same results can be seen with the second specimen. As the relaxation occurs the beta points at the beginning and end of every cycle increase.

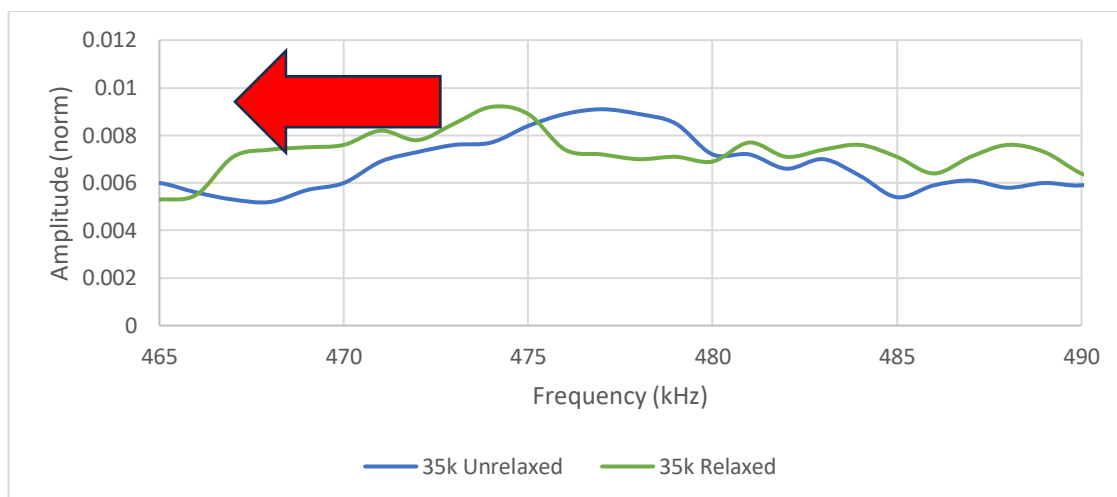


Figure 61: 5Hz Specimen 2 - Unrelaxed vs Relaxed - 35k

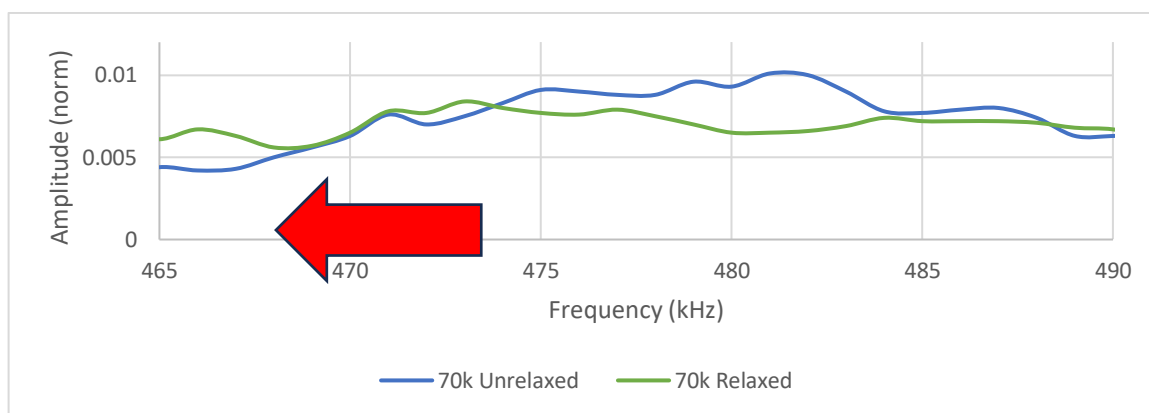


Figure 62: 5Hz Specimen 2 - Unrelaxed vs Relaxed - 70k

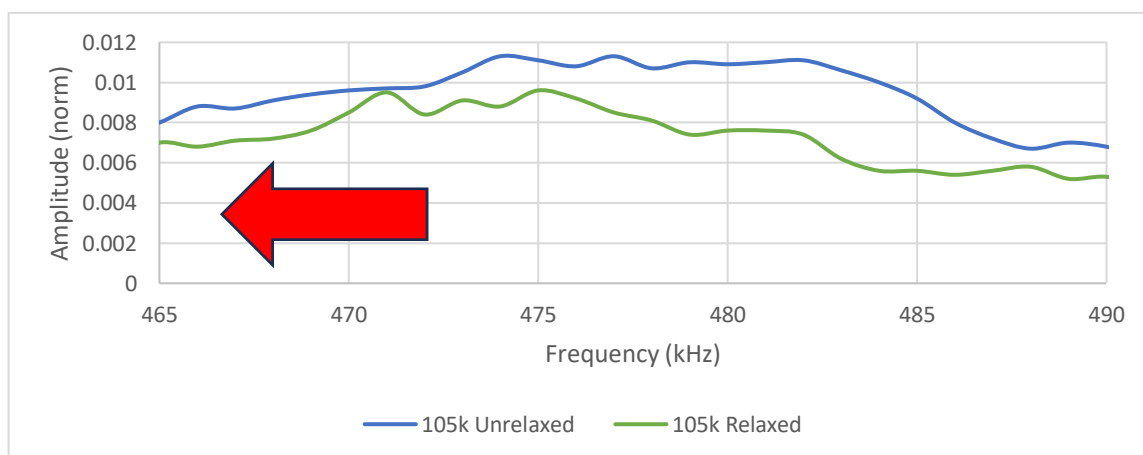


Figure 63: 5Hz Specimen 2 - Unrelaxed vs Relaxed - 105k

A noticeable shift occurs within all three relaxation periods of the second sample. The shift confirms the results of the first sample and indicates that the material is regaining strength throughout the relaxation cycle. The shift during the third relaxation cycle is more visible in this specimen. This difference is minuscule and can be contributed to the variability in the life of aluminum.

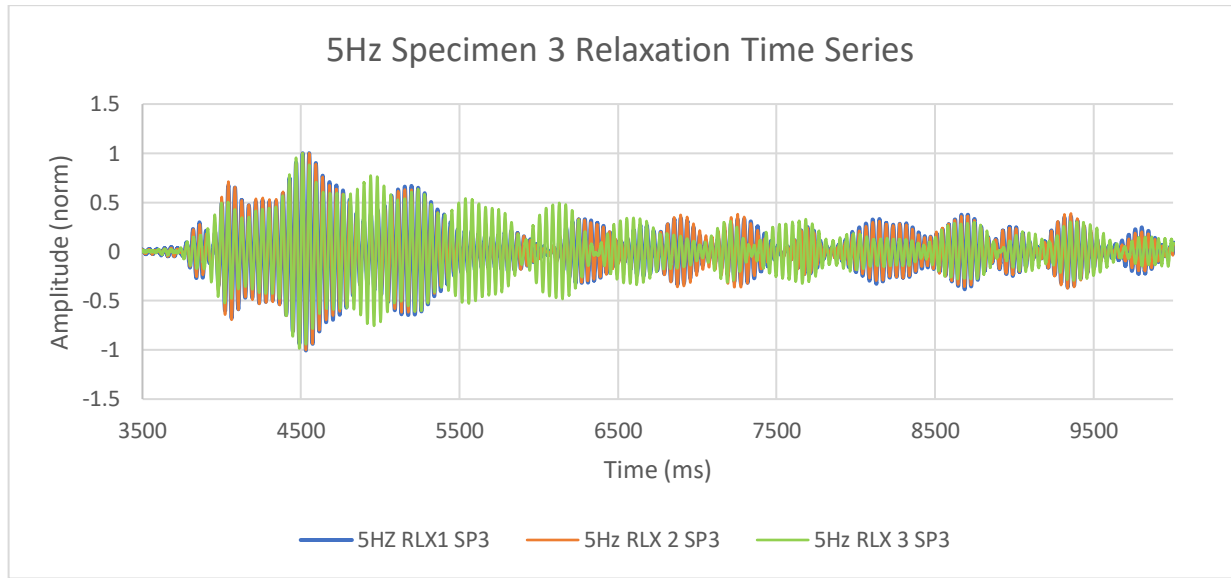


Figure 64: 5Hz Sp3 Time Series

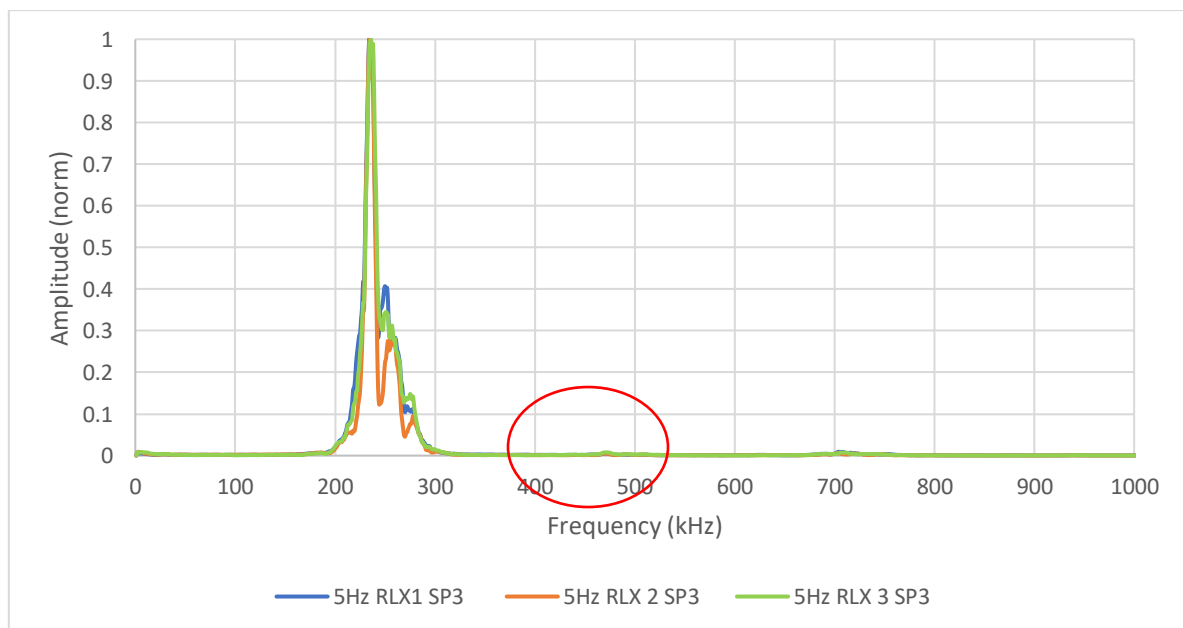


Figure 65: 5Hz Sp3 FFT Full View

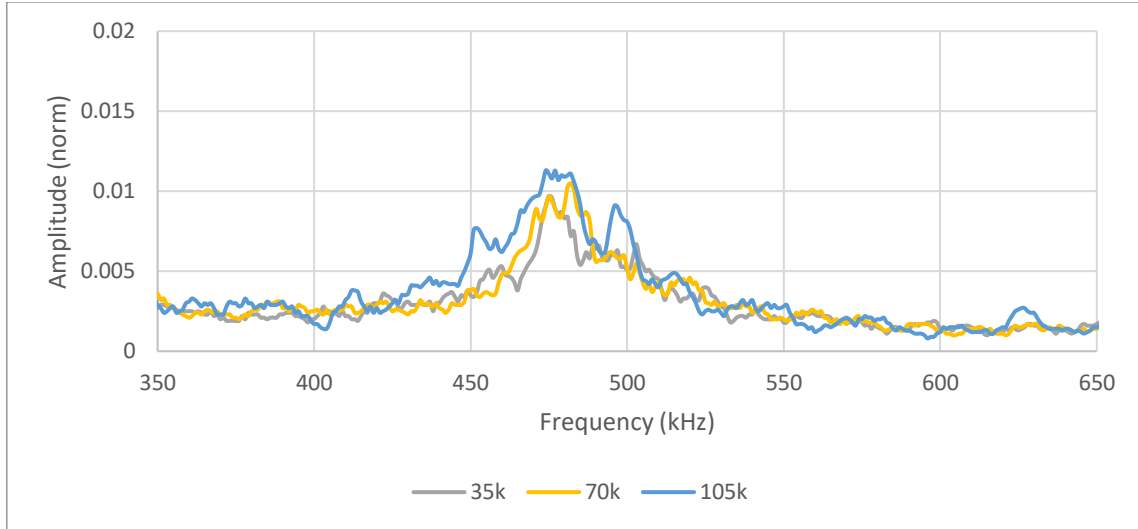


Figure 66: FFT Analysis of 5Hz Specimen 3

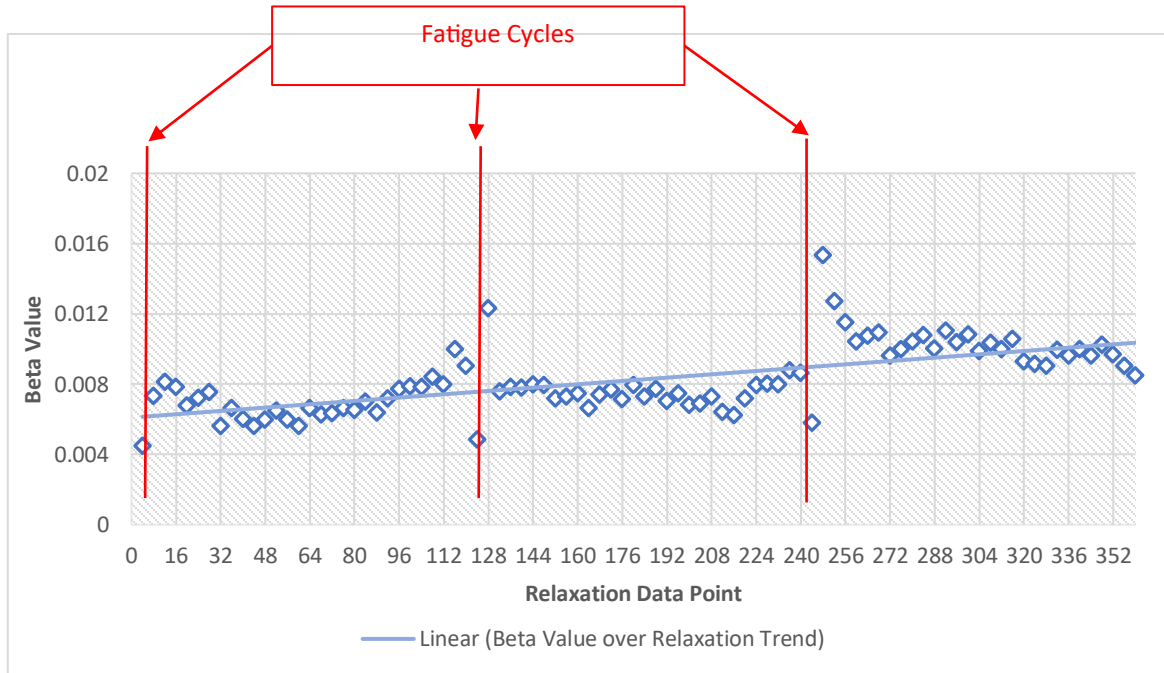


Figure 67: Second Harmonic Beta Value vs All Relaxation Cycles – SP3

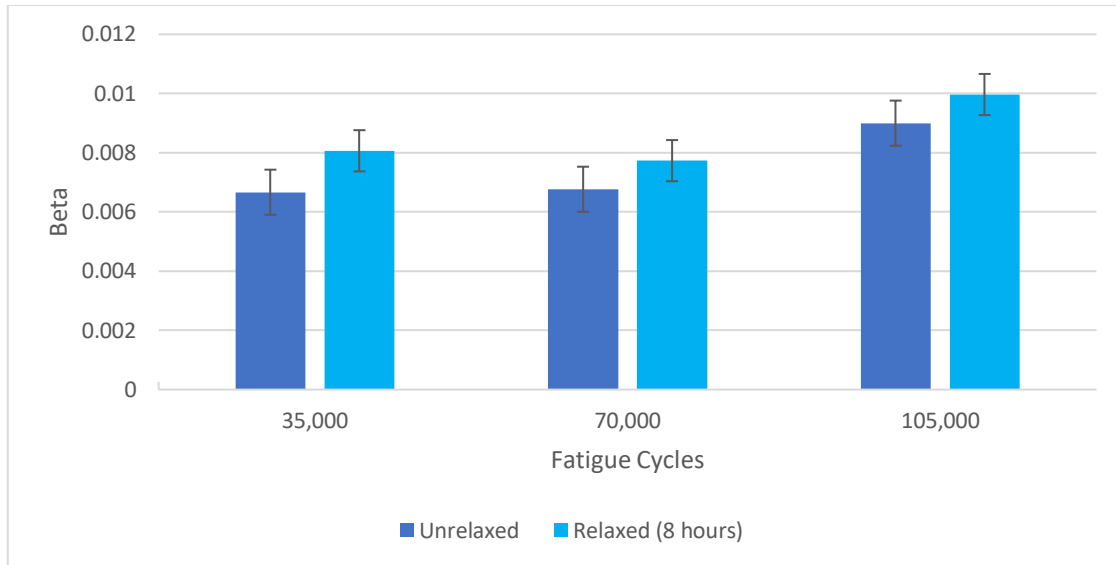


Figure 68: 5Hz Specimen 3 - Average Beta Values before and after Relaxation Period

The results of the FFT graph and the beta values for the third specimen follow the same pattern set in the first two specimen. The peaks of the second and third harmonic are within the expected range for all three of the unrelaxed points take. The beta values also fall within a similar range and follow the same expected trend. This trend indicates partial restoration in the materials strength. The results in figure 68 also show the same pattern that throughout each relaxation period some strength is restored.

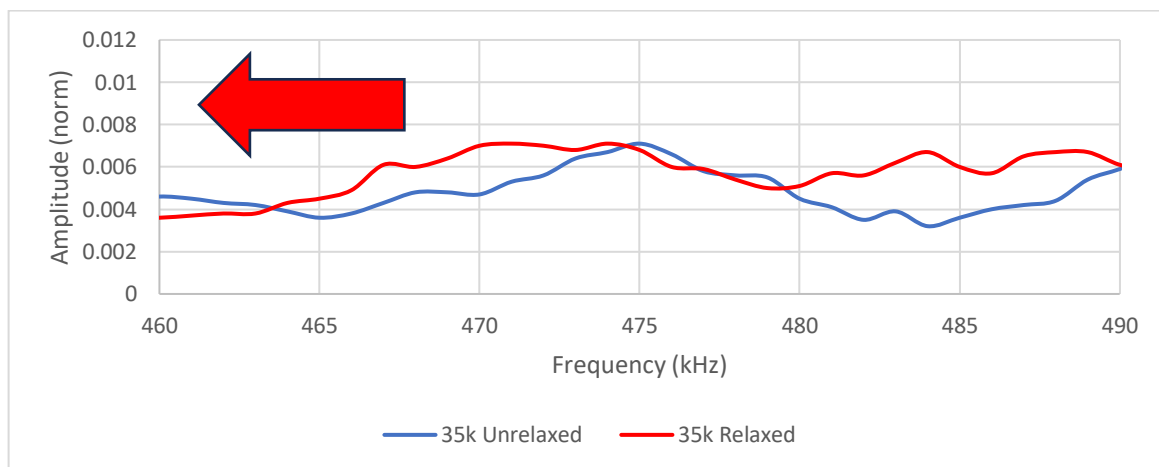


Figure 69: 5Hz Specimen 3 - Unrelaxed vs Relaxed - 35k

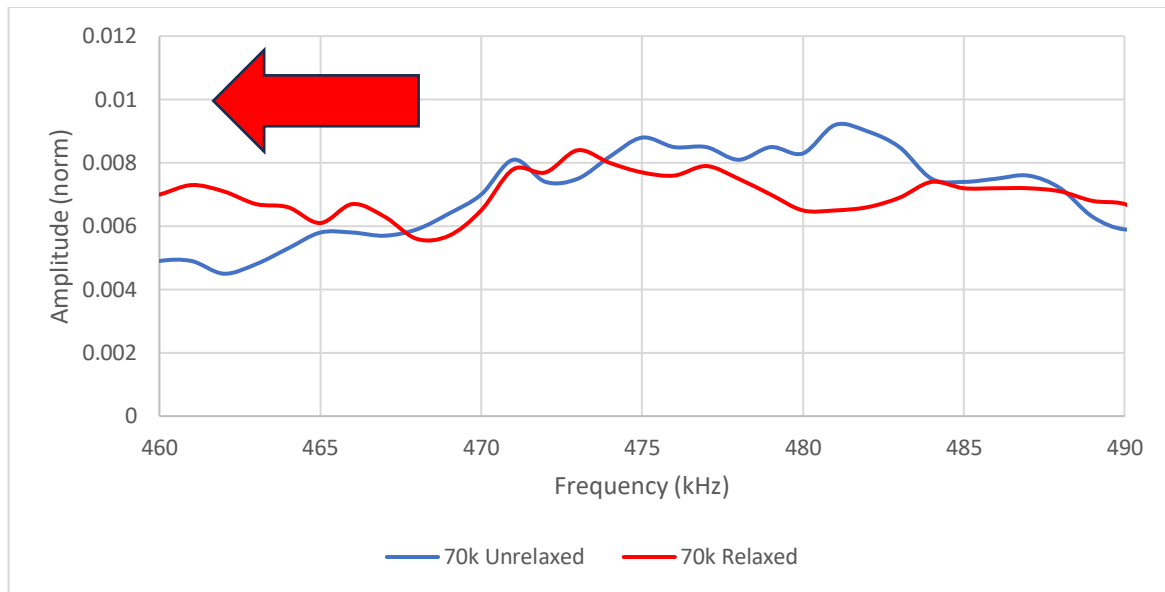


Figure 70: 5Hz Specimen 3 - Unrelaxed vs Relaxed - 70k

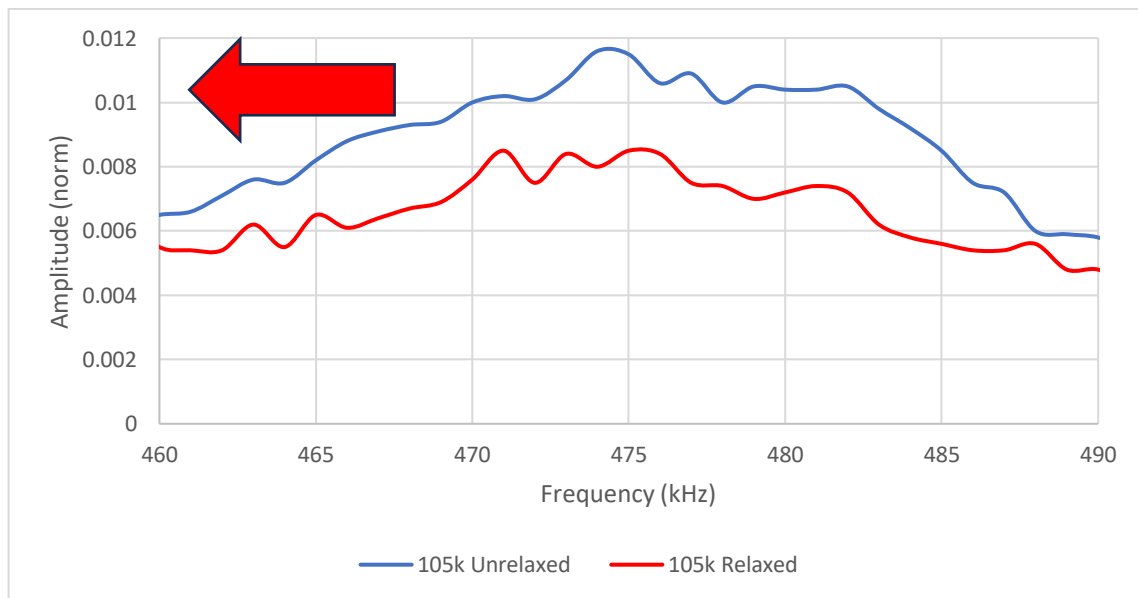


Figure 71: 5Hz Specimen 3 - Unrelaxed vs Relaxed - 105k

A noticeable shift occurs in the in all three FFT beta peaks in specimen three as well. The peak is more distinct in the first two points and less obvious in the third. Once again, this distinction could indicate that more plastic damage occurred inside the material and that more damage was introduced.

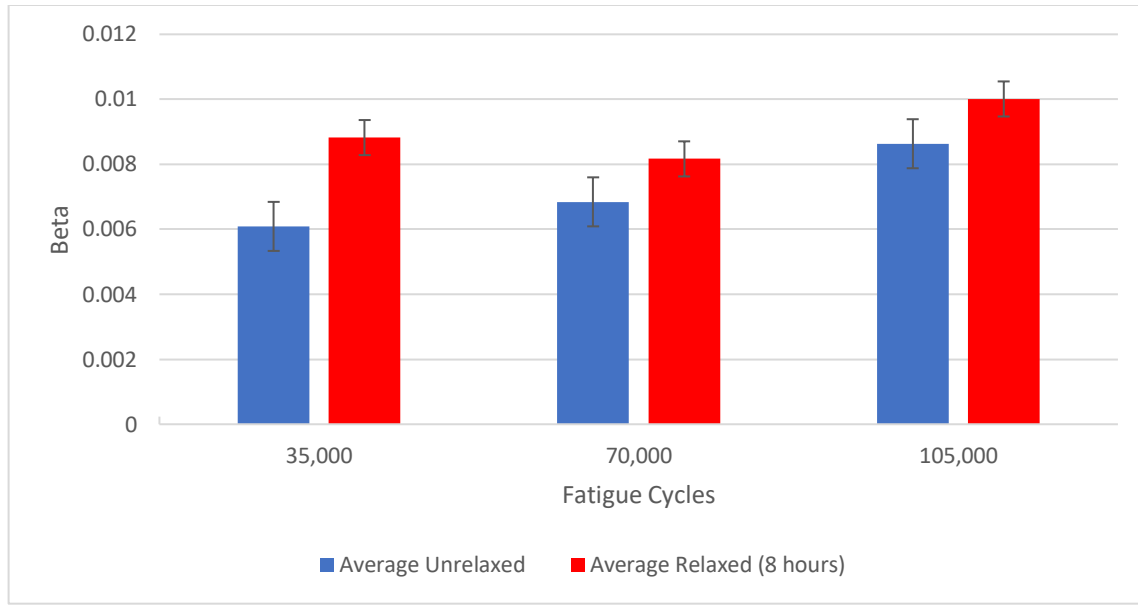


Figure 72: Average Beta Value for all 5Hz Specimen

4.5.2 FFT Results – 3Hz

The results from the 3Hz specimen follow a similar pattern to the results from the 5Hz. All of the results are not directly comparable due to issues with the tensile machine that caused the changes in testing parameters. Even with these changes some results are still comparable, the only major changes that occur is slight decreases in energy output of the PZTs. Due to less introduction of damage slight increases in the beta values are observed. Overall similar patterns emerge in both sets of data.

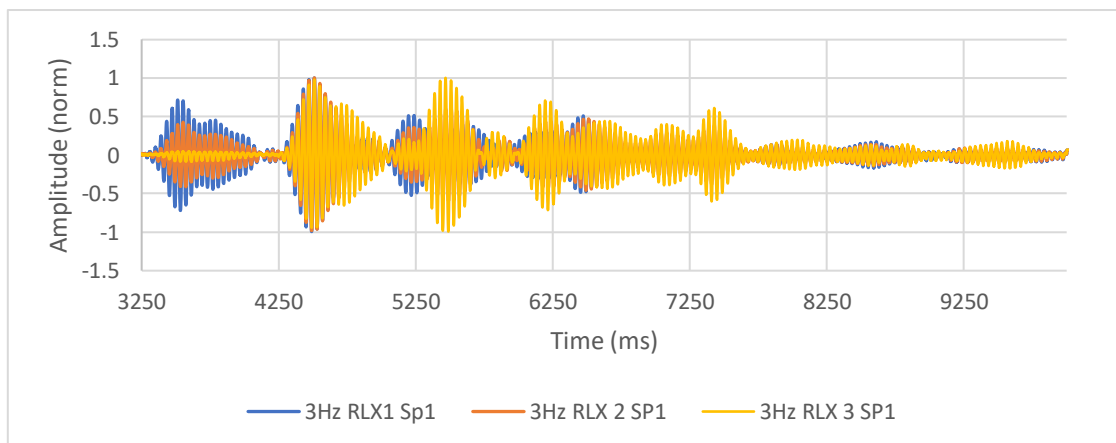


Figure 73: 3Hz Sp1 Time Series

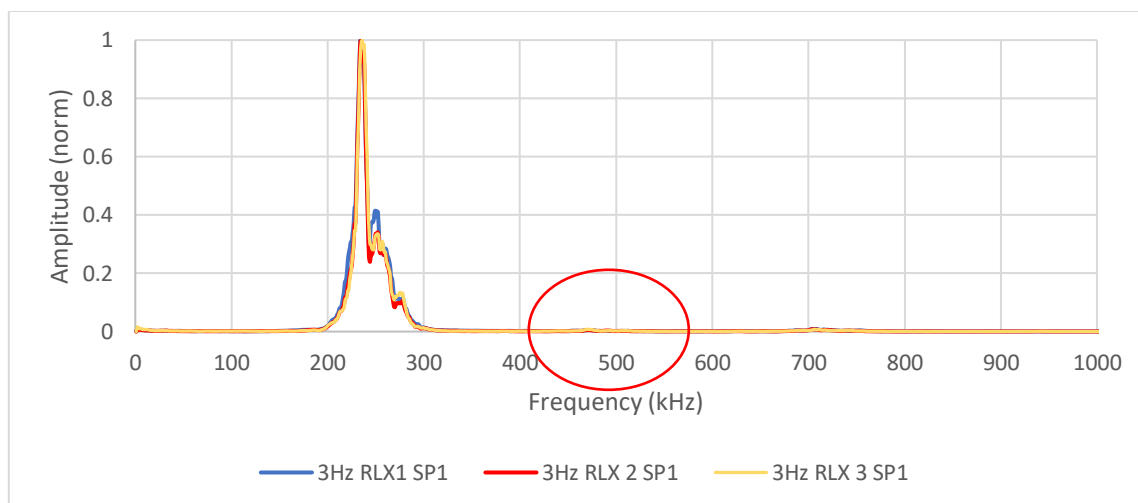


Figure 74: 3Hz Sp1 FFT Full View

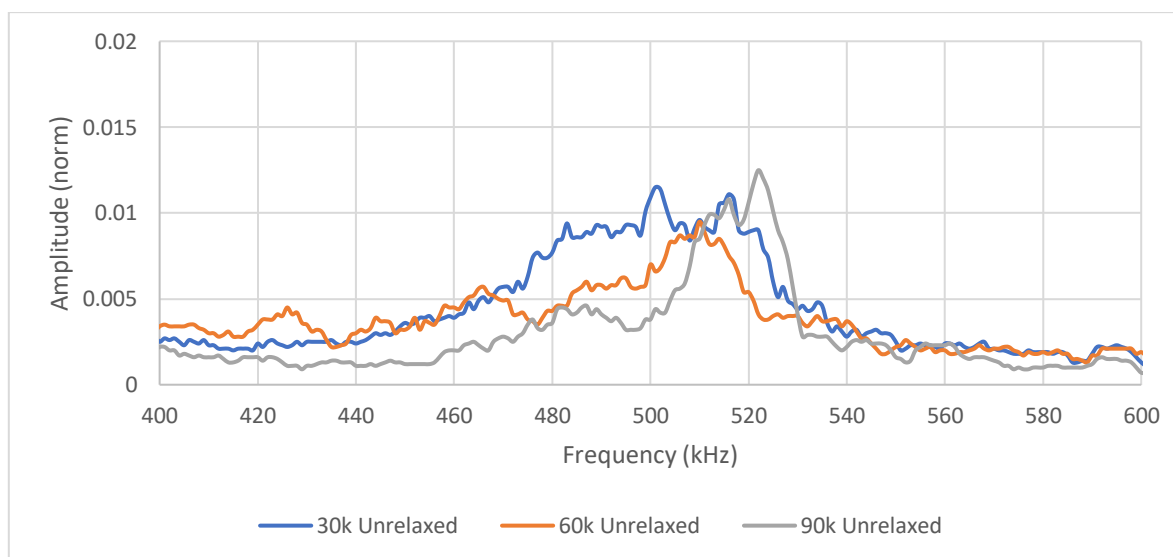


Figure 75: FFT Analysis of 3Hz Specimen 1

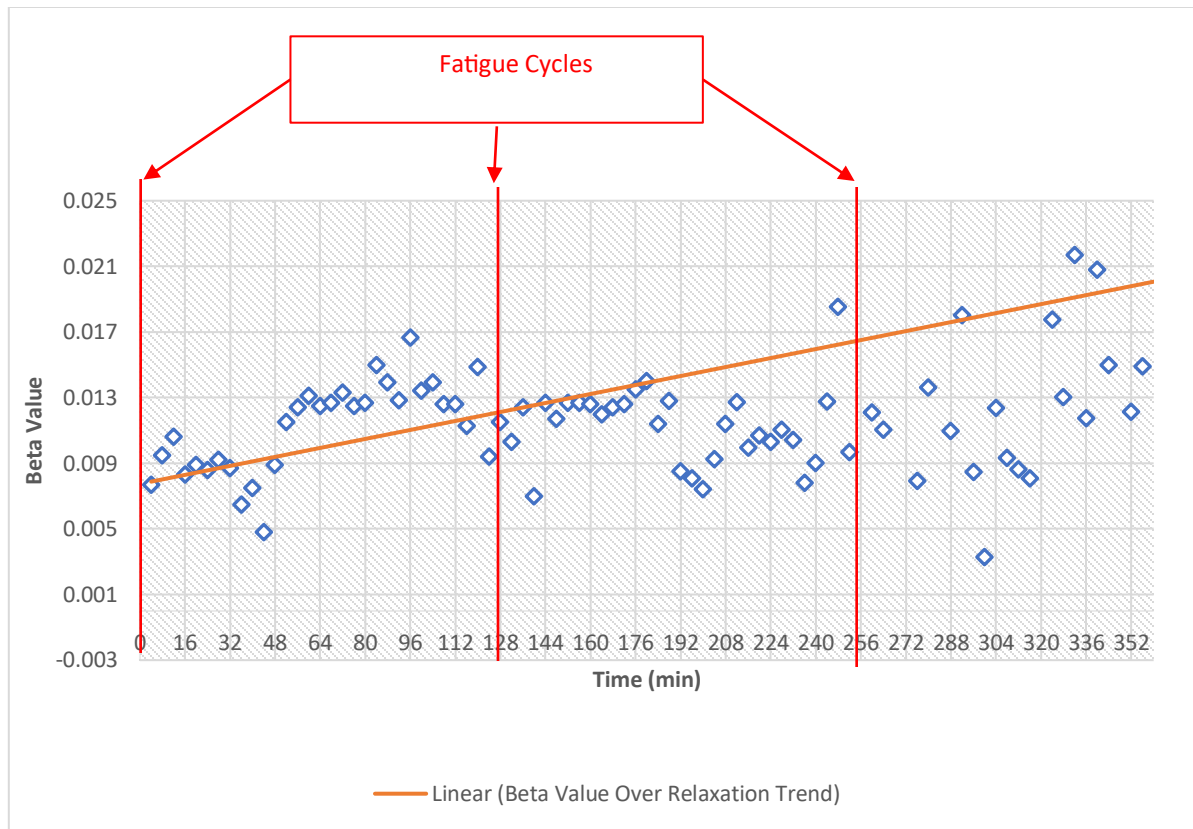


Figure 76: Second Harmonic Beta Value vs All Relaxation Cycles – SP1

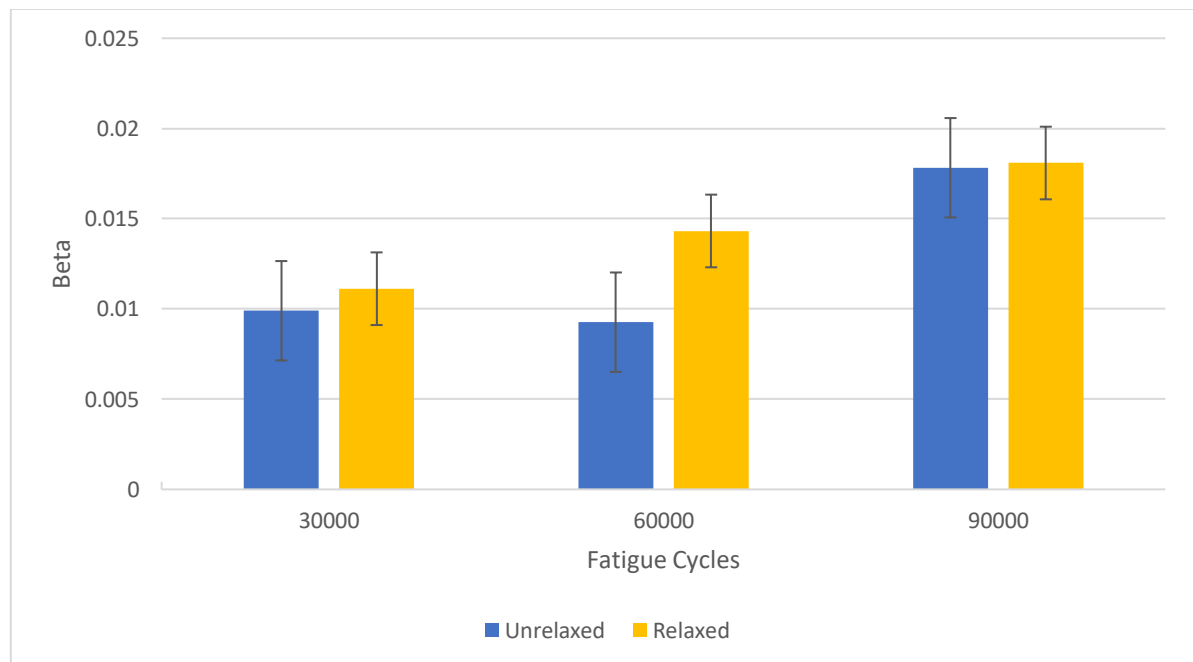


Figure 77: 3Hz Specimen 1 - Average Beta Values before and after Relaxation Period

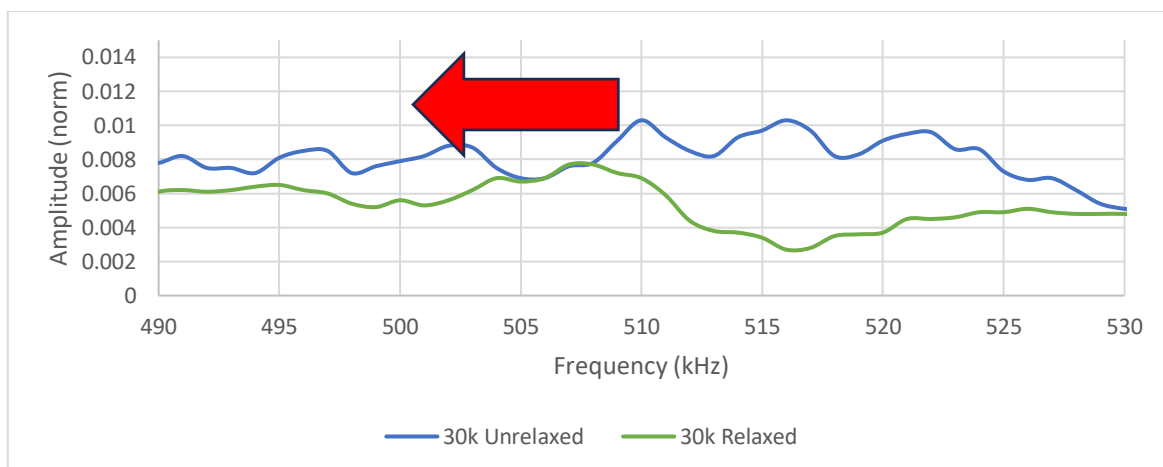


Figure 78: 3Hz Specimen 1 - Unrelaxed vs Relaxed - 30k

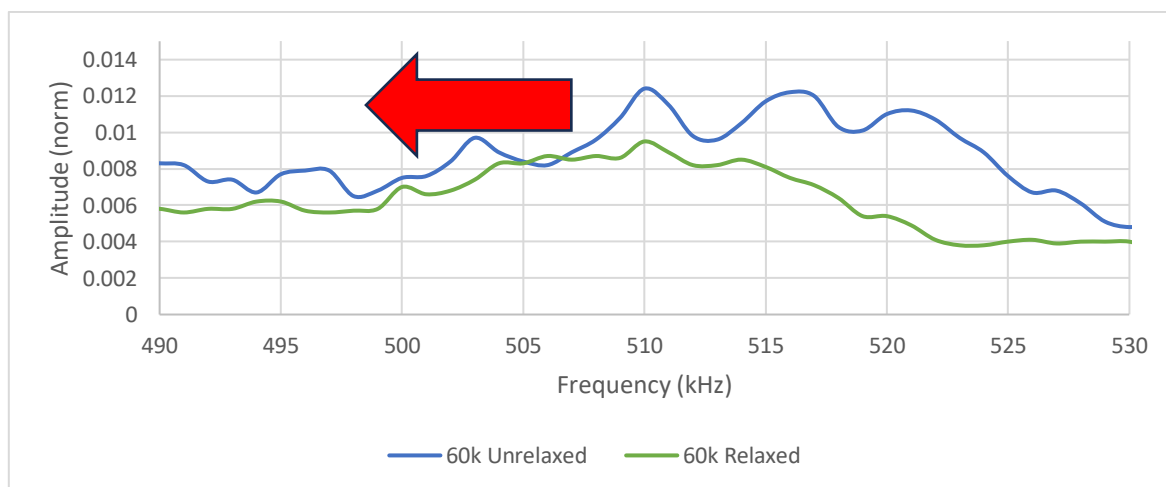


Figure 79: 3Hz Specimen 1 - Unrelaxed vs Relaxed - 60k

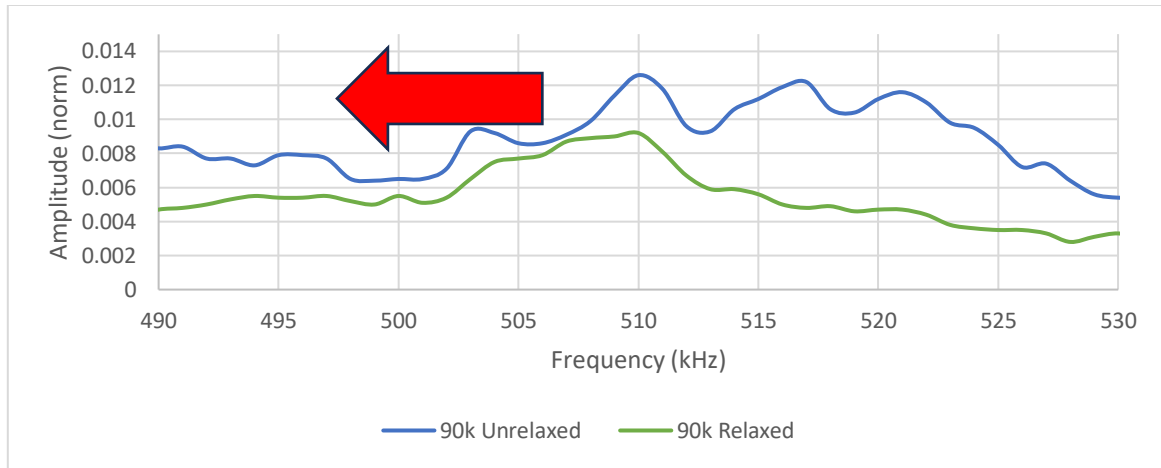


Figure 80: 3Hz Specimen 1 - Unrelaxed vs Relaxed - 90k

Shifts are visible in all three sets of data from the first specimen when comparing relaxed and unrelaxed data. This is still indicating a shift towards the left which indicates an increase in the strength throughout relaxation. Slightly increased beta values can be seen due to a decrease in damage introduced in the material. This in turn decreases the amount of recovery though the relaxation phases. For specimen 1 most of the recovery is seen in the third phase of relaxation. This is likely due to the culmination of damage introduced through the three fatigue cycles.

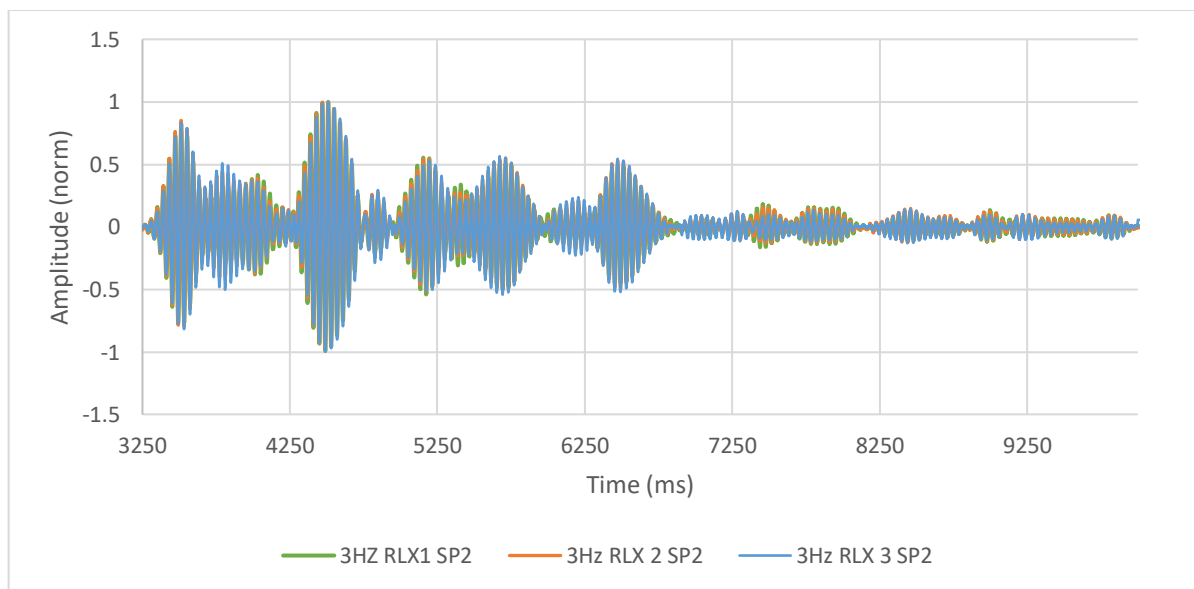


Figure 81: 3Hz Sp2 Time Series

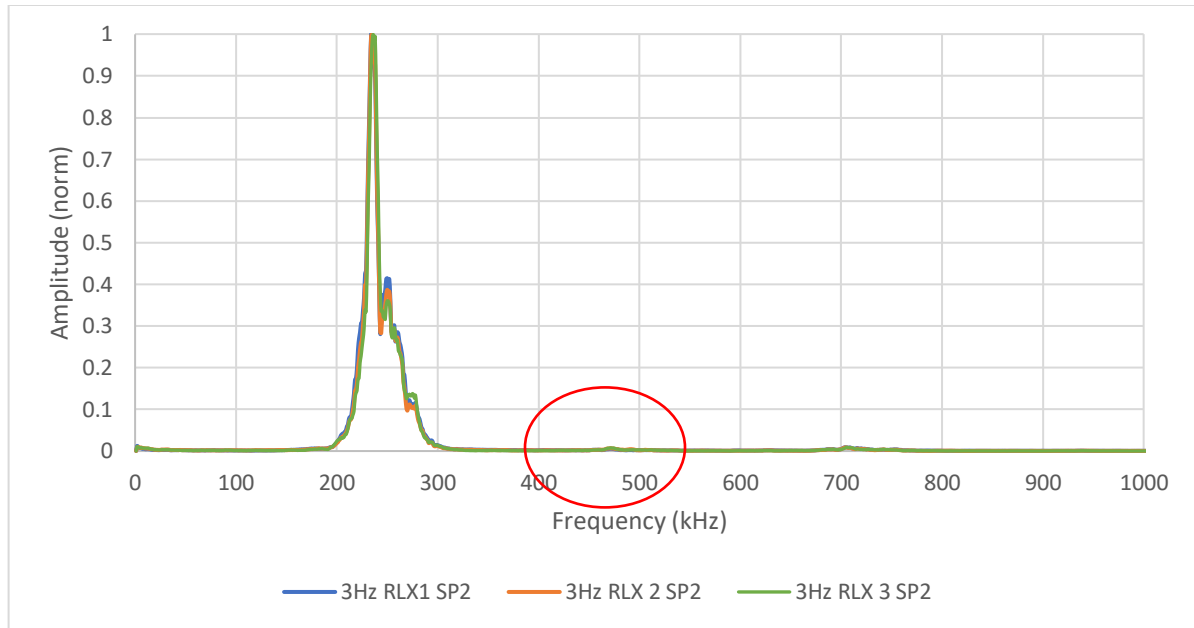


Figure 82: 3Hz Sp2 FFT Full View

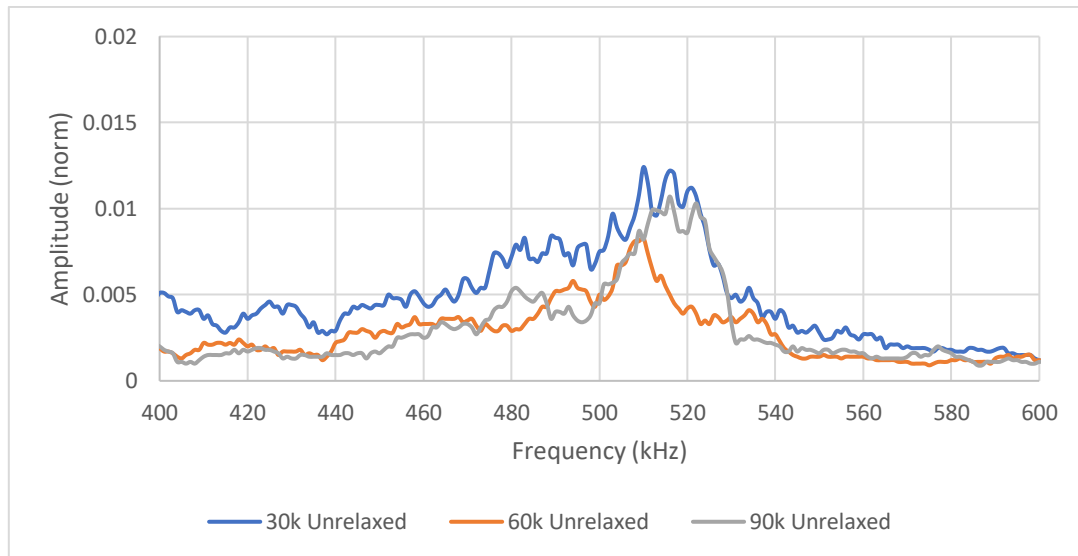


Figure 83: FFT Analysis of 3Hz Specimen 2

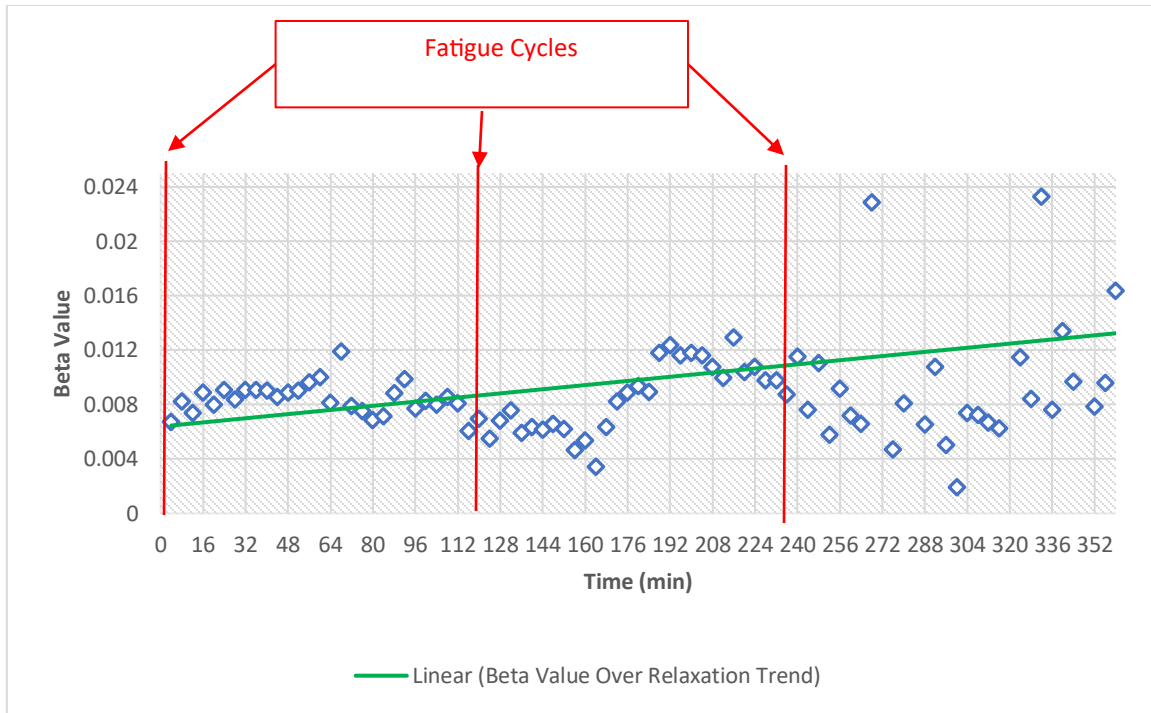


Figure 84: Second Harmonic Beta Value vs All Relaxation Cycles – SP2

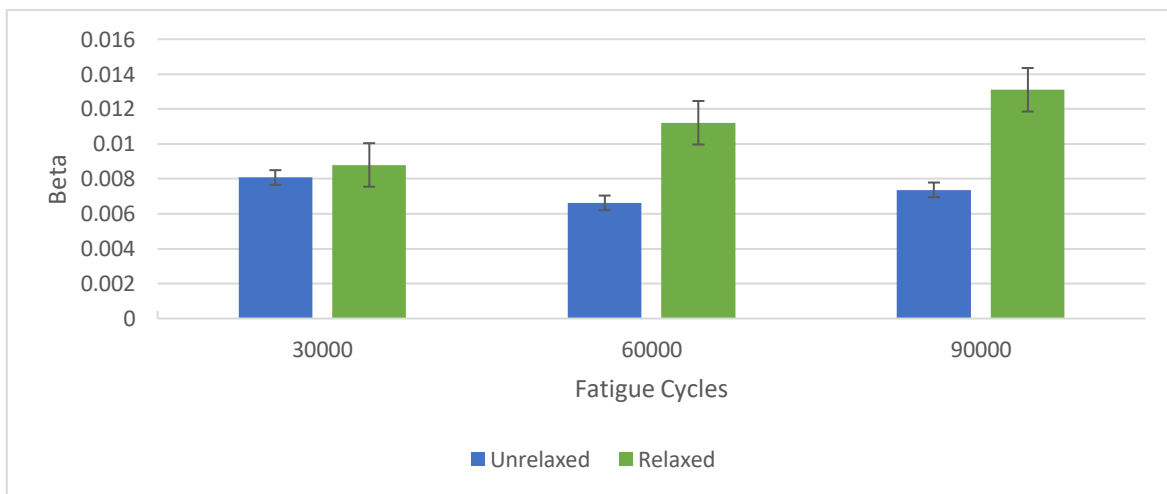


Figure 85: 3Hz Specimen 2 - Average Beta Values before and after Relaxation Period

Similar results are also found in the second 3Hz specimen. It can be observed from the results that the beta values follow the same trend as previous samples and indicate material strength increases. A notable point is the slight decrease throughout the second relaxation cycles. The outlier point is likely due to the amount of damage introduced and the variability in the life of aluminum.

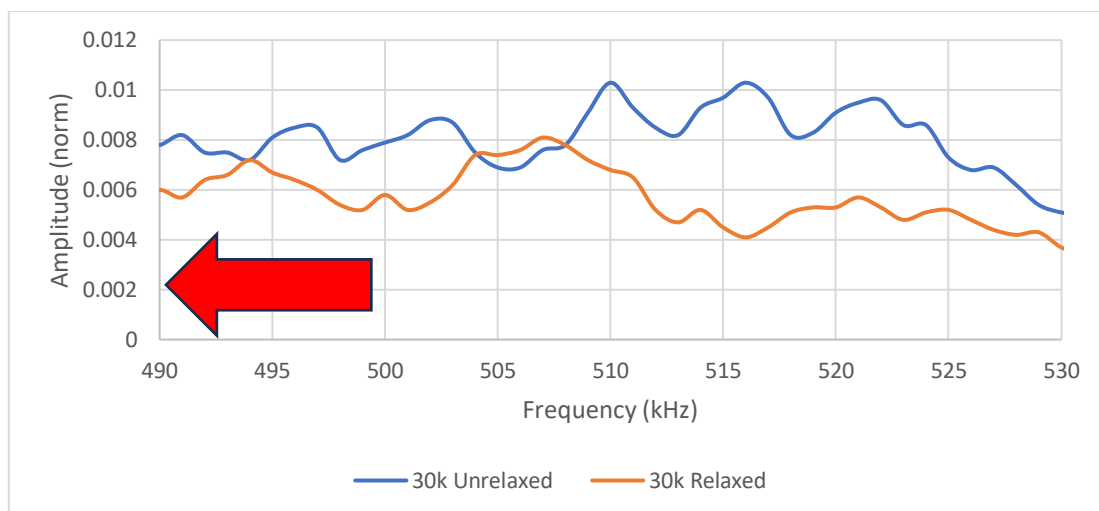


Figure 86: 3Hz Specimen 2 - Unrelaxed vs Relaxed - 30k

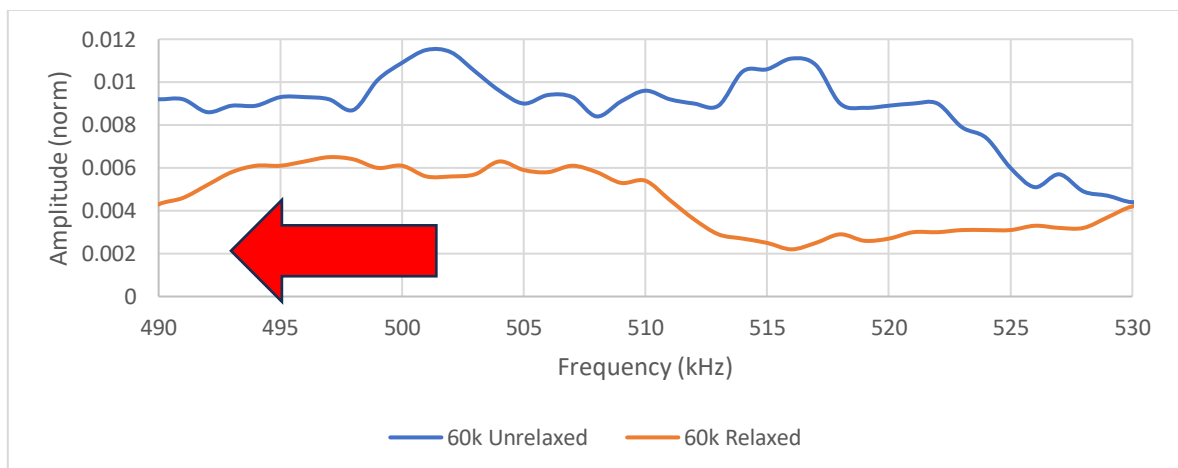


Figure 87: 3Hz Specimen 2 - Unrelaxed vs Relaxed - 60k

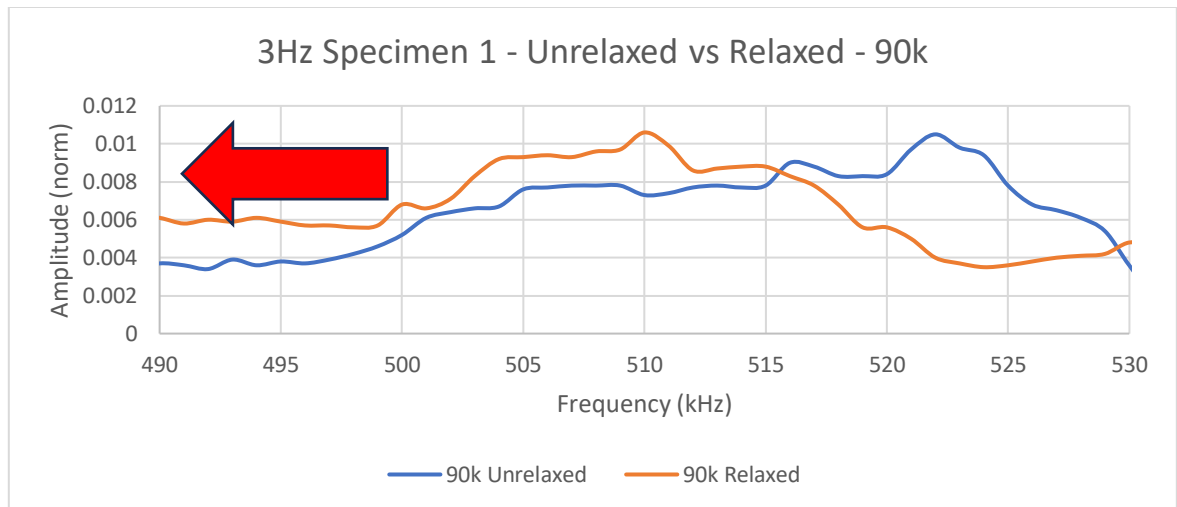


Figure 88: 3Hz Specimen 2 - Unrelaxed vs Relaxed - 90k

The beta graphs also follow a similar pattern when compared to previous test and previous composite research. The shift in the data values indicate that the material is regaining small amounts of strength the longer it is in relaxation. The absence of a major shift in the second relaxation period relates to the decrease in the beta value and is an outlier compared to previous cycles.

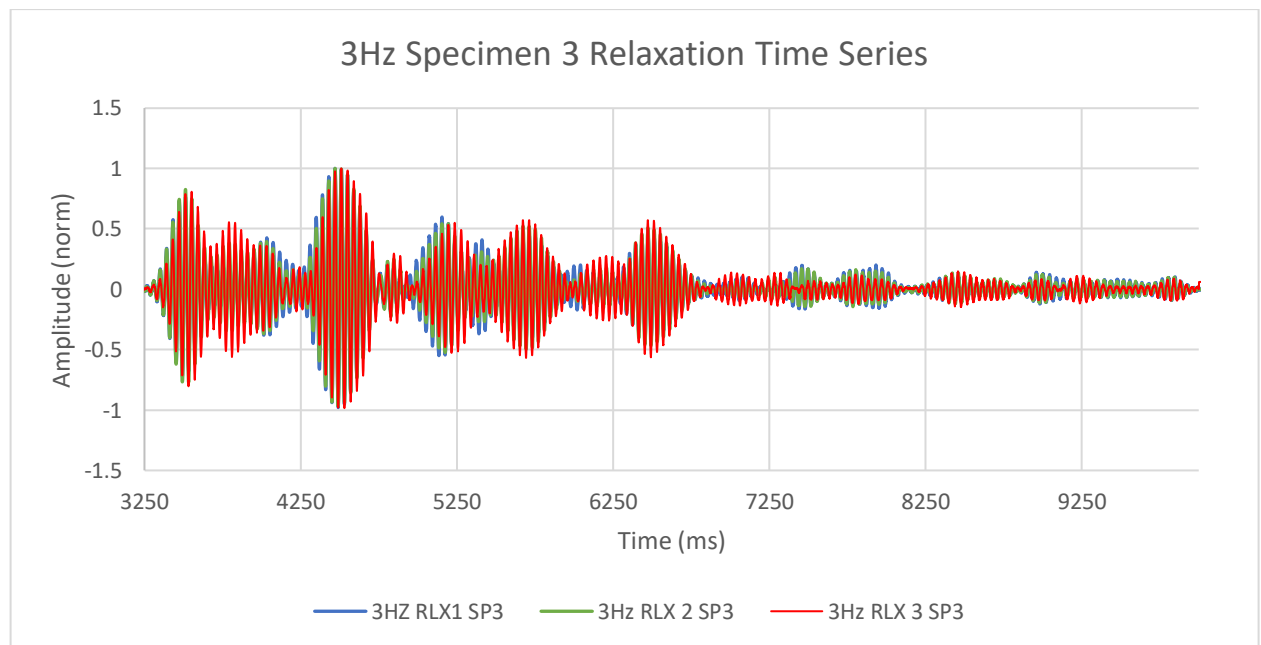


Figure 89: 3Hz Sp3 Time Series

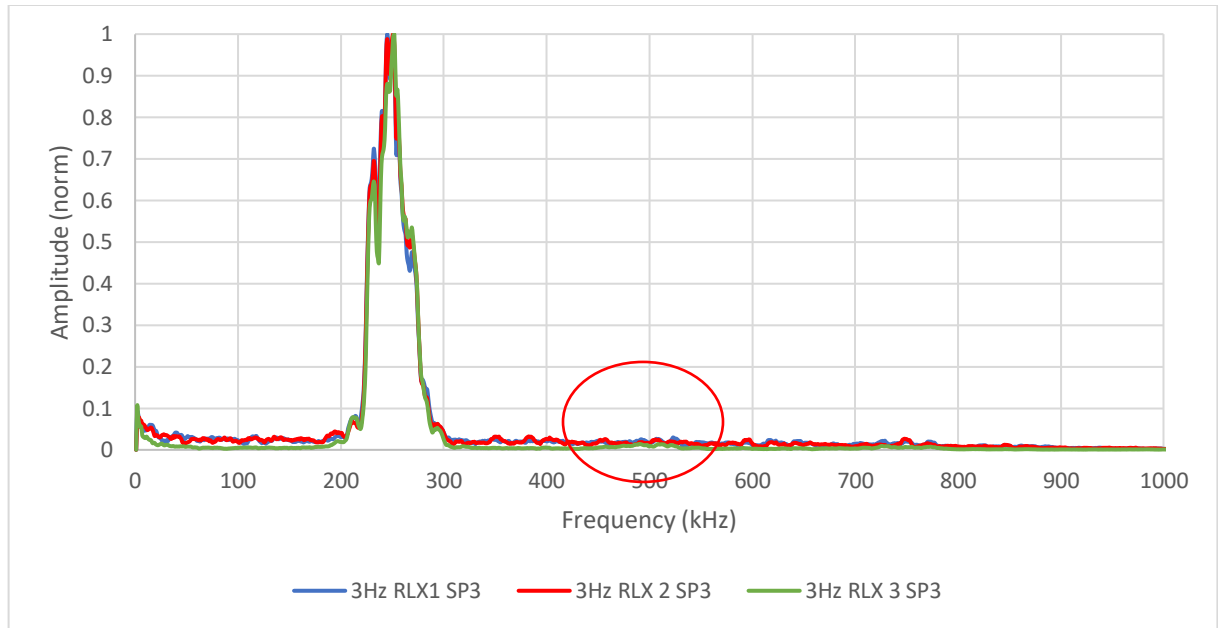


Figure 90: 3Hz Sp3 FFT Full View

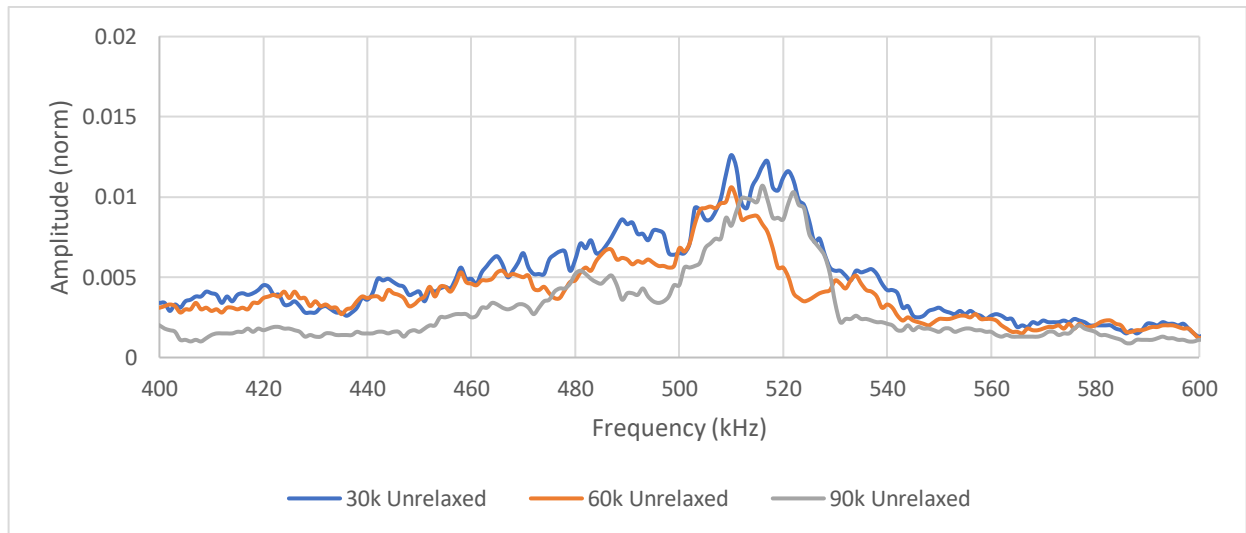


Figure 91: FFT Analysis of 3Hz Specimen 3

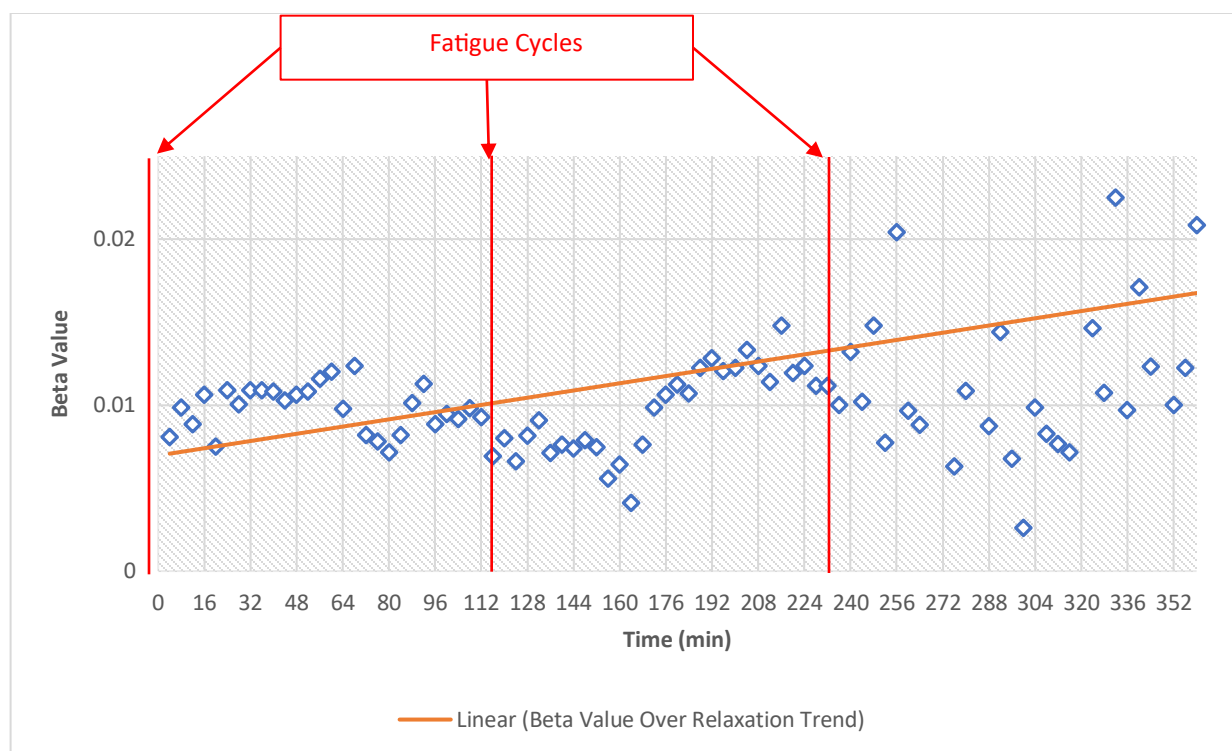


Figure 92: Second Harmonic Beta Value vs All Relaxation Cycles – SP3

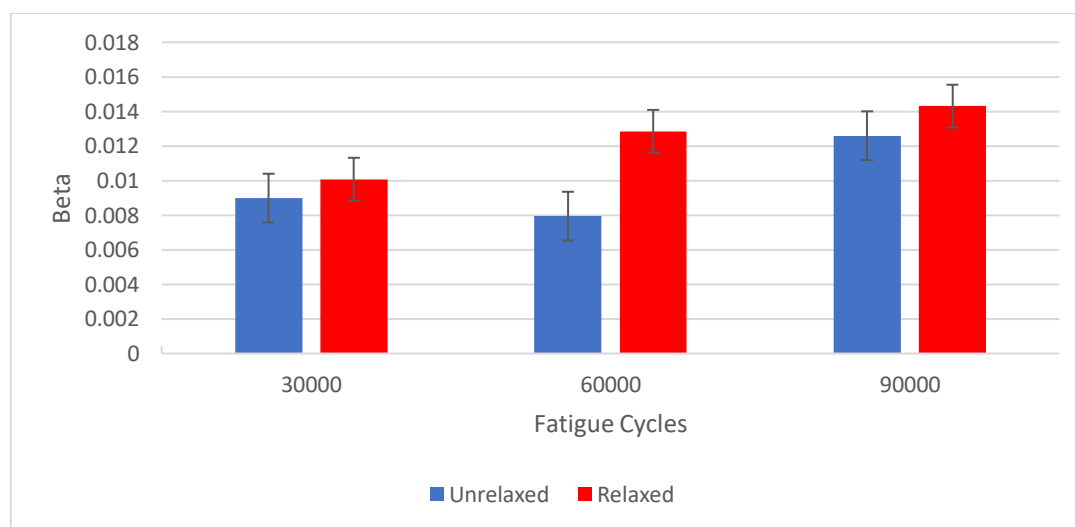


Figure 93: 3Hz Specimen 3 - Average Beta Values before and after Relaxation Period

The third and final specimen follow the same pattern previous established. The pattern in all 5Hz data and 3Hz data are used to confirm the findings. In all examples a pattern is established that indicates the material regains partial strength during relaxation. This can also be verified with previous research and establishes a connection between isotropic material and composite material. Specimen three exhibits three clear shifts at the beginning and end of relaxation and verifies the results to show the strength regained due to the slight decrease in frequency on the FFT analysis graph. The results are shown in figures 93 – 95.

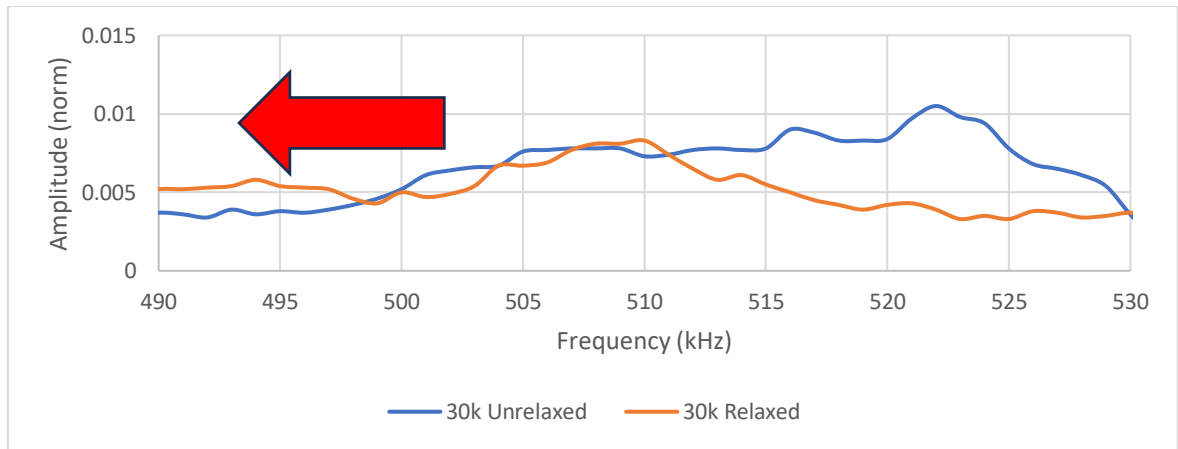


Figure 94: 3Hz Specimen 3 - Unrelaxed vs Relaxed - 30k

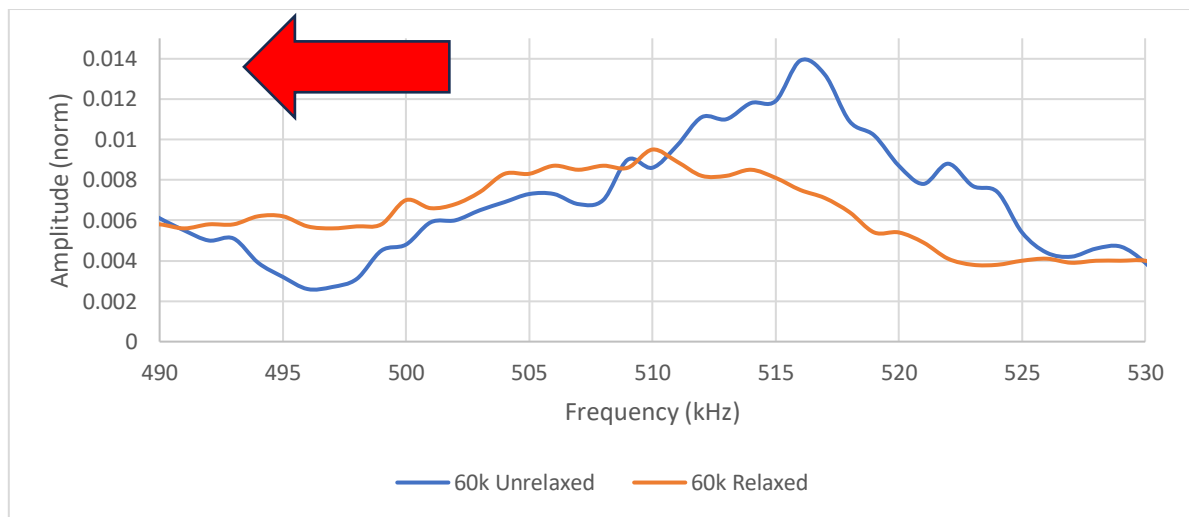


Figure 95: 3Hz Specimen 3 - Unrelaxed vs Relaxed - 60k

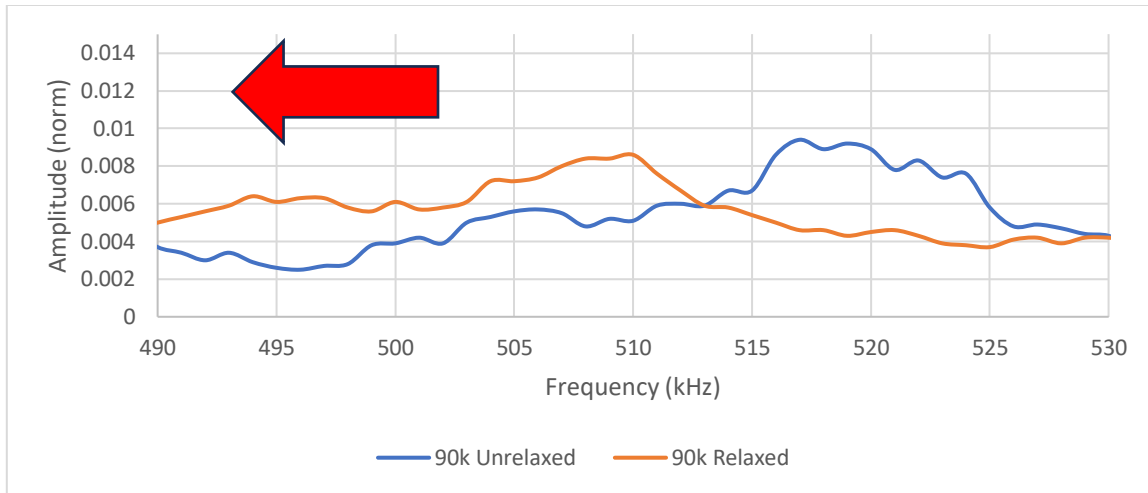


Figure 96: 3Hz Specimen 3 - Unrelaxed vs Relaxed - 90k

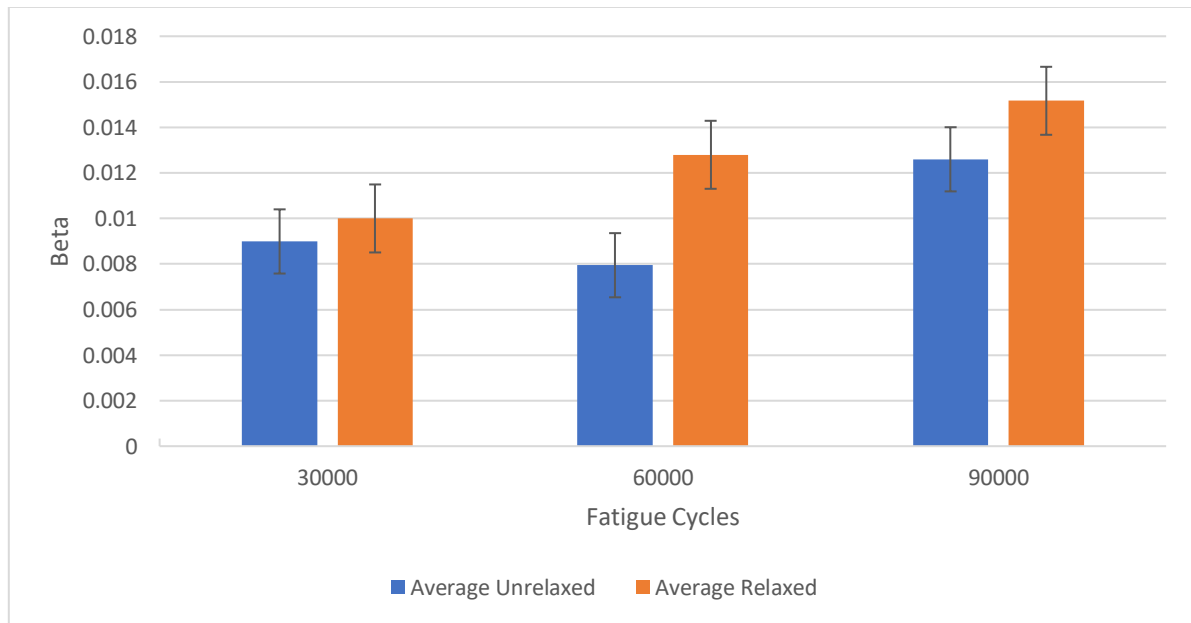


Figure 97: Average Beta Value for all 3Hz Specimen

Figure 97 shows the averages for the beta values of all three specimens run at 3Hz with error bars. Figure 72 shows the average for all 5Hz specimens. Throughout all three cycles and all three specimens at both frequencies the beta values increase throughout the relaxation period. This increase for all six specimens shows that the material regained strength throughout the relaxation period due to the increase in beta values and the relation between material strength and beta.

4.5.3 Velocity Results – 5Hz

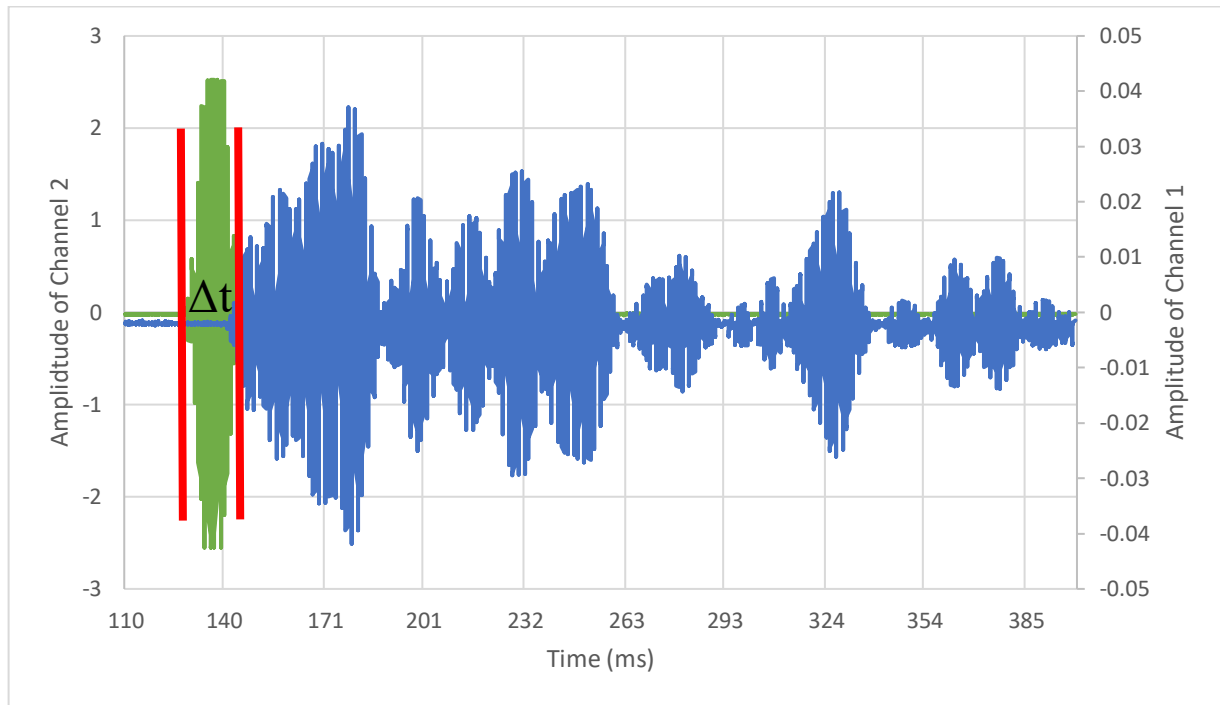


Figure 98: Amplitude vs Time Graph for 5Hz Specimen

The graphs above in figure 98 show an example of the signal that was sent directly to the oscilloscope from the function generator in orange and the signal received through the material in blue. The figure is a generic example and was consistently the same throughout all 540 data points take through relaxation of all 6 specimen. The time from the beginning of the first signal to the beginning of the second signal was used to give a time estimate of the signal through the material. This time was used in conjunction with the distance between the centers of the round PZT patches to give a velocity of the material. The beginning of the first and second signals is shown with a red line and gives the ranges used to find Δt .

The velocity data is shown below for all 5Hz specimen. The velocity is a property of the material that can be used to evaluate the strength returning to the material during relaxation. A point was taken at the beginning, middle, and end of each relaxation period. The time was evaluated and used with the distance

to estimate the velocity of the signal through the material at the three points. If the material life was to increase the material velocity would also increase due to the medium the signal travels through. The material would travel faster through solid material indicating that that if the velocity increased the material would have regained some of its strength. The relaxation velocity data for all three specimens can be seen below and all indicate increases in the signal's velocity and in turn an increase in the materials strength.

The velocities for all 5Hz specimens are shown below in figure 102 and show that as the material experiences relaxation after fatigue the velocity increases which indicates a positive increase in material strength throughout the relaxation. Overall, the velocity decreases as damage is introduced through all three fatigue cycles.

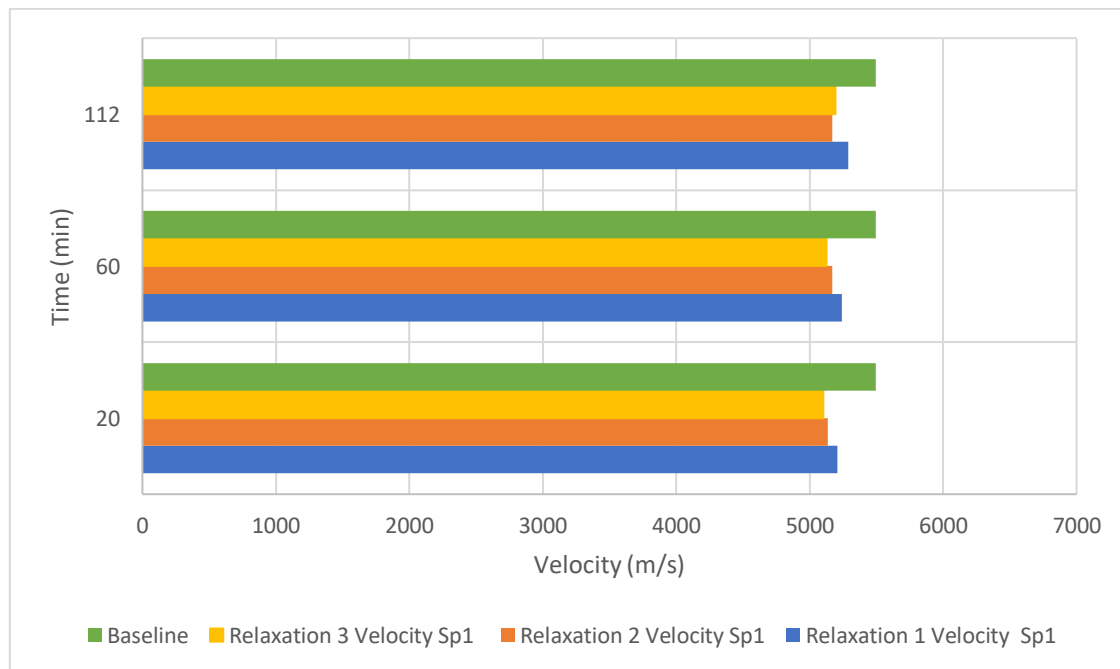


Figure 99: Specimen 1 – Relaxation Velocity

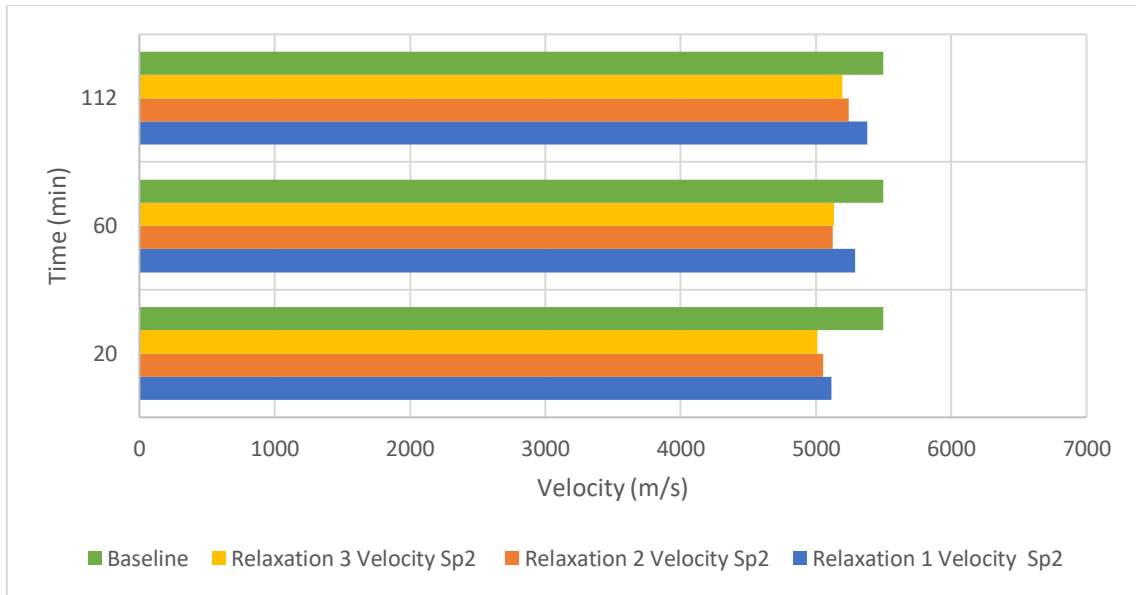


Figure 100: Specimen 2 Relaxation Velocity

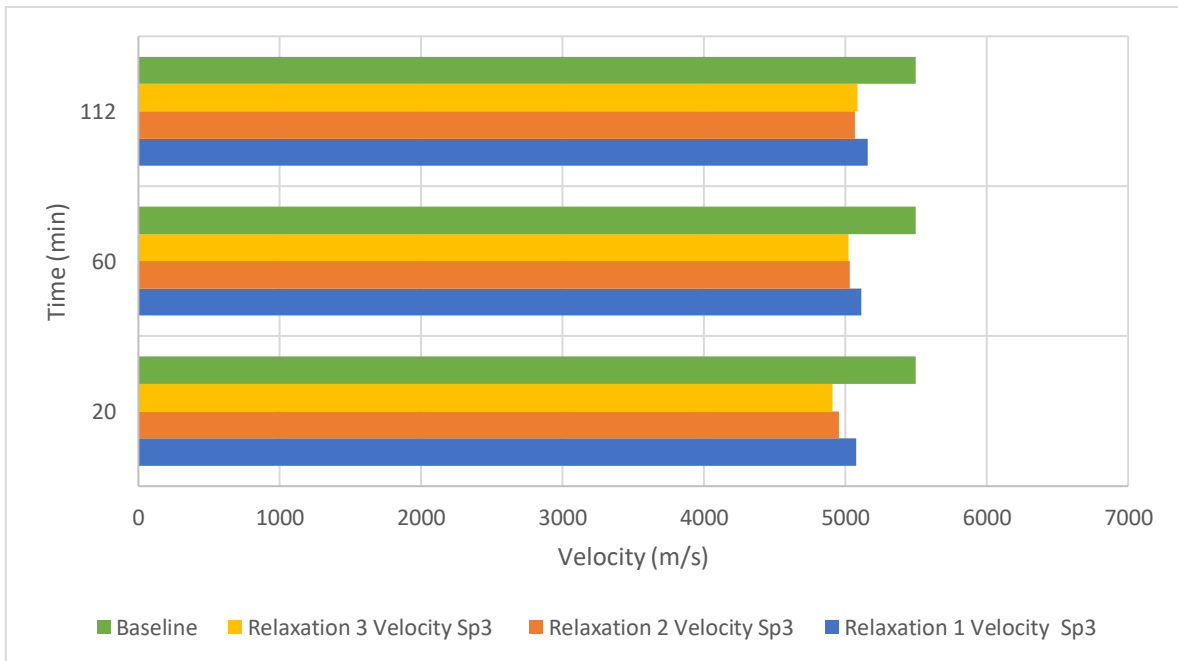


Figure 101: Specimen 3 – Relaxation Velocity

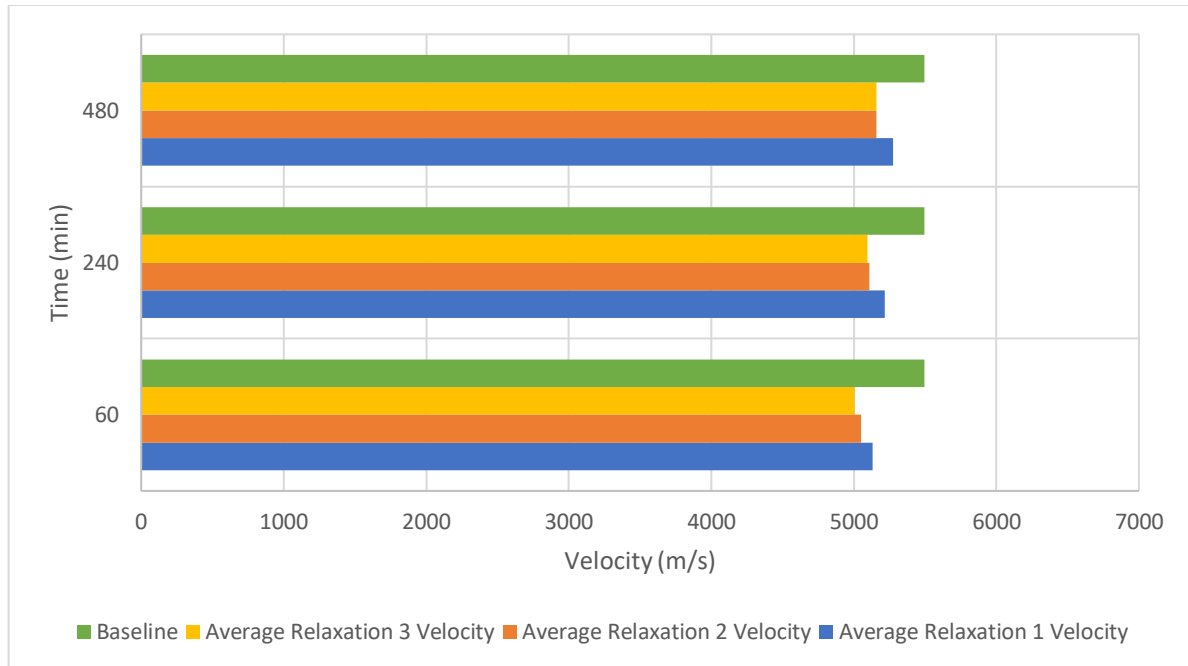


Figure 102: 5Hz Average Velocity for all Three Specimen

4.5.4 Velocity Results – 3Hz

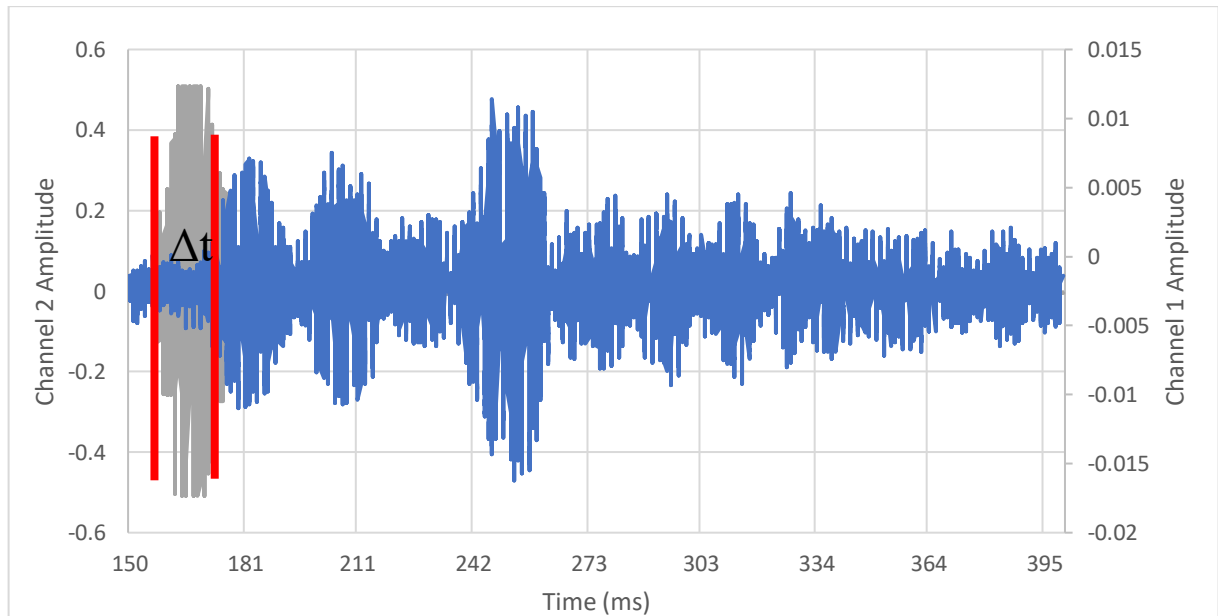


Figure 103: Amplitude vs Time Graph for 3Hz Specimen

The setup is the same for the 3Hz specimen, The red indicates the direct signal from the function generator and the blue indicates the signal from the material. The signal through the material has units that can be seen on the right and are lower than the direct signal. It is noted that the decrease in signal strength is due to loss of signal through the material.

The velocity also follows the previously established conditions. Points were taken in the same points of the data set and the distance between the PZTs and the time between the waves were used to calculate velocity. The increase in the velocity of all three specimens indicates that the material is regaining a portion of its strength throughout the relaxation phase. This supports the results from the FFT analysis.

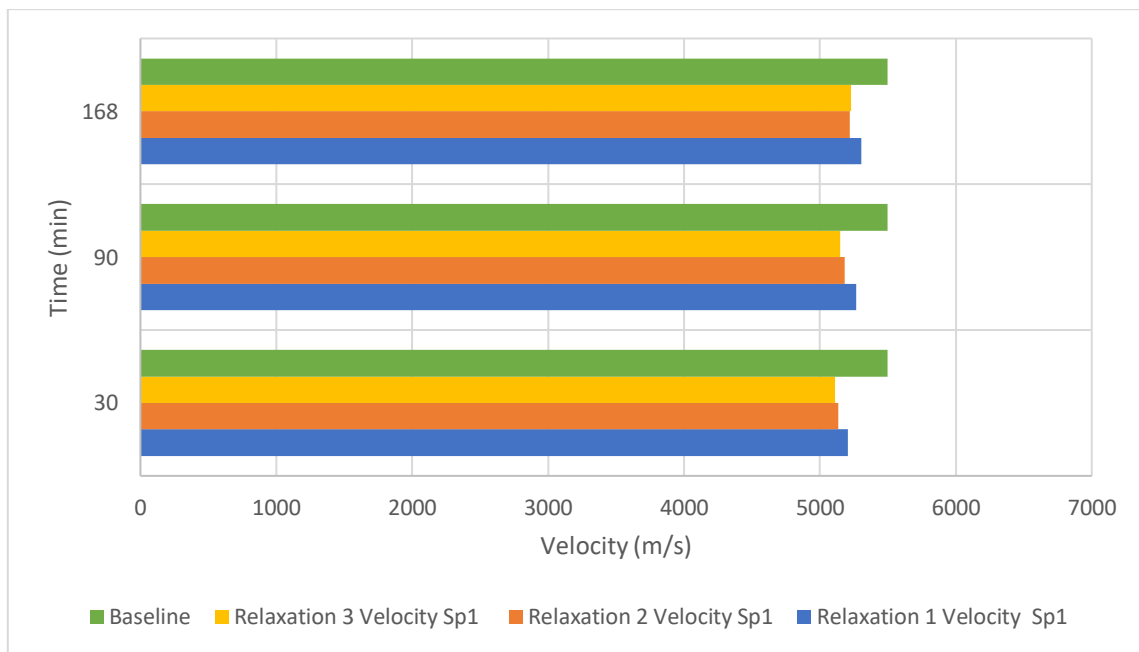


Figure 104: 3Hz - Specimen 1 - Relaxation Velocity

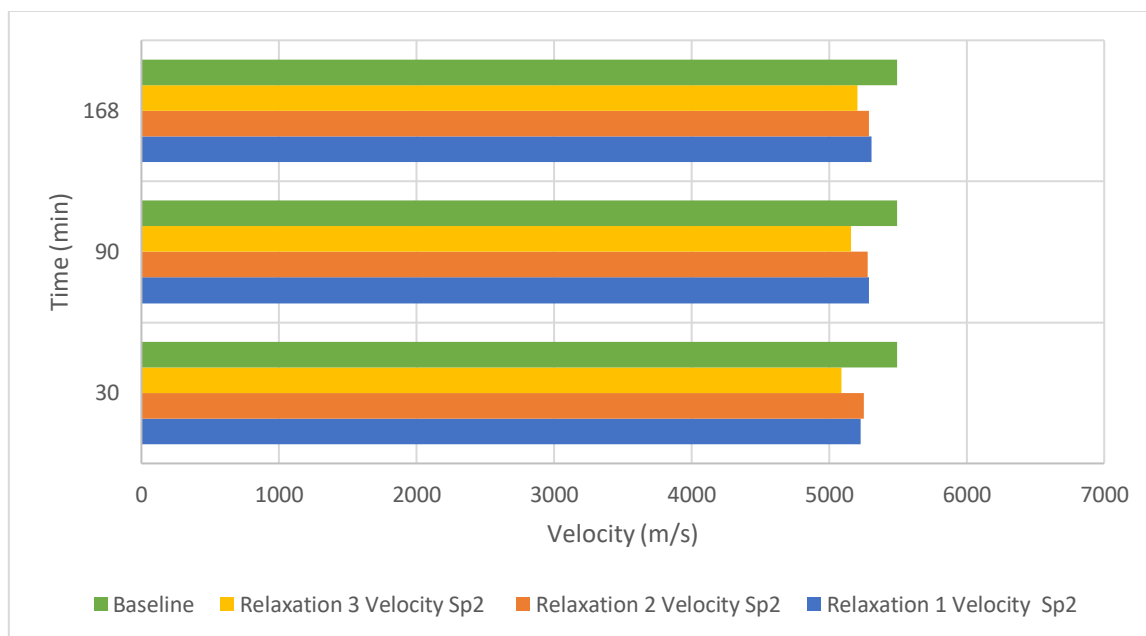


Figure 105: 3Hz - Specimen 2 - Relaxation Velocity

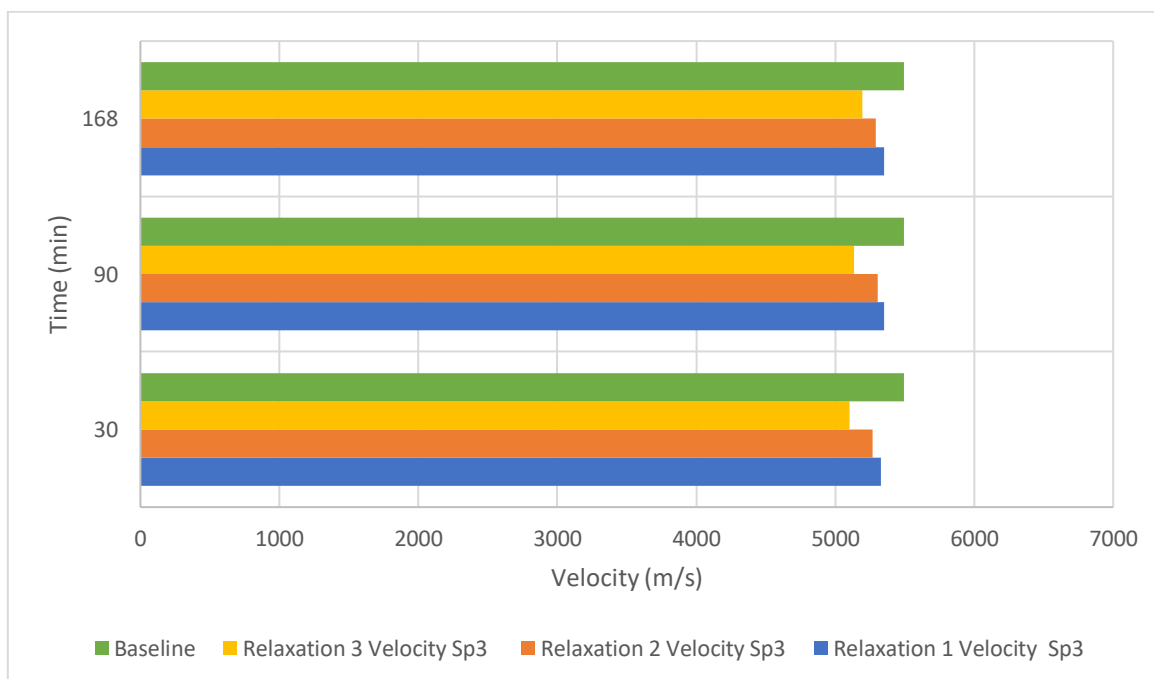


Figure 106: 3Hz - Specimen 3 - Relaxation Velocity

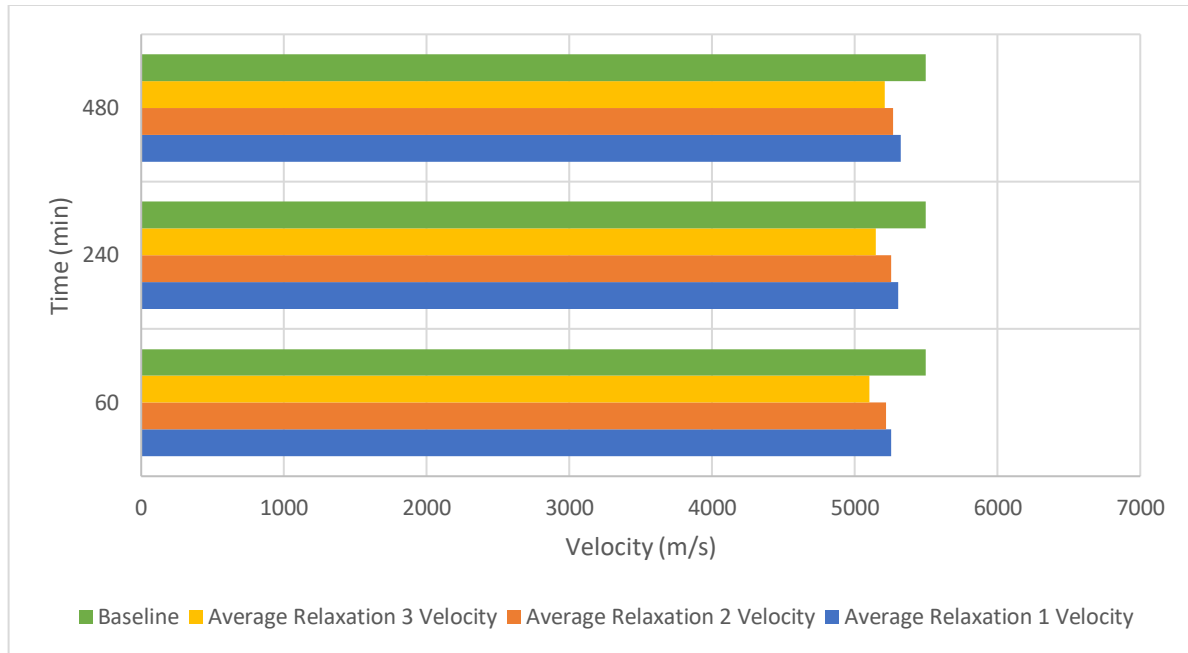


Figure 107: 3Hz Average Velocity for all Three Specimens

The velocity of all three specimens is shown in figures 104-106 an average of all three specimens is shown in figure 107 and they all show an increase in the velocity over the relaxation but a decrease throughout the entire testing procedure which indicates permanent material damage.

4.5.5 Total Max Stress of 5Hz and 3Hz Samples

The total max stress for each tensile specimen shows important information about the specimen as a whole and is a significant aspect of the research. The graphs below show a clear lowering of max stress the material can endure before and after energy harvesting. The increase in max stress in the three hertz sample is due to a decrease in the total number of cycles and the decrease in force that applied due to the premature breaking of the specimen at three hertz and 35,000 cycles. The graphs show an average of 8% strength that is lost after the energy harvesting for 5Hz and a 13% decrease in average strength through the 3Hz samples that energy was harvested from.

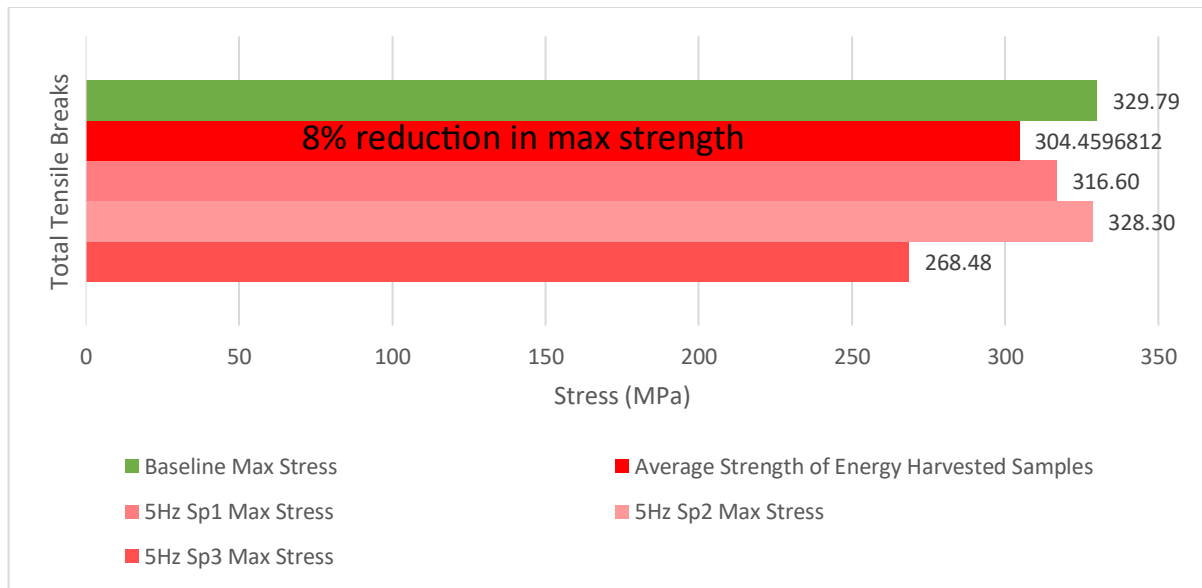


Figure 108: Max Stress for 5Hz Samples

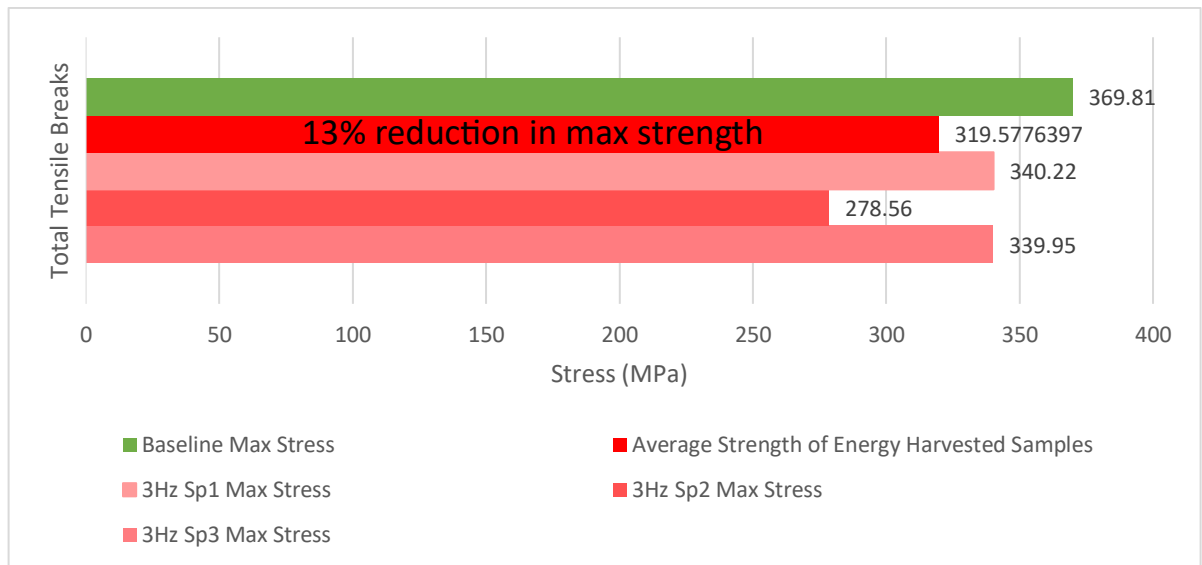


Figure 109: Max Stress for 3Hz Samples

4.6 Analysis of Data and Results

Overall, the data shows multiple things throughout the fatiguing and relaxation phases conducted through the testing. The first major point for analysis focused on harvesting energy from the material and the effect that the harvesting would have on the materials properties. The data partially supports the hypothesis that harvesting would influence the material properties but does not support that harvesting the energy increases the materials life, rather the opposite is true. As energy is extracted from the material the ultimate tensile strength of the material decreases.

The second major testing area was the effect of relaxation on the damage introduced through the energy harvesting and fatiguing of the specimen. The area focused on two major analysis tools. The first tool used the time response data and FFT to analysis to convert to a frequency response. After normalization the FFT generated three distinct points or harmonics. The changes of these harmonics can be used to show many properties of the material and changes the material undergoes when in relaxation. The relaxation phase also looked at signal velocity through the material to determine changes in the velocity as the material was in a relaxed state. This data was used to determine connections between all fatigue phases, all relaxation phases, and connection in the beginning and end of the relaxation phases.

CHAPTER 5

FINDINGS, CONCLUSION, AND RECOMMENDATIONS

5.1 Discussion of Findings and Results

The purpose of this research was to analyze an isotropic material, aluminum 6061, to determine the effects that using smart materials have on the materials properties. The study also aimed to determine the effects that relaxation has on isotropic materials and compare the results to the effects relaxation has on composite materials.

Through a series of testing, it has been found that using piezoelectric material to harvest energy from a testing specimen of aluminum 6061 while the material is fatigue decreases the overall life of the material. The decrease in material life follows principles of energy conservation and shows that as the energy is extracted the internal energy of the material decreases resulting in lower material strength. This is also directly supported by through experimentation and simulation and established a link between material strength and the amount of energy harvested.

The second phase of the study was to evaluate the effects of relaxation on isotropic material and compare the results with a similar study that tested relaxation effects on composite materials. Analysis was conducted to look at two major areas to verify the results. Physical material properties of material velocity were used to measure the velocity of a material that had been fatigued to determine how and if the velocity changed while the material was relaxed. The second was looking at nonlinear FFT analysis of a time response and using FFT to convert the time response to frequency response. The frequency response was evaluated with several methods to evaluate the results. After the Frequency graph was normalized three distinct points appear. The points are referred to as the first, second, and third harmonics. The second harmonic was evaluated through six samples that each experienced 3 fatigue cycles and 3 relaxation periods. The second harmonics peak point is referred to as beta in previous studies. Throughout testing the beta value shifts. Information regarding material properties and strength can be evaluated using this beta value. Throughout all relaxation periods the beta value can be seen increasing. This increase indicates that the

material is regaining partial strength through its relaxation. The beta value was also compared at the beginning and end of each relaxation period to determine the change in material strength through each phase. Using the points at the beginning and end of each relaxation period, a leftward shift is seen from the relaxed peak of the data. This leftward shift indicates a positive increase in the strength of the material. The results of this follow the results of the composite study. The material's velocity was also measured to confirm the results of the FFT. Using piezoelectric material, the signal was sent through the material in intervals during relaxation; this signal was also sent directly to the function generator. The difference between the time of the first signal's receipt and the second was used to calculate the velocity. The material velocity increases throughout the relaxation periods and indicates the material strength also partially returns.

The overall research had four components. The specimen's tensile strength, specimens that experienced a fatigue load, harvesting energy during the fatigue load, and the tensile strength after the fatigue load. The premise of the research lies in tying together these four things with linear velocity data and nonlinear ultrasonic beta value data that was extracted during the relaxation period. The two major concepts look at the combination of these principles to establish the connection between the energy harvesting and the material strength and the relaxation effects that occur in the material. The two are tied together through the material strength and the effects that the energy harvesting, and relaxation have on the material. The energy harvesting actively extracts energy from the material and the relaxation partially restores the material's strength as shown by the increase in velocity, the upward trend of beta values, and the second harmonic shift that occurs during relaxation. The amount of energy that is extracted from the material as the material gets weaker from fatigue shows a correlation between the material and the energy that is extracted. This is verified through the simulation that was conducted in COMSOL. Overall, the two test areas conducted in this study are connected in a major way. The results show the effects that both have on the material and how the two are opposites when comparing the effects that occur in the material.

5.2 Conclusion of Research

Effect of low frequency vibration energy harvesting on Aluminum structures has been investigated in this research. To quantify the energy harvesting effect, both numerical and experimental studies are designed, performed, and analyzed. Numerical studies are performed by commercial finite element-based software COMSOL Multiphysics. In the numerical study, controlled fatigue loads are applied throughout the fatigue cycles and material properties are decreases as the fatigue cycles increased. The simulation results show that as the elastic modulus of Aluminum decreased, the extracted energy is decreased as well. To perform the experimental study, two sets of specimens are prepared following ASTM standards. The first sets of specimens are reserved for baseline tests that includes baseline tensile and fatigue tests. The second set is reserved for fatigue tests with varying fatigue loads (3 Hz and 5 Hz). To quantify the experimental results, guided waves are utilized (add frequency of the actuating PZT) to estimate the linear (wave velocity) and non-linear (normalized second harmonic frequency) parameter of ultrasonic waves. From these experiments, it is found that as energy is extracted from isotropic material, the non-linear beta values increase over three sets of relaxation periods. On the other hand, the linear wave velocity decreases for the same periods of relaxation. Finally, the ultimate strength material of all specimens is estimated. It is as the specimens without energy harvesting have higher remaining ultimate strength compared to the specimens with energy harvesting. A decrease of 8% of strength is shown in the 5Hz samples and 12% decrease in strength is shown in the 3Hz samples. This finding partially supports the hypothesis as the material properties are affected by energy harvesting, however, the effect is not a positive increase in strength. The experimental results confirm the simulation results and establish a direct correlation between material strength and the amount of energy that is harvested. The study also confirmed that isotropic materials behave in a similar way to composite materials when the material is in a relaxed state after the introduction of force.

5.3 Recommendations of Improvements

There are several improvements that can be made with the current research. An increase in the number of tests conducted gives more information and more trends to look for. An increase in the number of frequencies that are tested could also generate more results that build upon the assertions of this research. Due to the premature breaking in specimens that occurred more research into the other frequencies can be tested.

5.4 Recommendations for Future Work

Future work may include looking into different linear and nonlinear methods to test other properties in the material through a similar fatigue-relaxation cycle. Looking at the effects that energy harvesting has on other material properties is also another opportunity that is now open due to the established connection between material properties and energy harvesting with vibrational PZT smart material.

REFERENCES

- Anton, Steven R., and Henry A. Sodano. "A Review of Power Harvesting Using Piezoelectric Materials (2003–2006)." *Smart Materials and Structures* 16, no. 3 (2007/05/18 2007): R1. <https://doi.org/10.1088/0964-1726/16/3/R01>.
- Beeby, S. P., M. J. Tudor, and N. M. White. "Energy Harvesting Vibration Sources for Microsystems Applications." *Measurement Science and Technology* 17, no. 12 (2006/10/26 2006): R175. <https://doi.org/10.1088/0957-0233/17/12/R01>.
- Bergmann Tiest, Wouter M. "Tactual Perception of Material Properties." *Vision Research* 50, no. 24 (2010/12/01/ 2010): 2775-82. <https://doi.org/https://doi.org/10.1016/j.visres.2010.10.005>. <https://www.sciencedirect.com/science/article/pii/S0042698910004967>.
- Chandra Kandpal, Bhaskar, D. K. Gupta, Ashok Kumar, Ashish Kumar Jaisal, Atul Kumar Ranjan, Ankit Srivastava, and Prashant Chaudhary. "Effect of Heat Treatment on Properties and Microstructure of Steels." *Materials Today: Proceedings* 44 (2021/01/01/ 2021): 199-205. <https://doi.org/https://doi.org/10.1016/j.matpr.2020.08.556>. <https://www.sciencedirect.com/science/article/pii/S2214785320364385>.
- Covaci, Corina, and Aurel Gontean. "Piezoelectric Energy Harvesting Solutions: A Review." *Sensors* 20, no. 12 (2020): 3512. <https://www.mdpi.com/1424-8220/20/12/3512>.
- Domanski, Marian, and John Webb. "A Review of Heat Treatment Research." *Lithic Technology* 32, no. 2 (2007/01/01 2007): 153-94. <https://doi.org/10.1080/01977261.2007.11721052>.
- Dreyfuss, R. "Standard Practice for Conducting Force Controlled Constant Amplitude Axial Fatigue Tests of Metallic Materials." *Annual Book of ASTM. American Society for Testing and Materials* (2003): 515-19.
- EIA, U.S. *Forms of Energy*. Independent Statistics and Analysis, 2023.
- . *How Much Electricity Is Lost in Electricity Transmission and Distribution in the United States?*, 2022.
- Elvin, Niell G., and Alex A. Elvin. "A Coupled Finite Element—Circuit Simulation Model for Analyzing Piezoelectric Energy Generators." *Journal of Intelligent Material Systems and Structures* 20, no. 5 (2009/03/01 2008): 587-95. <https://doi.org/10.1177/1045389X08101565>.
- Erturk, A., and D. J. Inman. "An Experimentally Validated Bimorph Cantilever Model for Piezoelectric Energy Harvesting from Base Excitations." *Smart Materials and Structures* 18, no. 2 (2009/01/13 2009): 025009. <https://doi.org/10.1088/0964-1726/18/2/025009>.

- Fan, Kangqi, Jianwei Chang, Fengbo Chao, and Witold Pedrycz. "Design and Development of a Multipurpose Piezoelectric Energy Harvester." *Energy conversion and management* 96 (2015): 430-39. <https://doi.org/10.1016/j.enconman.2015.03.014>.
- Farshchi Yazdi, Seyed Amir Fouad, Alberto Corigliano, and Raffaele Ardito. "3-D Design and Simulation of a Piezoelectric Micropump." *Micromachines* 10, no. 4 (2019): 259. <https://www.mdpi.com/2072-666X/10/4/259>.
- Glynne-Jones, P., M. J. Tudor, S. P. Beeby, and N. M. White. "An Electromagnetic, Vibration-Powered Generator for Intelligent Sensor Systems." *Sensors and Actuators A: Physical* 110, no. 1 (2004/02/01/ 2004): 344-49. <https://doi.org/https://doi.org/10.1016/j.sna.2003.09.045>. <https://www.sciencedirect.com/science/article/pii/S0924424703005995>.
- Howells, Christopher A. "Piezoelectric Energy Harvesting." *Energy conversion and management* 50, no. 7 (2009): 1847-50. <https://doi.org/10.1016/j.enconman.2009.02.020>.
- Inkson, B. J. "2 - Scanning Electron Microscopy (Sem) and Transmission Electron Microscopy (Tem) for Materials Characterization." In *Materials Characterization Using Nondestructive Evaluation (Nde) Methods*, edited by Gerhard Hübschen, Iris Altpeter, Ralf Tschuncky and Hans-Georg Herrmann, 17-43: Woodhead Publishing, 2016.
- Kim, Heung Soo, Joo-Hyong Kim, and Jaehwan Kim. "A Review of Piezoelectric Energy Harvesting Based on Vibration." *International Journal of Precision Engineering and Manufacturing* 12, no. 6 (2011/12/01 2011): 1129-41. <https://doi.org/10.1007/s12541-011-0151-3>.
- Kornbluh, Roy, Ron Pelrine, Qibing Pei, Richard Heydt, Scott Stanford, Seajin Oh, and Joseph Eckerle. "Electroelastomers: Applications of Dielectric Elastomer Transducers for Actuation, Generation, and Smart Structures." Paper presented at the SPIE Smart Structures and Materials + Nondestructive Evaluation and Health Monitoring, 2002.
- LaVan, D. A., and W. N. Sharpe. "Tensile Testing of Microsamples." *Experimental Mechanics* 39, no. 3 (1999/09/01 1999): 210-16. <https://doi.org/10.1007/BF02323554>.
- Lee, Yung-Li. *Fatigue Testing and Analysis: Theory and Practice*. Vol. 13: Butterworth-Heinemann, 2005.
- Lerch, R. "Simulation of Piezoelectric Devices by Two- and Three-Dimensional Finite Elements." *IEEE Transactions on Ultrasonics, Ferroelectrics, and Frequency Control* 37, no. 3 (1990): 233-47. <https://doi.org/10.1109/58.55314>.
- Lesics. "Understanding Piezoelectric Effect! Youtube." United States, 2021. https://www.youtube.com/watch?v=_XABS0dR15o.
- Liao, Yabin, and Henry A. Sodano. "Structural Effects and Energy Conversion Efficiency of Power Harvesting." *Journal of Intelligent Material Systems and Structures* 20, no. 5 (2009): 505-14.

- <https://doi.org/10.1177/1045389x08099468>.
- <https://journals.sagepub.com/doi/abs/10.1177/1045389X08099468>.
- Ma, Hongbao, Kuan-Jiunn Shieh, and Tracy X Qiao. "Study of Transmission Electron Microscopy (Tem) and Scanning Electron Microscopy (Sem)." *Nat. Sci* 4, no. 3 (2006): 14-22.
- Mateu, Loreto, and Francesc Moll. *Review of Energy Harvesting Techniques and Applications for Microelectronics*. Microtechnologies for the New Millennium 2005. Vol. 5837: SPIE, 2005. <https://doi.org/10.1117/12.613046>.
- Meade, Daniel. "Investigation of Mechanically Fatigued Low-Frequency Energy Harvesting Effect on Isotropic Materials." IMECE 2023, New Orleans, LA, ASME, 2023.
- Mitcheson, P. D., P. Miao, B. H. Stark, E. M. Yeatman, A. S. Holmes, and T. C. Green. "Mems Electrostatic Micropower Generator for Low Frequency Operation." *Sensors and Actuators A: Physical* 115, no. 2 (2004/09/21/ 2004): 523-29. <https://doi.org/https://doi.org/10.1016/j.sna.2004.04.026>. <https://www.sciencedirect.com/science/article/pii/S0924424704002985>.
- Mitcheson, P. D., E. M. Yeatman, G. K. Rao, A. S. Holmes, and T. C. Green. "Energy Harvesting from Human and Machine Motion for Wireless Electronic Devices." *Proceedings of the IEEE* 96, no. 9 (2008): 1457-86. <https://doi.org/10.1109/JPROC.2008.927494>.
- Mohammed, Azad, and Avin Abdullah. "Scanning Electron Microscopy (Sem): A Review." Paper presented at the Proceedings of the 2018 International Conference on Hydraulics and Pneumatics—HERVEX, Băile Govora, Romania, 2018.
- Patra, Subir, Hossain Ahmed, Mohammadsadegh Saadatzi, and Sourav Banerjee. "Effect of Time-Dependent Strength Recovery of Composite Materials: Quantification through Higher Order Ultrasonic Non-Linearity Using Lamb Waves." *Journal of Nondestructive Evaluation, Diagnostics and Prognostics of Engineering Systems* 3, no. 1 (2020): 1-10. <https://doi.org/10.1115/1.4045011>.
- Patra, Subir, and Sourav Banerjee. "Material State Awareness for Composites Part I: Precursor Damage Analysis Using Ultrasonic Guided Coda Wave Interferometry (Cwi)." *Materials* 10, no. 12 (2017): 1436. <https://www.mdpi.com/1996-1944/10/12/1436>.
- Popovici, Dorina, Alexandru Gheorghe, Florea Ioan Hantila, Florin Constantinescu, Mihai Maricar, and Miruna Nitescu. *Modeling and Simulation of Piezoelectric Devices*. IntechOpen Rijeka, 2008.
- Rashad, Magdi, Navid Khordehgah, Alina Żabnieńska-Góra, Lujean Ahmad, and Hussam Jouhara. "The Utilisation of Useful Ambient Energy in Residential Dwellings to Improve Thermal Comfort and Reduce Energy Consumption." *International Journal of Thermofluids* 9 (2021/02/01/ 2021): 100059. <https://doi.org/https://doi.org/10.1016/j.ijft.2020.100059>. <https://www.sciencedirect.com/science/article/pii/S266620272030046X>.
- Roylance, David. "Stress-Strain Curves." *Massachusetts Institute of Technology study, Cambridge* (2001).

- Shenck, N. S., and J. A. Paradiso. "Energy Scavenging with Shoe-Mounted Piezoelectrics." *IEEE Micro* 21, no. 3 (2001): 30-42. <https://doi.org/10.1109/40.928763>.
- Shu, Y. C., and I. C. Lien. "Analysis of Power Output for Piezoelectric Energy Harvesting Systems." *Smart Materials and Structures* 15, no. 6 (2006/09/25 2006): 1499. <https://doi.org/10.1088/0964-1726/15/6/001>. <https://dx.doi.org/10.1088/0964-1726/15/6/001>.
- Stadtländer, CTKH. "Scanning Electron Microscopy and Transmission Electron Microscopy of Mollicutes: Challenges and Opportunities." *Modern research and educational topics in microscopy* 1 (2007): 122-31.
- Staworko, Micha, and Tadeusz Uhl. "Modeling and Simulation of Piezoelectric Elements-Comparison of Available Methods and Tools." *Mechanics/AGH University of Science and Technology* 27, no. 4 (2008): 161-71.
- Surmenev, Roman A., Tetiana Orlova, Roman V. Chernozem, Anna A. Ivanova, Ausrine Bartasyte, Sanjay Mathur, and Maria A. Surmeneva. "Hybrid Lead-Free Polymer-Based Nanocomposites with Improved Piezoelectric Response for Biomedical Energy-Harvesting Applications: A Review." *Nano Energy* 62 (2019/08/01/ 2019): 475-506. <https://doi.org/https://doi.org/10.1016/j.nanoen.2019.04.090>. <https://www.sciencedirect.com/science/article/pii/S221128551930391X>.
- Taylor, G. W., J. R. Burns, S. A. Kammann, W. B. Powers, and T. R. Welsh. "The Energy Harvesting Eel: A Small Subsurface Ocean/River Power Generator." *IEEE Journal of Oceanic Engineering* 26, no. 4 (2001): 539-47. <https://doi.org/10.1109/48.972090>.
- Weibull, Waloddi. *Fatigue Testing and Analysis of Results*. Elsevier, 2013.
- Yang, Yi, Zhiyuan Chen, Qin Kuai, Junrui Liang, Jingjing Liu, and Xiaoyang Zeng. "Circuit Techniques for High Efficiency Piezoelectric Energy Harvesting." *Micromachines* 13, no. 7 (2022): 1044. <https://www.mdpi.com/2072-666X/13/7/1044>.
- Yildirim, Tanju, Mergen H. Ghayesh, Weihua Li, and Gursel Alici. "A Review on Performance Enhancement Techniques for Ambient Vibration Energy Harvesters." *Renewable and Sustainable Energy Reviews* 71 (2017/05/01/ 2017): 435-49. <https://doi.org/https://doi.org/10.1016/j.rser.2016.12.073>. <https://www.sciencedirect.com/science/article/pii/S1364032116311273>.
- Zhou, Weilie, Robert Apkarian, Zhong Lin Wang, and David Joy. "Fundamentals of Scanning Electron Microscopy (Sem)." In *Scanning Microscopy for Nanotechnology: Techniques and Applications*, edited by Weilie Zhou and Zhong Lin Wang, 1-40. New York, NY: Springer New York, 2007.